



Universiteit
Leiden
The Netherlands

Constructing traveling fronts at the savanna-forest transition zone

Vossen, N.C.M. van

Citation

Vossen, N. C. M. van. *Constructing traveling fronts at the savanna-forest transition zone.*

Version: Not Applicable (or Unknown)

License: [License to inclusion and publication of a Bachelor or Master thesis in the Leiden University Student Repository](#)

Downloaded from: <https://hdl.handle.net/1887/4171445>

Note: To cite this publication please use the final published version (if applicable).

N.C.M. van Vossen

Constructing traveling fronts at the
savanna-forest transition zone

Master thesis

August 22, 2022

Thesis supervisors: Prof. dr. A. Doelman
Dr. S. Banerjee



Leiden University
Mathematical Institute

Contents

1	Introduction	3
2	Methods	5
2.1	Model formulation	5
2.1.1	Introducing the spatial system	6
2.1.2	Introducing the travelling wave solution	7
2.2	Relations between the characters of the fixed points in the temporal and the spatial system	7
2.3	Geometric singular perturbation theory	8
2.3.1	Fenichel's first theorem	9
2.3.2	Fenichel's second theorem	9
2.4	Numerical schemes	9
3	Analysis of the nonspatial model	12
3.1	Scaling of the system	12
3.1.1	Critical points and their character	14
3.1.2	Phase planes	17
3.2	Spatially extended savanna-forest model	18
3.2.1	Critical points and their character	18
4	Constructing traveling fronts	23
4.1	The fast and slow limits	24
4.2	Fast sub-system	24
4.2.1	Critical points and their character	25
4.2.2	Hamiltonian	26
4.2.3	Phase plane	28
4.3	Slow system on \mathcal{M}_0^0	29
4.3.1	Critical points and their character	30
4.3.2	Phase plane	30
4.3.3	Hamiltonian	31
4.4	Slow system on \mathcal{M}_0^+	32
4.4.1	Critical points and their character	33
4.4.2	Phase planes	33
4.4.3	Hamiltonian	34
4.5	Heteroclinic connection in the 4D space	36
4.5.1	Intersection of the manifolds	36
4.5.2	Finding condition for heteroclinic connection using Hamiltonians	36

4.5.3	Heteroclinic connection for $c \neq 0$	37
4.6	Numerical simulations	38
4.6.1	Travelling front	38
4.6.2	Standing front	41
5	A more realistic model: saturation with respect to forest trees	45
5.1	Four dimensional system	48
5.2	Fast and slow sub-system	48
5.3	Heteroclinic orbit	50
5.3.1	Orbit from $(0, 0)$ on \mathcal{M}_0^+	52
5.3.2	Combine dynamics of fast and slow system	52
5.3.3	Heteroclinic orbit in fast system	53
5.3.4	Intersection of the orbits on \mathcal{M}_0^0 and \mathcal{M}_0^+	54
5.4	Fast jump	55
5.5	Finding the fast jump numerically	56
6	Front (in-)stability	59
6.1	Intersection homoclinic orbits	60
6.2	Fast jump	60
6.3	Condition for fingering fronts	61
6.4	Numerical simulations in 2D (Still have to do these simulations for the second extended model)	62
7	Discussion	65
A	Matlab codes	69
A.1	Unextended model	69
A.1.1	Main code for using pdepe	69
A.1.2	Defining equations for pdepe	70
A.1.3	Defining initial condition for pdepe	70
A.1.4	Defining boundary conditions for pdepe	71
A.1.5	Finding still front	71
A.2	Extended model: saturation term in F- and S-equation	72
A.3	Unextended model 2D	73
A.4	Heteroclinic orbit	76
A.4.1	Heteroclinic orbit for (2.7)	76
A.4.2	Heteroclinic orbit for (5.4)	76
A.4.3	Heteroclinic orbit for (6.2)	77
A.4.4	Defining equations for ode45	78

Chapter 1

Introduction

Savannas are defined by Gillison (1983) as tropical grasslands with scattered individual trees. These are located throughout the tropics in all continents, but mostly in America, Africa and Australia (Solbrig, 1996). Savanna covers approximately one-sixth of all land surface on earth (Grace, José, Meir, Miranda, & Montes, 2006). The characteristics of savanna changes with the precipitation gradient. For example, if there are small increases in precipitation, the plant productivity may increase. This happens because these increases cause a decrease in interception and evaporation. On the other hand, large increases can decrease the plant productivity. For instance due to overflow or deep soil infiltration (Berry & Kulmatiski, 2017). Towards humid ends of the savanna, the savanna gives way to tropical forests. We will analyse a model that describes the savanna-forest transition zone. In this zone, both savanna and forest can be observed under similar climatic conditions when rainfall is moderate (Oliveras & Malhi, 2016). Spatial processes like dispersal plays an important roll as well (Goel, Guttal, Levin, & Staver, 2018). We will incorporate all these compontens into the model.

We first give ecological background, which shows that this problem is of interest. Forest and savanna constitute approximately 35 percent of all land surface on earth. Moreover they are the predominant biomes of the tropical regions of the world (Ametsitsi, 2021). The savanna-forest boundary is the most common transition of the tropical regions (Oliveras & Malhi, 2016). The research of Kershaw (1992) has shown that savanna-forest boundaries have shifted in the past and other studies have shown that these boundaries will also continue to shift (D. Schwartz, 2013). Forest encroachment into savannas is occurring worldwide (Mitchard & Flintrop, 2013). This could occur due to the action of intricate anthropogenic and biophysical drivers (Janssen et al., 2018), which is a disturbing phenomenon, because tropical forests contribute to climate change reduction. Forest trees remove net CO_2 from the atmosphere and store it as biomass (Bonan, 2008). Tropical forest are predicted to experience more climatic changes. This includes increased temperatures, change in rainfall patterns and possibly longer dry seasons (Cuni-Sanchez et al., 2016). That is why it is important that we get a better understanding of the savanna-forest boundaries. Furthermore how these boundaries may respond to climatic changes.



Figure 1.1: Savanna-forest boundary in regions of Western Ghats, Karnataka, India (Goel, 2020).

The interface between two distinct ecosystem states is called a front (Bel, Hagberg, & Meron, 2012), (Zelnik & Meron, 2018). In this thesis we will construct such a front with the help of mathematical and numerical analysis in a spatial model of the savanna-forest transition zone. This model has two variables, \hat{f} and \hat{s} , which represents the fire biomass and the savanna biomass respectively.

$$\begin{cases} \frac{d\hat{f}}{d\tau} = r_F \hat{f} \left(1 - \frac{\hat{f}}{K_F}\right) - \eta f_F \hat{s} \hat{f} - d_F \hat{f} \\ \frac{d\hat{s}}{d\tau} = r_S \hat{s} \left(1 - \frac{\hat{s}}{K_S}\right) - d\hat{f} \hat{s} - (\eta f_S \hat{s} + d_S) \hat{s} \end{cases} \quad (1.1)$$

This model consists of many parameters. We will explain their meaning and their significance in the next section. Because dispersal plays an important role in the savanna-forest transition zone, we add diffusion terms to both equations. This system has a clear separation in spatial scales, hence we can use geometric singular perturbation theory. We will introduce this theory in section 2.3.

In the third section we will analyse the model. First we non-dimensionalize the system, this procedure reduces the amount of parameter values, which makes it easier to analyse the system. Later on in this section we will analyse this dimensionless system. We will determine the critical values and their character, which we can use to plot their phase planes. This already helps us finding the front solution we that we are looking for. In the next section we will use this to find a heteroclinic connection. This heteroclinic connection goes from a pure forest state to a pure grass state. This solution is called the bi-stable front.

Furthermore we change the system by adding a saturation term, which makes the model more ecological relevant. Again we will show that a front solution exists for this system. Analysing this model analytically is really complicated, hence we use numerical tools to show this. Lastly we will plot these travelling fronts for both systems numerically. We compare these simulations to our analytical findings. We start by simulating solutions in one dimension. Afterwards we repeat this in two dimensions. Fingering fronts is a pattern that has been observed in other models (Fernandez-Oto, Tzuk, & Meron, 2019). We try to find out whether our model can give these patterns. We derive a condition that is needed for fingering fronts to exist. We will also use two dimensional simulations to find these fingering fronts for the savanna-forest transition model. Finally, we end this thesis by a short discussion section.

Chapter 2

Methods

2.1 Model formulation

Finding a model that describes the savanna-forest boundaries would help to predict how these boundaries will evolve over time. First we study the non-spatial model (1.1), which is a two dimensional system of first order ordinary differential equations. This system has two state variables \hat{f} and \hat{s} . \hat{f} and \hat{s} represent the forest biomass density and the savanna biomass density respectively. The savanna biomass includes C4 grasses and savanna trees, which are both shade intolerant as well as fire resistant.

Because the state variables represent the area that is covered by the biomass, we consider a logistic growth. Then both of the state variables can increase independently until a certain carrying capacity is reached (Murray, 2002).

We have many parameters in system (1.1), later on we are going to scale the system and reduce this number of parameters. The parameters r_S and r_F represent the growth rate of the savanna and forest vegetation respectively. The parameters K_S and K_F are the carrying capacities that are incorporated into the system. d_S and d_F are the removal rates of the savanna vegetation and the forest trees, resulting from various factors. Lastly, the parameter d represents the effect of shading of the forest trees on the savanna grasses.



Figure 2.1: Fire at the savanna-forest boundary (Staver, 2011).

Fire also has an impact on the savanna-forest transition dynamics. We incorporate this into our model. The parameter f_S is the sensitivity of the savanna biomass to fire. Because the savanna vegetation itself is a fuel to fire, the rate of loss of savanna biomass is modeled by $-\eta f_S \hat{s}^2$ in (1.1). We also add a term in the first equation of (1.1) that incorporates the effect of fire, because fire also causes loss of forest biomass. Similarly, f_F represents the sensitivity of the forest biomass to fire. The rate of loss of forest biomass is modeled by $-\eta f_F \hat{s} \hat{f}$, where η is the frequency in which a fire occurs. We multiply by \hat{f} in this term, because this loss due to fire must be directly proportional to the present forest biomass density.

In order to analyse this system we non-dimensionalise system (1.1). We show how we have done this procedure in section 3.1. The non-dimensionalised model is the following

$$\begin{cases} \frac{df}{dt} = f(\alpha - f - as) & =: A(f, s) \\ \frac{ds}{dt} = s(\beta - bf - \mu s) & =: B(f, s). \end{cases} \quad (2.1)$$

We remark that this equation is very similar to the well known modified Lotka-Volterra model described in Braun (1983).

$$\begin{cases} \frac{dx}{dt} = ax - bxy - ex^2 \\ \frac{dy}{dt} = -cy + dxy - fy^2. \end{cases} \quad (2.2)$$

This model describes predator-pray interactions. The variables $x(t)$ and $y(t)$ represent the prey- and predator population over time respectively. System (2.1) is equal to the Lotka-Volterra equations with $a = \alpha$, $b = a$, $c = -\beta < 0$, $d = -b < 0$, $e = 1$ and $f = \mu$.

2.1.1 Introducing the spatial system

We want to add a spatial variable to the system. Hence we add a diffusion term to the system (Murray, 2002), then it becomes the following

$$\begin{cases} \frac{\partial F}{\partial t} = F(\alpha - F - aS) + \Delta F \\ \frac{\partial S}{\partial t} = S(\beta - bF - \mu S) + \frac{1}{\epsilon^2} \Delta S. \end{cases} \quad (2.3)$$

Where Δ is the Laplace operator is equal to $\Delta = \frac{\partial^2}{\partial x^2} + \frac{\partial^2}{\partial y^2}$ in two dimensions. The diffusion coefficient of the F -equation is equal to 1. We set the diffusion coefficient of the S -equation equal to $\frac{1}{\epsilon^2}$, where $0 < \epsilon \ll 1$. This is because grasses are the main component of the savanna and that diffuses much faster than forest trees Oliveras and Malhi (2016). Moreover, we only look into one spatial dimension, this already gives us a lot of information about how this equation describes the savanna-forest boundary. So then we have $\Delta F = \frac{\partial^2 F}{\partial x^2}$ and $\Delta S = \frac{\partial^2 S}{\partial x^2}$.

In the next section we want to analyse the spatially extended model (2.3). First we look at the stationary equation: $\frac{\partial f}{\partial t} = \frac{\partial s}{\partial t} = 0$. This gives us this system of two stationary second order ordinary differential equations

$$\begin{cases} \frac{d^2 f}{dx^2} = f(f + as - \alpha) \\ \frac{d^2 s}{dx^2} = \epsilon^2 s(bf + \mu s - \beta). \end{cases} \quad (2.4)$$

We can rewrite this two dimensional system of second order ordinary differential equations in a four dimensional system of first order ordinary differential equations. We do this by defining the following variables $p := \frac{df}{dx}$ and $q := \frac{1}{\epsilon} \frac{ds}{dx}$, then we get

$$\begin{cases} \frac{df}{dx} = p & =: U(f, p, s, q) \\ \frac{dp}{dx} = f(f + as - \alpha) & =: V(f, p, s, q) \\ \frac{ds}{dx} = \epsilon q & =: W(f, p, s, q) \\ \frac{dq}{dx} = \epsilon s(bf + \mu s - \beta) & =: Z(f, p, s, q). \end{cases} \quad (2.5)$$

2.1.2 Introducing the travelling wave solution

At the savanna forest transition zone is observed that the savanna can invade the forest or the other way around. Hence we introduce a wave solution to (2.3) in order to describe this phenomenon. Then we take $F = F(x, t) = f(\xi)$ and $S = S(x, t) = s(\xi)$, with $\xi = x - ct$. Then we get $\Delta F = \frac{\partial^2 f}{\partial x^2} = \frac{d^2 f}{d\xi^2}$ and $\Delta S = \frac{\partial^2 s}{\partial x^2} = \frac{d^2 s}{d\xi^2}$ and $\frac{\partial F}{\partial t} = -c \frac{df}{d\xi}$ and $\frac{\partial S}{\partial t} = -c \frac{ds}{d\xi}$. Then we get a two dimensional system of second order ordinary differential equations

$$\begin{cases} \frac{d^2 f}{d\xi^2} = -c \frac{df}{d\xi} + f(f - \alpha + as) \\ \frac{d^2 s}{d\xi^2} = \epsilon^2 \left[-c \frac{ds}{d\xi} + s(\mu s - \beta + bf) \right]. \end{cases} \quad (2.6)$$

If we define the variables $p := \frac{df}{d\xi}$ and $q := \frac{1}{\epsilon} \frac{ds}{d\xi}$ we can rewrite this system into a system of four first order ordinary differential equations as well

$$\begin{cases} \frac{df}{d\xi} = p \\ \frac{dp}{d\xi} = -cp + f(f - \alpha + as) \\ \frac{ds}{d\xi} = \epsilon q \\ \frac{dq}{d\xi} = \epsilon(-\epsilon cq + s(\mu s - \beta + bf)). \end{cases} \quad (2.7)$$

In order to analyse this system we use geometric singular perturbation theory. In section 2.3 we explain this theory and in section 4 we apply it to system (2.7).

2.2 Relations between the characters of the fixed points in the temporal and the spatial system

In this section we will look into the relations between (\bar{F}, \bar{S}) and $(\bar{F}, 0, \bar{S}, 0)$ as critical points of (2.3) and (2.5). For both systems we only look at one spatial dimension, hence system (2.3) becomes

$$\begin{cases} \frac{\partial F}{\partial t} = F(\alpha - F - aS) + \frac{\partial^2 F}{\partial x^2} \\ \frac{\partial S}{\partial t} = S(\beta - bF - \mu S) + \frac{1}{\epsilon^2} \frac{\partial^2 S}{\partial x^2}. \end{cases} \quad (2.8)$$

We state the following lemma's that describe the relation between the characters of the fixed points in these systems.

Lemma 2.2.1. *Let $\bar{P} = (\bar{F}, 0, \bar{S}, 0)$ be a critical point of (2.5) that corresponds to a stable trivial state (\bar{F}, \bar{S}) of (2.8) on \mathbb{R} , then $\dim(W^s(\bar{P})) = \dim(W^u(\bar{P})) = 2$: \bar{P} is a saddle of (2.5) (Doelman, n.d.)*

Lemma 2.2.2. *If $\dim(W^s(\bar{P})) = \dim(W^u(\bar{P})) = 2$ and (\bar{F}, \bar{S}) is stable as solution of the reaction ODE (2.1), then (\bar{F}, \bar{S}) is stable as solution of (2.8) on \mathbb{R} (Doelman, n.d.).*

In the next section we will determine the critical points and their characters of systems (2.1) and (2.5). Afterwards we can use these lemma's to derive the characters of the critical points of (2.8).

2.3 Geometric singular perturbation theory

System (2.7) has a clear separation in spatial scales. Geometric singular perturbation theory is very useful for these types of problems, this theory uses different scales to understand the global structure of the phase space (Hek, 2009). The basic equations that this theory considers are singularly perturbed systems of first order ordinary differential equations, that have two different time-scales. These are of the form

$$\begin{cases} \dot{\mathbf{u}} = g(\mathbf{u}, \mathbf{v}, \epsilon), \\ \dot{\mathbf{v}} = \epsilon h(\mathbf{u}, \mathbf{v}, \epsilon), \end{cases} \quad (2.9)$$

where $\dot{\cdot} = \frac{d}{dt}$, $0 < \epsilon \ll 1$, $\mathbf{u} \in \mathbb{R}^k$ and $\mathbf{v} \in \mathbb{R}^l$ with $k, l \geq 1$. The functions f and g must be at least C^1 . System (2.9) is called the fast system and t is called the fast scale. To get the slow system, we introduce a change the slow scale. For the first equation we get $\dot{\mathbf{u}} = \frac{d\mathbf{u}}{dt} = \frac{d\mathbf{u}}{d\tau} \frac{d\tau}{dt} = \epsilon \frac{d\mathbf{u}}{d\tau} = \epsilon \mathbf{u}'$, where $' = \frac{d}{d\tau}$. In the same way we get $\dot{\mathbf{v}} = \epsilon \mathbf{v}'$ for the second equation. So the slow system becomes

$$\begin{cases} \epsilon \mathbf{u}' = g(\mathbf{u}, \mathbf{v}, \epsilon), \\ \mathbf{v}' = h(\mathbf{u}, \mathbf{v}, \epsilon), \end{cases} \quad (2.10)$$

The fast and the slow system are equivalent, but only as long as $\epsilon \neq 0$ holds. For both systems we can take the limit $\epsilon \rightarrow 0$, these limits are respectively given by

$$\begin{cases} \dot{\mathbf{u}} = g(\mathbf{u}, \mathbf{v}, 0), \\ \dot{\mathbf{v}} = 0, \end{cases} \quad (2.11)$$

and

$$\begin{cases} 0 = g(\mathbf{u}, \mathbf{v}, 0), \\ \mathbf{v}' = h(\mathbf{u}, \mathbf{v}, 0). \end{cases} \quad (2.12)$$

These systems are approximations for the full system where $\epsilon \neq 0$ holds, but where ϵ is sufficiently small. However, in both systems we miss information about one of the equations. The goal of geometric singular perturbation theory is to analyse and combine the dynamics of the two systems with limit $\epsilon \rightarrow 0$, which gives an insight to the dynamics of the full system (2.9). Because the limit sets are lower dimensional and we can analyse them in more details. And by combining this knowledge of the fast and slow pieces of orbits, which is obtained in the fast and slow limits, we can construct the global singular structures.

2.3.1 Fenichel's first theorem

We remark that system (2.12) describes the slow dynamics on the set $g(\mathbf{u}, \mathbf{v}, 0)$. This set is equal to the set of critical points of (2.11). The critical manifold \mathcal{M}_0 is defined as the l -dimensional manifold that is contained in the set $g(\mathbf{u}, \mathbf{v}, 0) = 0$. To get more knowledge of the full system we can analyse the slow dynamics on this manifold \mathcal{M}_0 , so we analyse the system $\mathbf{v}' = h(\mathbf{u}, \mathbf{v}, 0)$ on \mathcal{M}_0 . Fenichel's first theorem (2.3.1) says that if the manifold \mathcal{M}_0 is normally hyperbolic, it persists for $0 < \epsilon \ll 1$ as a manifold \mathcal{M}_ϵ with a slow flow on it. Before we state Fenichel's theorem we define normal hyperbolicity.

Definition 2.3.1. (*Normal hyperbolicity*) A manifold \mathcal{M} is called normally hyperbolic when the eigenvalues λ of the Jacobian $\frac{\partial g}{\partial \mathbf{u}}(\mathbf{u}, \mathbf{v}, 0)|_{\mathcal{M}}$ are uniformly bounded away from the imaginary axis (Hek, 2009).

Theorem 2.3.1. (Fenichel) *Suppose $\mathcal{M}_0 \subset \{g(\mathbf{u}, \mathbf{v}, 0) = 0\}$ is compact, possibly with boundary, and normally hyperbolic. Suppose g and h are smooth. Then for $\epsilon > 0$ and sufficiently small, there exists a manifold $\mathcal{M}_\epsilon, \mathcal{O}(\epsilon)$ close and diffeomorphic to \mathcal{M}_0 , that is locally invariant under the flow of the full problem (2.9) (Hek, 2009).*

The theorem states that under these conditions \mathcal{M}_ϵ is locally invariant under the flow of the full problem under these conditions, which means that orbits on this manifold can leave this manifold in the slow direction, via the the boundary of \mathcal{M}_ϵ , but via the directions not perpendicular to it (Hek, 2009). It also states that \mathcal{M}_ϵ is a small perturbation of $\mathcal{O}(\epsilon)$ of \mathcal{M}_0 .

2.3.2 Fenichel's second theorem

Fenichel's first theorem guarantees the existence of the slow manifold \mathcal{M}_0 and gives an $\mathcal{O}(\epsilon)$ approximation for the flow on it. The second theorem gives more information about the stable and unstable manifolds of \mathcal{M}_0 and \mathcal{M}_ϵ . It is already known that hyperbolic fixed points of ordinary differential equations persists under small perturbations, as well as their stable and unstable manifolds (Wiggins, 1990). This holds for the normally hyperbolic critical manifold \mathcal{M}_0 as well, this is stated in Fenichel's second theorem (2.3.2). In this theorem we require $\mathcal{M}_0 \subset g(\mathbf{u}, \mathbf{v}, 0) = 0$ to be a normally hyperbolic critical manifold, that has an $l + m$ -dimensional stable manifold $W^s(\mathcal{M}_0)$ and an $l + n$ -dimensional unstable manifold $W^u(\mathcal{M}_0)$, such that $m + n = k$ holds. This is the case whenever the Jacobian $\frac{\partial g}{\partial \mathbf{u}}(\mathbf{u}, \mathbf{v}, 0)|_{\mathcal{M}}$ has m eigenvalues with negative real part and n eigenvalues with positive real part.

Theorem 2.3.2. (Fenichel) *Suppose $\mathcal{M}_0 \subset \{g(\mathbf{u}, \mathbf{v}, 0) = 0\}$ is compact, possibly with boundary, and normally hyperbolic, and suppose f and g are smooth. Then for $\epsilon > 0$ and sufficiently small, there exists manifolds $W^s(\mathcal{M}_\epsilon)$ and $W^u(\mathcal{M}_\epsilon)$, that are $\mathcal{O}(\epsilon)$ close and diffeomorphic to $W^s(\mathcal{M}_0)$ and $W^u(\mathcal{M}_0)$, respectively, and that are locally invariant under the flow of (2.9) (Hek, 2009).*

The stable and unstable manifolds $W^s(\mathcal{M}_\epsilon)$ and $W^u(\mathcal{M}_\epsilon)$ also have respective dimensions $l + m$ and $l + n$.

In the next chapters of this thesis we apply this theory to our system (2.5).

2.4 Numerical schemes

We use geometric singular perturbation theory to analyse the system analytically. We would also like to reproduce the analytical findings numerically. We start by doing simulations in one

dimension, hence we look into system (2.8) We want to implement this system in our Matlab code. The Matlab function `pdepe` solves a system of partial differential equations that are parabolic or elliptic with one spatial variable x and time t (MATLAB, 2010).

For our numerical simulations we take the following domain $\Omega = [0, L] \subset \mathbb{R}$, with $L = 100$. We take the stepsize equal to stepsize $h = 0.2$ and our running time to $T = 500$. We implement these values in the Matlab code in A.1.1. We also defined our parameter values in this code. We saved all these values in parameter vector P . This is what the vector P looks like

$$P = (\alpha, a, \beta, b, \mu)^\top.$$

In this code we also call the function `pdepe` and plot the solution for different time values. In our theoretical calculations we used $\Omega = \mathbb{R}$, now we look at a finite domain. Before we can implement our system in our Matlab code we have to rewrite it in a form that the `pdepe` solver expects. The standard form that `pdepe` expects is

$$\omega \left(x, t, \mathbf{u}, \frac{\partial \mathbf{u}}{\partial x} \right) \frac{\partial \mathbf{u}}{\partial t} = x^{-m} \frac{\partial}{\partial x} \left[x^m \varphi \left(x, t, \mathbf{u}, \frac{\partial \mathbf{u}}{\partial x} \right) \right] + \psi \left(x, t, \mathbf{u}, \frac{\partial \mathbf{u}}{\partial x} \right) \quad (2.13)$$

Rewriting (2.8) to this form gives us the following variable, functions and constants

$$\mathbf{u} = \begin{pmatrix} F \\ S \end{pmatrix}, \quad m = 0, \quad \omega = 1, \quad \varphi = \begin{pmatrix} \frac{\partial F}{\partial x} \\ \frac{1}{\epsilon^2} \frac{\partial S}{\partial x} \end{pmatrix}, \quad \psi = \begin{pmatrix} F(\alpha - F - aS) \\ S(\beta - bF - \mu S) \end{pmatrix}.$$

We implemented this equation in the MATLAB code `eqn.m` given in A.1.2. We also have to define our initial conditions. Because we will be looking for a front solution we take fronts as initial conditions. Here we define the initial condition for forest biomass F_0 and savanna biomass S_0 .

$$F_0 := \frac{1}{2} \left(1 + \tanh \left(-x + \frac{L}{2} \right) \right), \quad S_0 := \frac{1}{2} \left(1 + \tanh \left(x - \frac{L}{2} \right) \right)$$

In figure 2.2 we plotted the graphs of these initial conditions.

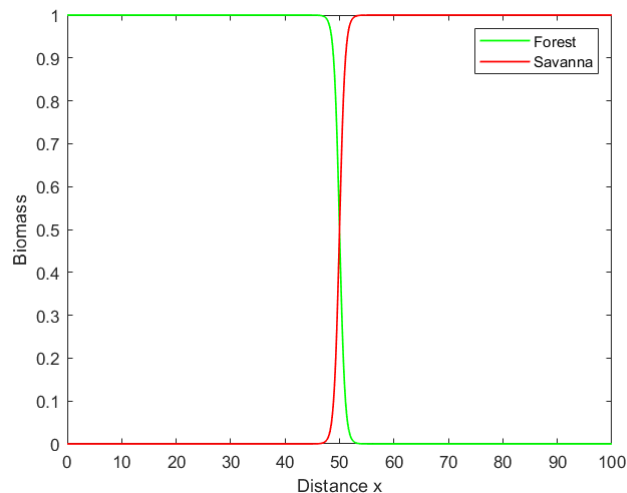


Figure 2.2: The green and the red plots represent the initial condition of the forest biomass and the savanna biomass respectively.

We implemented these functions in `initial.m` in A.1.3. Now we have almost set everything up in order to run the code. We still have to define the boundary conditions. We use Neumann boundary conditions, because we want zero flux at the boundaries. For problems posed on the interval $a \leq x \leq b$, the boundary conditions apply for all t and either $x = a$ or $x = b$. Matlab requires the boundary conditions to be of the form

$$p(x, t, \mathbf{u}) + q(x, t) \varphi \left(x, t, \mathbf{u}, \frac{\partial \mathbf{u}}{\partial x} \right) = 0.$$

Filling in \mathbf{u} and φ gives us the following system of equations

$$\begin{pmatrix} p_1(x, t, F, S) \\ p_2(x, t, F, S) \end{pmatrix} + \begin{pmatrix} q(x, t) \frac{\partial F}{\partial x} \\ q(x, t) \frac{1}{\epsilon^2} \frac{\partial S}{\partial x} \end{pmatrix} = \begin{pmatrix} 0 \\ 0 \end{pmatrix}$$

The domain that we consider is $[0, L]$. If we choose $\begin{pmatrix} p_1(x, t, F, S) \\ p_2(x, t, F, S) \end{pmatrix} \Big|_{x=0} = \begin{pmatrix} p_1(x, t, F, S) \\ p_2(x, t, F, S) \end{pmatrix} \Big|_{x=L} = \begin{pmatrix} 0 \\ 0 \end{pmatrix}$ and $q(x, t)|_{x=0} = q(x, t)|_{x=L} = 1$. Because if we choose p and q in this way we have zero flux at the boundary. These are the boundary conditions that we use

$$\frac{\partial F}{\partial x} \Big|_{x=0} = \frac{\partial S}{\partial x} \Big|_{x=0} = \frac{\partial F}{\partial x} \Big|_{x=L} = \frac{\partial S}{\partial x} \Big|_{x=L} = 0. \quad (2.14)$$

We implemented the boundary conditions in `bc.m` in A.1.4. Now we can call function `pdepe` with the line `sol = pdepe(m,@eqn,@initial,@bc,x,t,[],P)`.

Chapter 3

Analysis of the nonspatial model

3.1 Scaling of the system

We want to study system (1.1) to learn more about the savanna-forest boundary. This system has many parameters, but we can reduce this number. We start by reducing the number of parameters, because it makes analysing this system easier. We do this by scaling the system. Before we can do this, we rewrite the system a little. We also add two diffusion terms to the system, with diffusion coefficients D_F and D_S .

$$\begin{cases} \frac{\partial \hat{F}}{\partial \tau} = r_F \hat{F} \left(1 - \frac{\hat{F}}{K_F}\right) - \eta f_F \hat{S} \hat{F} - d_F \hat{F} + D_F \hat{\Delta} \hat{F} \\ \frac{\partial \hat{S}}{\partial \tau} = r_S \hat{S} \left(1 - \left(\frac{1}{K_S} + \frac{\eta f_S}{r_S}\right) \hat{S}\right) - d \hat{F} \hat{S} - d_S \hat{S} + D_S \hat{\Delta} \hat{S} \end{cases} \quad (3.1)$$

$\hat{\Delta}$ is the Laplace operator, which is equal to $\hat{\Delta} = \frac{\partial^2}{\partial \hat{x}^2} + \frac{\partial^2}{\partial \hat{y}^2}$. We want to make this system dimensionless. Because that way, we will have less parameters to deal with. Furthermore we can scale τ in such a way that the r_F term in the first equation disappears. Therefore we do choose the following scaling

$$F = \frac{1}{K_F} \hat{F}, \quad S = \left(\frac{1}{K_S} + \frac{\eta f_S}{r_S}\right) \hat{S}, \quad t = r_F \tau, \quad x = \hat{x} \sqrt{\frac{r_F}{D_F}}, \quad y = \hat{y} \sqrt{\frac{r_F}{D_F}}$$

By using the chain rule, we can express $\frac{\partial \hat{F}}{\partial \tau}$ in terms of t and our new variable f .

$$\begin{aligned} \frac{\partial \hat{F}}{\partial \tau} &= \frac{\partial \hat{F}}{\partial F} \frac{\partial F}{\partial \tau} \\ &= K_F \frac{\partial F}{\partial \tau} \\ &= K_F \frac{\partial F}{\partial t} \frac{\partial t}{\partial \tau} \\ &= r_F K_F \frac{\partial F}{\partial t}, \end{aligned}$$

Now we express $\frac{\partial \hat{S}}{\partial \tau}$ in terms of t and s in the same way

$$\frac{\partial \hat{S}}{\partial \tau} = \left(\frac{r_F}{\frac{1}{K_S} + \frac{\eta f_s}{r_S}} \right) \frac{\partial S}{\partial t}.$$

Next we want to rewrite the diffusion term in the \hat{F} equation

$$\begin{aligned} \hat{\Delta} \hat{F} &= \frac{\partial^2 \hat{F}}{\partial \hat{x}^2} + \frac{\partial^2 \hat{F}}{\partial \hat{y}^2} \\ &= \frac{\partial}{\partial \hat{x}} \left[\frac{\partial \hat{F}}{\partial \hat{x}} \right] + \frac{\partial}{\partial \hat{y}} \left[\frac{\partial \hat{F}}{\partial \hat{y}} \right] \\ &= \frac{\partial}{\partial \hat{x}} \left[\frac{\partial \hat{F}}{\partial F} \frac{\partial F}{\partial \hat{x}} \right] + \frac{\partial}{\partial \hat{y}} \left[\frac{\partial \hat{F}}{\partial F} \frac{\partial F}{\partial \hat{y}} \right] \\ &= K_F \left(\frac{\partial}{\partial \hat{x}} \left[\frac{\partial F}{\partial \hat{x}} \right] + \frac{\partial}{\partial \hat{y}} \left[\frac{\partial F}{\partial \hat{y}} \right] \right) \\ &= K_F \left(\frac{\partial}{\partial \hat{x}} \left[\frac{\partial F}{\partial x} \frac{\partial x}{\partial \hat{x}} \right] + \frac{\partial}{\partial \hat{y}} \left[\frac{\partial F}{\partial y} \frac{\partial y}{\partial \hat{y}} \right] \right) \\ &= K_F \sqrt{\frac{r_F}{D_F}} \left(\frac{\partial}{\partial \hat{x}} \left[\frac{\partial F}{\partial x} \right] + \frac{\partial}{\partial \hat{y}} \left[\frac{\partial F}{\partial y} \right] \right) \\ &= K_F \frac{r_F}{D_F} \left(\frac{\partial^2 F}{\partial x^2} + \frac{\partial^2 F}{\partial y^2} \right) \\ &= K_F \frac{r_F}{D_F} \Delta F. \end{aligned}$$

In the same manner we find

$$\hat{\Delta} \hat{S} = \left(\frac{1}{\frac{1}{K_S} + \frac{\eta f_s}{r_S}} \right) \frac{r_F}{D_F} \Delta S.$$

If we substitute these derivatives, $\hat{F} = K_F F$ and $\hat{S} = \left(\frac{1}{\frac{1}{K_S} + \frac{\eta f_s}{r_S}} \right) S$ into (3.1), the equations only depend on the variables F and S .

$$\left\{ \begin{array}{l} r_F K_F \frac{\partial F}{\partial t} = r_F K_F F (1 - F) - \eta f_F K_F \left(\frac{1}{\frac{1}{K_S} + \frac{\eta f_S}{r_S}} \right) S F - d_F K_F F + K_F r_F \Delta F \\ \left(\frac{r_F}{\frac{1}{K_S} + \frac{\eta f_S}{r_S}} \right) \frac{\partial S}{\partial t} = \left(\frac{r_S}{\frac{1}{K_S} + \frac{\eta f_S}{r_S}} \right) S (1 - S) - \left(\frac{d K_F}{\frac{1}{K_S} + \frac{\eta f_S}{r_S}} \right) F S \\ \quad - \left(\frac{d_S}{\frac{1}{K_S} + \frac{\eta f_S}{r_S}} \right) S + \left(\frac{r_F}{\frac{1}{K_S} + \frac{\eta f_S}{r_S}} \right) \frac{D_S}{D_F} \Delta S \end{array} \right. \quad (3.2)$$

We can simplify these equations by dividing the first equation by $r_F K_F$ and the second on by $\frac{r_F}{\frac{1}{K_S} + \frac{\eta f_S}{r_S}}$.

$$\left\{ \begin{array}{l} \frac{\partial F}{\partial t} = F (1 - F) - \left(\frac{\eta f_F}{r_F \left(\frac{1}{K_S} + \frac{\eta f_S}{r_S} \right)} \right) S F - \frac{d_F}{r_F} F + \Delta F \\ \frac{\partial S}{\partial t} = \frac{r_S}{r_F} S (1 - S) - \frac{d K_F}{r_F} F S - \frac{d_S}{r_F} S + \frac{D_S}{D_F} \Delta S \end{array} \right. \quad (3.3)$$

We can easily simplify these equations by defining the following constants

$$\mu = \frac{r_S}{r_F}, \quad b = \frac{d K_F}{r_F}, \quad n = \frac{d_S}{r_F}, \quad a = \frac{\eta f_F}{r_F \left(\frac{1}{K_S} + \frac{\eta f_S}{r_S} \right)}, \quad m = \frac{d_F}{r_F}, \quad \delta = \frac{D_S}{D_F}.$$

Substituting them gives us the scaled system below.

$$\left\{ \begin{array}{l} \frac{\partial F}{\partial t} = F(1 - F) - a S F - m F + \Delta F \\ \frac{\partial S}{\partial t} = \mu S(1 - S) - b F S - n S + \delta \Delta S. \end{array} \right. \quad (3.4)$$

We can rewrite this system to (2.1), then we take $\Delta F = \Delta S = 0$. We also choose $\alpha = 1 - m$ and $\beta = \mu - n$, later on in this thesis we show that both of these parameters must be positive.

3.1.1 Critical points and their character

To determine the critical points, we first have to determine the nullclines. These are the lines on which $A(f, s) = 0$ or $B(f, s) = 0$ holds. $A(f, s) = 0$ gives us

$$f = 0 \text{ or } f + as = \alpha,$$

setting the second equation to zero gives

$$s = 0 \text{ or } bf + \mu s = \beta.$$

Combining these nullclines gives us the critical points

$$(0, 0), \left(0, \frac{\beta}{\mu}\right), (\alpha, 0), (f^*, s^*) = \left(\frac{a\beta - \alpha\mu}{ab - \mu}, \frac{\alpha b - \beta}{ab - \mu}\right).$$

We would like to know if these points are stable or unstable, this will yield information about solutions of our equation. Our goal is to find a front solution, hence we are looking for a heteroclinic connection from $(\alpha, 0)$ to $\left(0, \frac{\beta}{\mu}\right)$. These points represent the pure forest state and the pure grass state respectively. Because we want to find a bi-stable front, we want to choose our parameters in such a way that $(\alpha, 0)$ and $\left(0, \frac{\beta}{\mu}\right)$ are both stable nodes.

We continue with determining the character and stability of the equilibria. For this we look at the linearised system of (2.1). The linearised system yields primary information about the behavior of system (2.1) (Meiss, 2017). We compute the Jacobian matrix $J(f, s)$ for (2.1)

$$J(f, s) = \begin{pmatrix} \frac{\partial A}{\partial f} & \frac{\partial A}{\partial s} \\ \frac{\partial B}{\partial f} & \frac{\partial B}{\partial s} \end{pmatrix} = \begin{pmatrix} -2f - as + \alpha & -af \\ -bs & -2\mu s - bf + \beta \end{pmatrix}.$$

If we evaluate the Jacobian in the point critical point $(0, 0)$ we get

$$J(0, 0) = \begin{pmatrix} \alpha & 0 \\ 0 & \beta \end{pmatrix}$$

Because this is a diagonal matrix, we can directly see that the eigenvalues are α and β , which are both positive values. This means that $(0, 0)$ is an unstable node. Now we evaluate the Jacobian in $\left(0, \frac{\beta}{\mu}\right)$, we get:

$$J\left(0, \frac{\beta}{\mu}\right) = \begin{pmatrix} -\frac{a\beta}{\mu} + \alpha & 0 \\ -\frac{b\beta}{\mu} & -\beta \end{pmatrix}.$$

This is a lower triangular matrix, hence we know that the eigenvalues are equal to the values on the diagonal. So the eigenvalues are equal to $\lambda_1 = -\frac{a\beta}{\mu} + \alpha$ and $\lambda_2 = -\beta$. We want both eigenvalues to be negative, because then we know that the critical point is a stable node. In order for λ_2 to be negative β must be positive. For λ_1 we distinguish two cases

$$\lambda_1 = -\frac{a\beta}{\mu} + \alpha \begin{cases} < 0, & \text{if } \frac{\alpha}{a} < \frac{\beta}{\mu}, \text{ so } \left(0, \frac{\beta}{\mu}\right) \text{ is a stable node,} \\ > 0, & \text{if } \frac{\alpha}{a} > \frac{\beta}{\mu}, \text{ so } \left(0, \frac{\beta}{\mu}\right) \text{ is a saddle.} \end{cases}$$

So we conclude that the condition $\frac{\alpha}{a} < \frac{\beta}{\mu}$ must hold.

For $(\alpha, 0)$ we have:

$$J(\alpha, 0) = \begin{pmatrix} -\alpha & -a\alpha \\ 0 & -b\alpha + \beta \end{pmatrix}.$$

Now we have a upper triangular matrix, which also has its eigenvalues on the diagonal. Hence the eigenvalues are equal to $\lambda_1 = -\alpha$ and $\lambda_2 = -b\alpha + \beta$. Just like for the previous critical value we want both eigenvalues to be negative. This can only hold when $\alpha > 0$ holds, because then we have $\lambda_1 < 0$. Again we distinguish two separate cases

$$\lambda_2 = -b\alpha + \beta \begin{cases} < 0, & \text{if } \frac{\beta}{b} < \alpha, \text{ so } (\alpha, 0) \text{ is a stable node,} \\ > 0, & \text{if } \frac{\beta}{b} > \alpha, \text{ so } (\alpha, 0) \text{ is a saddle.} \end{cases}$$

Hence we also choose $\frac{\beta}{b} < \alpha$. Lastly we evaluate the Jacobian in (f^*, s^*)

$$\begin{aligned} J(f^*, s^*) &= \begin{pmatrix} -2f^* - as^* + \alpha & -af^* \\ -bs^* & -2\mu s^* - bf^* + \beta \end{pmatrix} \\ &= \begin{pmatrix} -f^* & -af^* \\ -bs^* & -\mu s^* \end{pmatrix} \end{aligned}$$

The last equality holds because, we know that the equalities $f^* + as^* = \alpha$ and $bf^* + \mu s^* = \beta - 1$ hold for this critical point. To determine the eigenvalues we first compute the characteristic polynomial

$$\begin{aligned} \det(\lambda I - J(f^*, s^*)) &= \begin{vmatrix} \lambda + f^* & af^* \\ bs^* & \lambda + \mu s^* \end{vmatrix} \\ &= \lambda^2 + \lambda(f^* + \mu s^*) + \mu f^* s^* - abf^* s^*. \end{aligned}$$

Setting the characteristic polynomial to zero gives us the eigenvalues:

$$\lambda_{\pm} = -\frac{1}{2}(f^* + \mu s^*) \pm \frac{1}{2}\sqrt{(f^* + \mu s^*)^2 - 4(\mu f^* s^* - abf^* s^*)}$$

We notice that for (f^*, s^*) we also have two possible characters

$$\begin{cases} \lambda_- < 0 < \lambda_+, & \text{if } ab > \mu, \text{ so } (f^*, s^*) \text{ is a saddle,} \\ \lambda_{\pm} < 0, & \text{if } ab < \mu, \text{ so } (f^*, s^*) \text{ is a stable node.} \end{cases}$$

We have already shown that $\frac{\alpha}{a} < \frac{\beta}{\mu}$ holds. We can rewrite this condition into $\mu < \frac{\beta a}{\alpha}$. We also know that $\frac{\beta}{b} < \alpha$ holds, which we can rewrite into $b > \frac{\beta}{\alpha}$. Combining these conditions gives us $\mu < ab$, thus we know that λ_- is negative and that λ_+ is positive. Thus we can conclude that (f^*, s^*) is a saddle.

In this section we found the characters of the different critical values. This gives us a lot of information about the behavior of system (2.1). The next step is to determine the phase planes for different parameter values.

3.1.2 Phase planes

Now that we know the characters of the critical values, we can plot the phase plane of system (2.1). The critical point $(0, 0)$ is always an unstable node. This is not true for the other critical values, we saw that $\left(0, \frac{\beta}{\mu}\right)$ and $(\alpha, 0)$ switch characters at the parameter values $\frac{\alpha}{a} = \frac{\beta}{\mu}$ and $\frac{\beta}{b} = \alpha$ respectively. That is why the phase plane looks different in these four cases.

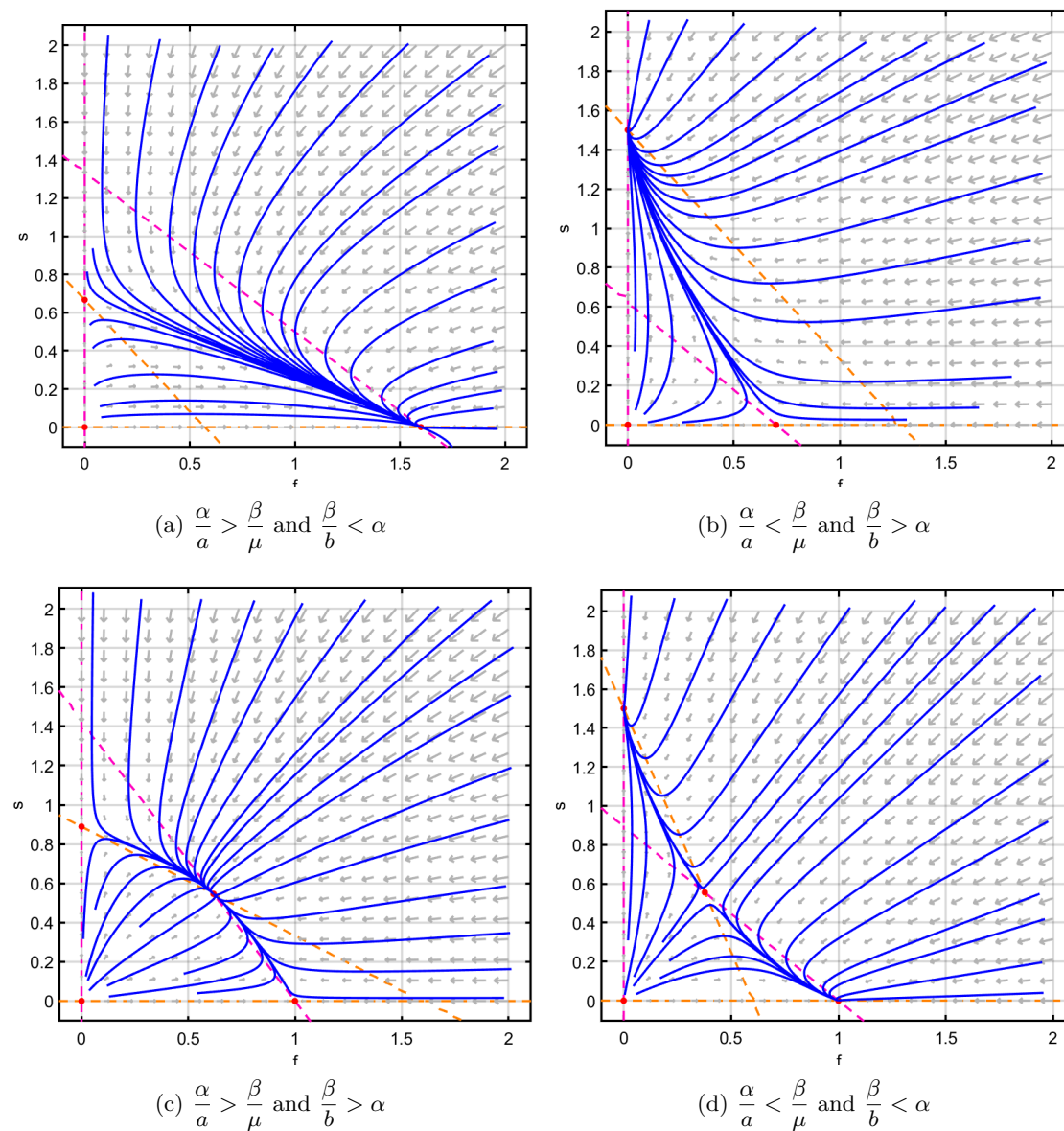


Figure 3.1: The phase planes of system (2.1) for four different choices of parameter values.

The orange and the pink nullclines represent $\frac{df}{dt} = 0$ and $\frac{ds}{dt} = 0$ respectively.

In figures (3.1a) and (3.1b) the nontrivial critical point (f^*, s^*) does not lie in the first quadrant. In figure 3.1a $(0, \beta/\mu)$ is a saddle and $(\alpha, 0)$ is a stable node. For figure 3.1b the opposite holds, here holds that $(0, \beta/\mu)$ is a stable node and that $(\alpha, 0)$ is a saddle. $(\alpha, 0)$ and $(0, \beta/\mu)$ are the only stable nodes in the first quadrant in the phase planes (3.1a) and (3.1b) respectively. Furthermore we can prove that all solutions remain bounded and that there cannot exist any periodic orbits. Hence we know that all solutions of (2.1) approach these critical points as t approaches infinity (Braun, 1983).

In the case of figures (3.1c) and (3.1d) (f^*, s^*) does lie in the first quadrant. In figure 3.1c this critical point is a stable node and both $(0, \beta/\mu)$ and $(\alpha, 0)$ are saddles. In figure 3.1d it is the other way around, there we have that (f^*, s^*) is a saddle and $(0, \beta/\mu)$ and $(\alpha, 0)$ are stable nodes. We are interested in this case, where the system exhibits bistability. Only in this case a connection from $(\alpha, 0)$ to $(0, \beta/\mu)$ is possible.

We are also curious to see if there is a possibility that a connection between one of the fixed points $(\alpha, 0)$ and $(0, \beta/\mu)$ and the mixed state $(f^*, s^*) = \left(\frac{a\beta - \alpha\mu}{ab - \mu}, \frac{\alpha b - \beta}{ab - \mu} \right)$ exists. For a connection between $(\alpha, 0)$ and (f^*, s^*) , both of these fixed points need to be stable. Hence we know that the conditions $\frac{\beta}{b} < \alpha$ and $ab < \mu$ must hold. This implies that the inequalities $\alpha b - \beta > 0$ and $ab - \mu < 0$ hold. Thus we know that s^* is negative. So even if there exists a heteroclinic connection between $(\alpha, 0)$ and (f^*, s^*) , this would be ecologically irrelevant. We have the same problem with the connection between $(0, \beta/\mu)$ and (f^*, s^*) . Stability for both of these fixed points requires $\frac{\alpha}{a} < \frac{\beta}{\mu}$ and $ab < \mu$. Which implies $\alpha\beta - \mu\alpha > 0$ and $ab - \mu < 0$. In this case we have $f^* < 0$, which makes this heteroclinic connection ecologically irrelevant as well.

3.2 Spatially extended savanna-forest model

In this section we want to analyse the spatially extended model (2.3) that we defined in section 2.1. We will look at the stationary system that we have rewritten into a four dimensional system of ordinary differential equations (2.5).

3.2.1 Critical points and their character

We start by determining the critical points, to do this we determine the nullclines. In order to determine the nullclines, we set all four equations in (2.5) equal to zero. $U(f, p, s, q) = 0$ gives that $p = 0$ must hold and $V(f, p, s, q) = 0$ implies that $f = 0$ or $f = \alpha - as$. $W(f, p, s, q) = 0$ and $Z(f, p, s, q) = 0$ give nullclines $q = 0$ and $s \in \left\{ 0, \frac{\beta - bf}{\mu} \right\}$ respectively. From combining these nullclines we can conclude that the system has these four critical points:

$$(0, 0, 0, 0), \left(0, 0, \frac{\beta}{\mu}, 0 \right), (\alpha, 0, 0, 0), (f^*, 0, s^*, 0).$$

Where f^* and s^* are the solutions of the system of these two equations

$$\begin{cases} f = \alpha - as \\ s = \frac{\beta - bf}{\mu} \end{cases}$$

Solving these equations gives us the non-trivial critical point

$$(f^*, 0, s^*, 0) = \left(\frac{a\mu - a - \beta + m\mu}{ab - \mu}, 0, \frac{b - bm - \mu + n}{ab - \mu}, 0 \right).$$

Just like for system (2.1) we want to determine the characters of the critical points. So we look at the linearised system of (2.5) by computing the Jacobian $J(f, p, s, q)$ of system (2.5)

$$J(f, p, s, q) = \begin{pmatrix} \frac{\partial U}{\partial V} & \frac{\partial U}{\partial V} & \frac{\partial U}{\partial V} & \frac{\partial U}{\partial V} \\ \frac{\partial f}{\partial W} & \frac{\partial p}{\partial W} & \frac{\partial s}{\partial W} & \frac{\partial q}{\partial W} \\ \frac{\partial f}{\partial Z} & \frac{\partial p}{\partial Z} & \frac{\partial s}{\partial Z} & \frac{\partial q}{\partial Z} \\ \frac{\partial f}{\partial f} & \frac{\partial p}{\partial p} & \frac{\partial s}{\partial s} & \frac{\partial q}{\partial q} \end{pmatrix} = \begin{pmatrix} 0 & 1 & 0 & 0 \\ 2f + as - \alpha & 0 & af & 0 \\ 0 & 0 & 0 & \epsilon \\ \epsilon bs & 0 & \epsilon(2\mu s + bf - \beta) & 0 \end{pmatrix}.$$

We start by evaluating the Jacobian in the trivial critical point $(0, 0, 0, 0)$.

$$J(0, 0, 0, 0) = \begin{pmatrix} 0 & 1 & 0 & 0 \\ -\alpha & 0 & 0 & 0 \\ 0 & 0 & 0 & \epsilon \\ 0 & 0 & -\epsilon\beta & 0 \end{pmatrix}.$$

We determine the characteristic polynomial of this matrix.

$$\begin{aligned} \det(\lambda I - J(0, 0, 0, 0)) &= \begin{vmatrix} \lambda & -1 & 0 & 0 \\ \alpha & \lambda & 0 & 0 \\ 0 & 0 & \lambda & -\epsilon \\ 0 & 0 & \epsilon\beta & \lambda \end{vmatrix} \\ &= \lambda \begin{vmatrix} \lambda & 0 & 0 \\ 0 & \lambda & -\epsilon \\ 0 & \epsilon\beta & \lambda \end{vmatrix} + \begin{vmatrix} \alpha & 0 & 0 \\ 0 & \lambda & -\epsilon \\ 0 & \epsilon\beta & \lambda \end{vmatrix} \\ &= (\lambda^2 + \alpha) \begin{vmatrix} \lambda & -\epsilon \\ \epsilon\beta & \lambda \end{vmatrix} \\ &= (\lambda^2 + \alpha) (\lambda^2 + \epsilon^2\beta) \end{aligned}$$

Setting the characteristic polynomial to zero gives us the two eigenvalues $\lambda_{1\pm} = \pm\sqrt{-\alpha}$ and $\lambda_{2\pm} = \pm\epsilon\sqrt{-\beta}$. We notice that $\lambda_{1\pm}, \lambda_{2\pm} \in i\mathbb{R}$ holds, because we know that $\alpha, \beta > 0$ holds.

Evaluating $\left(0, 0, \frac{\beta}{\mu}, 0\right)$ in the Jacobian gives us the following matrix

$$J\left(0, 0, \frac{\beta}{\mu}, 0\right) = \begin{pmatrix} 0 & 1 & 0 & 0 \\ a\frac{\beta}{\mu} - \alpha & 0 & 0 & 0 \\ 0 & 0 & 0 & \epsilon \\ \epsilon b\frac{\beta}{\mu} & 0 & \epsilon(2\beta - \beta) & 0 \end{pmatrix} = \begin{pmatrix} 0 & 1 & 0 & 0 \\ a\frac{\beta}{\mu} - \alpha & 0 & 0 & 0 \\ 0 & 0 & 0 & \epsilon \\ \epsilon b\frac{\beta}{\mu} & 0 & \epsilon\beta & 0 \end{pmatrix}.$$

We want to determine its eigenvalues, to do this we first determine the characteristic polynomial.

$$\begin{aligned}
\det\left(\lambda I - J\left(0, 0, \frac{\beta}{\mu}, 0\right)\right) &= \begin{vmatrix} \lambda & -1 & 0 & 0 \\ -a\frac{\beta}{\mu} + \alpha & \lambda & 0 & 0 \\ 0 & 0 & \lambda & -\epsilon \\ \epsilon b\frac{-\beta}{\mu} & 0 & -\epsilon\beta & \lambda \end{vmatrix} \\
&= \lambda \begin{vmatrix} \lambda & 0 & 0 \\ 0 & \lambda & -\epsilon \\ 0 & -\epsilon\beta & \lambda \end{vmatrix} + \begin{vmatrix} -a\frac{\beta}{\mu} + \alpha & 0 & 0 \\ 0 & \lambda & -\epsilon \\ \epsilon b\frac{-\beta}{\mu} & -\epsilon\beta & \lambda \end{vmatrix} \\
&= \left(\lambda^2 - a\frac{\beta}{\mu} + \alpha\right) \begin{vmatrix} \lambda & -\epsilon \\ -\epsilon\beta & \lambda \end{vmatrix} \\
&= \left(\lambda^2 - a\frac{\beta}{\mu} + \alpha\right) (\lambda^2 - \epsilon^2\beta)
\end{aligned}$$

Setting this expression to zero gives eigenvalues $\lambda_{1\pm} = \pm\sqrt{\frac{a\beta}{\mu} - \alpha}$ and $\lambda_{2\pm} = \pm\epsilon\sqrt{\beta}$. We know that $\frac{\alpha}{a} < \frac{\beta}{\mu}$ holds, thus we can conclude that $\lambda_{1-} < 0 < \lambda_{1+}$ must hold. We have also shown that $\beta > 0$ holds, hence we know $\lambda_{2-} < 0 < \lambda_{2+}$ must hold.

We continue like this for the other two critical values. Evaluating $(\alpha, 0, 0, 0)$ in $J(f, p, s, q)$ gives

$$J(\alpha, 0, 0, 0) = \begin{pmatrix} 0 & 1 & 0 & 0 \\ 2\alpha - \alpha & 0 & a\alpha & 0 \\ 0 & 0 & 0 & \epsilon \\ 0 & 0 & \epsilon(b\alpha - \beta) & 0 \end{pmatrix} = \begin{pmatrix} 0 & 1 & 0 & 0 \\ \alpha & 0 & a\alpha & 0 \\ 0 & 0 & 0 & \epsilon \\ 0 & 0 & \epsilon(b\alpha - \beta) & 0 \end{pmatrix}.$$

Then we determine the characteristic polynomial.

$$\begin{aligned}
\det(\lambda I - J(0, 0, 0, 0)) &= \begin{vmatrix} \lambda & -1 & 0 & 0 \\ -\alpha & \lambda & -a\alpha & 0 \\ 0 & 0 & \lambda & -\epsilon \\ 0 & 0 & +\epsilon(-b\alpha + \beta) & \lambda \end{vmatrix} \\
&= \lambda \begin{vmatrix} \lambda & -a\alpha & 0 \\ 0 & \lambda & -\epsilon \\ 0 & +\epsilon(-b\alpha + \beta) & \lambda \end{vmatrix} + \begin{vmatrix} -\alpha & -a\alpha & 0 \\ 0 & \lambda & -\epsilon \\ 0 & +\epsilon(-b\alpha + \beta) & \lambda \end{vmatrix} \\
&= (\lambda^2 - \alpha) \begin{vmatrix} \lambda & -\epsilon \\ +\epsilon(-b\alpha + \beta) & \lambda \end{vmatrix} - a\alpha(\lambda + 1) \begin{vmatrix} 0 & -\epsilon \\ 0 & \lambda \end{vmatrix} \\
&= (\lambda^2 - \alpha)(\lambda^2 + \epsilon^2(-b\alpha + \beta))
\end{aligned}$$

So we find the eigenvalues $\lambda_{1\pm} = \pm\sqrt{\alpha}$ and $\lambda_{2\pm} = \pm\epsilon\sqrt{b\alpha - \beta}$. We can directly see that $\lambda_{1-} < 0 < \lambda_{1+}$ holds. The same holds for the other eigenvalues $\lambda_{2-} < 0 < \lambda_{2+}$, because we have already shown that $\frac{\beta}{b} < \alpha$ holds.

Lastly we want to determine the character of critical point $(f^*, 0, s^*, 0)$. the evaluated Jacobian

in this point is the following.

$$J(f^*, 0, s^*, 0) = \begin{pmatrix} 0 & 1 & 0 & 0 \\ 2f^* + as^* - \alpha & 0 & af^* & 0 \\ 0 & 0 & 0 & \epsilon \\ \epsilon bs^* & 0 & \epsilon(2\mu s^* + bf^* - \beta) & 0 \end{pmatrix} = \begin{pmatrix} 0 & 1 & 0 & 0 \\ f^* & 0 & af^* & 0 \\ 0 & 0 & 0 & \epsilon \\ \epsilon bs^* & 0 & \epsilon\mu s^* & 0 \end{pmatrix}$$

The last equality holds because equalities $f^* + as^* = \alpha$ and $bf^* + \mu s^* = \beta$ hold for this critical point. Now we can determine the characteristic polynomial of this evaluated Jacobian.

$$\begin{aligned} \det(\lambda I - J(f^*, 0, s^*, 0)) &= \begin{vmatrix} \lambda & -1 & 0 & 0 \\ -f^* & \lambda & -af^* & 0 \\ 0 & 0 & \lambda & -\epsilon \\ -\epsilon bs^* & 0 & -\epsilon\mu s^* & \lambda \end{vmatrix} \\ &= \lambda \begin{vmatrix} \lambda & -af^* & 0 \\ 0 & \lambda & -\epsilon \\ 0 & -\epsilon\mu s^* & \lambda \end{vmatrix} + \begin{vmatrix} -f^* & -af^* & 0 \\ 0 & \lambda & -\epsilon \\ -\epsilon bs^* & -\epsilon\mu s^* & \lambda \end{vmatrix} \\ &= (\lambda^2 - f^*) \begin{vmatrix} \lambda & -\epsilon \\ -\epsilon\mu s^* & \lambda \end{vmatrix} + af^* \lambda \begin{vmatrix} 0 & -\epsilon \\ 0 & \lambda \end{vmatrix} + af^* \begin{vmatrix} 0 & -\epsilon \\ -\epsilon bs^* & \lambda \end{vmatrix} \\ &= (\lambda^2 - f^*)(\lambda^2 - \epsilon^2\mu s^*) - \epsilon^2 ab f^* s^* \\ &= \lambda^4 - (f^* + \epsilon^2\mu s^*)\lambda^2 + \epsilon^2 f^* s^* (\mu - ab) \end{aligned}$$

If we define $\sigma = \lambda^2$, we get the following quadratic expression for the characteristic polynomial.

$$\det(\lambda I - J(f^*, 0, s^*, 0)) = \sigma^2 - (f^* + \epsilon^2\mu s^*)\sigma + \epsilon^2 f^* s^* (\mu - ab)$$

Setting this to zero gives us the following expression for σ

$$\sigma_{\pm} = \frac{1}{2}(f^* + \epsilon^2\mu s^*) \pm \frac{1}{2}\sqrt{(f^* + \epsilon^2\mu s^*)^2 - 4\epsilon^2 f^* s^* (\mu - ab)}$$

If we substitute λ back into the expression and take the square roots of the left- and the right hand side we get the following four eigenvalues

$$\begin{aligned} \lambda_{+\pm} &= \pm \sqrt{\frac{1}{2}(f^* + \epsilon^2\mu s^*) + \frac{1}{2}\sqrt{(f^* + \epsilon^2\mu s^*)^2 - 4\epsilon^2 f^* s^* (\mu - ab)}} \\ \lambda_{-\pm} &= \pm \sqrt{\frac{1}{2}(f^* + \epsilon^2\mu s^*) - \frac{1}{2}\sqrt{(f^* + \epsilon^2\mu s^*)^2 - 4\epsilon^2 f^* s^* (\mu - ab)}}. \end{aligned}$$

We have already shown that $\mu > ab$ holds, hence we can conclude $\lambda_{+\pm} > 0$, $\lambda_{-\pm} < 0$.

In this four dimensional space we are looking for a heteroclinic connection from $(\alpha, 0, 0, 0)$ to $(0, 0, \frac{\beta}{\mu}, 0)$. This connection is a front connection between the stable background states. These background states are the pure trees and pure grass states. The corresponding critical points for system 2.8 are $(\alpha, 0)$ and $(\frac{\beta}{\mu}, 0)$. We have already determined that both $(\alpha, 0, 0, 0)$ and $(0, 0, \frac{\beta}{\mu}, 0)$ have two positive- and negative eigenvalues for system (2.5). Hence the stable- and unstable manifold of both of these critical points are two dimensional. We have also shown that

$(\alpha, 0)$ and $\left(\frac{\beta}{\mu}, 0\right)$ are stable as solution of the reaction ODE (2.1). Then we can apply lemma (2.2.2), which says that $(\alpha, 0)$ and $\left(\frac{\beta}{\mu}, 0\right)$ is stable as solution of (2.3). Hence we can talk about a bi-stable front connection.

Chapter 4

Constructing traveling fronts

The analysis of a system of four ordinary differential equations can be very complex. That is why we want to apply geometric singular perturbation theory. System (2.7) has a clear separation in spatial scales and is of the form (2.9). The functions in (2.9) are defined as follows in our case

$$\begin{aligned} g(\mathbf{u}, \mathbf{v}, \epsilon) &= g(f, p, s, q) = \begin{pmatrix} p \\ -cp + f(f + as - \alpha) \end{pmatrix} \\ h(\mathbf{u}, \mathbf{v}, \epsilon) &= h(f, p, s, q) = \begin{pmatrix} q \\ -\epsilon cq + s(bf + \mu s - \beta) \end{pmatrix}, \end{aligned} \quad (4.1)$$

with $\mathbf{u} = (f, p)^\top$, $\mathbf{v} = (s, q)^\top$. The functions f and g must be at least C^1 , which holds for functions (4.1).

System (2.9) is called the fast system and ξ is called the fast scale. To get the slow system, we introduce a change the slow scale $\chi = \epsilon\xi$. In order to rewrite this system in terms of χ we determine the derivatives with respect to χ . Using the chain rule we get $\frac{d\mathbf{u}}{d\xi} = \epsilon \frac{d\mathbf{u}}{d\chi}$ and

$\frac{d\mathbf{v}}{d\xi} = \epsilon \frac{d\mathbf{v}}{d\chi}$, thus the slow system becomes

$$\begin{cases} \epsilon \frac{df}{d\chi} = p \\ \epsilon \frac{dp}{d\chi} = -cp + f(f - \alpha + as) \\ \frac{ds}{d\chi} = q \\ \frac{dq}{d\chi} = -\epsilon cq + s(\mu s - \beta + bf). \end{cases} \quad (4.2)$$

4.1 The fast and slow limits

Now we can determine the fast and the slow limits (2.11) and (2.12). Taking the limit $\epsilon \rightarrow 0$ of (2.7) gives the following fast limit

$$\begin{cases} \frac{df}{d\xi} = p \\ \frac{dp}{d\xi} = -cp + f(f - \alpha + as) \\ \frac{ds}{d\xi} = 0 \\ \frac{dq}{d\xi} = 0. \end{cases} \quad (4.3)$$

We can determine the slow limit by taking $\epsilon \rightarrow 0$ of system (4.2)

$$\begin{cases} 0 = p \\ 0 = -cp + f(f + as - \alpha) \\ \frac{ds}{d\chi} = q \\ \frac{dq}{d\chi} = s(bf + \mu s - \beta). \end{cases} \quad (4.4)$$

These limits are approximations for the full system where $\epsilon > 0$ holds. These limit systems are only two dimensional instead of four, so we can analyse them in more detail. But the disadvantage is that both systems miss information about two of the equations. We use geometric singular perturbation theory to analyse and combine the dynamics of systems (4.3) and (4.4), which gives an insight in the dynamics of the full system (2.7).

The reduced system (4.4) is a dynamical system on the sets

$$\mathcal{M} = \{(f, p, s, q) \in \mathbb{R}^4 : p = 0, f(f + as - \alpha) = 0, s \geq 0, q \in \mathbb{R}\}.$$

In the rest of this thesis we refer to \mathcal{M} as critical manifolds. In section 4.2 we define these manifolds explicitly.

4.2 Fast sub-system

Note that $\frac{ds}{d\xi} = 0$ holds in the fast limit (4.3). Thus we know that $s(\xi)$ must be a constant function $s(\xi) \equiv s_0$. So we can write down the following system

$$\begin{cases} \frac{df}{d\xi} = p, & =: C(f, p) \\ \frac{dp}{d\xi} = -cp + f(f + as_0 - \alpha) & =: D(f, p). \end{cases} \quad (4.5)$$

This describes system (4.3) together with $\frac{ds}{d\xi} = 0$ and $\frac{dq}{d\xi} = 0$. We are going to analyse system (4.5) to learn more about the fast dynamics.

4.2.1 Critical points and their character

We want to determine the critical points of system (4.5), in order to do this we first determine its nullclines. $C(f, p) = 0$ gives $p = 0$ and $D(f, p) = 0$ together with $p = 0$ gives $f = 0$ or $f = \alpha - as_0$. Combining these equations gives us two critical points, $(0, 0)$ and $(\alpha - as_0, 0)$. This also gives us the following critical manifolds for system system (2.7) with $\epsilon \rightarrow 0$.

$$\begin{aligned}\mathcal{M}_0^0 &= \{(f, p, s, q) \mid f = 0, p = 0, s \geq 0, q \in \mathbb{R}\}, \\ \mathcal{M}_0^+ &= \{(f, p, s, q) \mid f = \alpha - as, p = 0, s \geq 0, q \in \mathbb{R}\}.\end{aligned}\tag{4.6}$$

We want to look at linearised the system. So first we determine the Jacobi matrix $J(f, p)$

$$J(f, p) = \begin{pmatrix} \frac{\partial C}{\partial f} & \frac{\partial C}{\partial p} \\ \frac{\partial D}{\partial f} & \frac{\partial D}{\partial p} \end{pmatrix} = \begin{pmatrix} 0 & 1 \\ 2f + as_0 - \alpha & -c \end{pmatrix}.$$

We start by evaluating the Jacobian in the trivial critical point

$$J(0, 0) = \begin{pmatrix} 0 & 1 \\ as_0 - \alpha & -c \end{pmatrix}.\tag{4.7}$$

We determine the characteristic polynomial in order to find the eigenvalues. We determine the characteristic polynomial in the same way as we did in section 3 a couple of times. For this evaluated Jacobian it's equal to $\lambda^2 + c\lambda + \alpha - as_0$. Setting this expression to zero gives us two eigenvalues $\lambda_{\pm} = \frac{1}{2} \left(-c \pm \sqrt{c^2 - 4(\alpha - as_0)} \right)$. We remark that $(0, 0)$ can have different characters depending on the parameter choices. We have a few different cases. For $c^2 > 4(\alpha - as_0)$ the expression in the square root is positive, otherwise it is negative. We get the following possibilities

$$\left\{ \begin{array}{l} \text{If } s_0 > \frac{\alpha}{a} \quad \lambda_- < 0 < \lambda_+, \text{ so } (0, 0) \text{ is a saddle,} \\ \text{If } s_0 < \frac{\alpha}{a} \quad c > 0 \text{ gives } \lambda_{\pm} < 0, \text{ so } (0, 0) \text{ is a stable node,} \\ \quad \quad \quad c < 0 \text{ gives } \lambda_{\pm} > 0, \text{ so } (0, 0) \text{ is an unstable node,} \\ \quad \quad \quad c = 0 \text{ gives } \lambda_{\pm} \in i\mathbb{R}, \text{ so } (0, 0) \text{ is a center.} \end{array} \right.$$

If $c^2 < 4(\alpha - as_0)$ holds, the expression in the square root is negative, therefore we have a nonzero imaginary part. So when $c > 0$ $(0, 0)$ is a stable focus and when $c < 0$ $(0, 0)$ is an unstable focus.

We remark that only for $s_0 > \frac{\alpha}{a}$ the manifold \mathcal{M}_0^0 is normally hyperbolic according to definition (2.3.1). So only where $s_0 > \frac{\alpha}{a}$ holds on \mathcal{M}_0^0 we can apply Fenichel's theorems. Otherwise we cannot state anything about the manifold \mathcal{M}_ϵ^0 , where $0 < \epsilon \ll 1$ holds.

Evaluating Jacobi matrix in the other critical point $(\alpha - as_0, 0)$ gives us this matrix

$$J(\alpha - as_0, 0) = \begin{pmatrix} 0 & 1 \\ 2(\alpha - as_0) + as_0 - \alpha & -c \end{pmatrix} = \begin{pmatrix} 0 & 1 \\ \alpha - as_0 & -c \end{pmatrix}$$

The characteristic polynomial of this matrix is equal to $\lambda^2 + c\lambda - \alpha + as_0$. Which gives us eigenvalues $\lambda_{\pm} = \frac{1}{2} \left(-c \pm \sqrt{c^2 - 4(-\alpha + as_0)} \right)$. For this critical point we can also expect different characters

depending on the parameter values. For $c^2 > 4(-\alpha + as_0)$, the expression in the square root is positive, so both eigenvalues on we have a nonzero imaginary part.

$$\left\{ \begin{array}{l} \text{If } s_0 > \frac{\alpha}{a} \\ \quad c > 0 \text{ gives } \lambda_{\pm} < 0, \text{ so } (\alpha - as_0, 0) \text{ is a stable node,} \\ \quad c < 0 \text{ gives } \lambda_{\pm} > 0, \text{ so } (\alpha - as_0, 0) \text{ is an unstable node,} \\ \quad c = 0 \text{ gives } \lambda_{\pm} \in i\mathbb{R}, \text{ so } (\alpha - as_0, 0) \text{ is a center.} \\ \text{If } s_0 < \frac{\alpha}{a} \\ \quad \lambda_- < 0 < \lambda_+, \text{ so } (\alpha - as_0, 0) \text{ is a saddle,} \end{array} \right.$$

If $c^2 < 4(-\alpha + as_0)$, then we have a nonzero imaginary part. So when $c > 0$, $(\alpha - as_0, 0)$ is a stable focus and when $c < 0$, $(\alpha - as_0, 0)$ is an unstable focus.

Now we would like to determine where normal hyperbolicity on \mathcal{M}_0^+ holds. Only when $s_0 < \frac{\alpha}{a}$ the eigenvalues of the evaluated Jacobian are bounded away from the imaginary axis. Hence definition (2.3.1) says that \mathcal{M}_0^+ is only normally hyperbolic for $s_0 < \frac{\alpha}{a}$. Hence it is only relevant to look at $s_0 < \frac{\alpha}{a}$ on \mathcal{M}_0^+ .

4.2.2 Hamiltonian

We remark that (4.5) is an Hamiltonian system if we take the wavespeed c equal to zero. Next we state the definition of a Hamiltonian system.

Definition 4.2.1. (Hamiltonian) A Hamiltonian system is a system of $2n$ ordinary differential equations of the form

$$\begin{cases} \frac{d\mathbf{p}}{dt} = -\frac{\partial H}{\partial \mathbf{q}} \\ \frac{d\mathbf{q}}{dt} = \frac{\partial H}{\partial \mathbf{p}} \end{cases} \quad (4.8)$$

where $H = H(t, \mathbf{p}, \mathbf{q})$, called the Hamiltonian, is a smooth real-valued function defined for $(t, \mathbf{p}, \mathbf{q}) \in \mathcal{O}$, an open set in $\mathbb{R}^1 \times \mathbb{R}^n \times \mathbb{R}^n$.

In order to determine the possible homoclinic and heteroclinic orbits of (4.5), we look at the Hamiltonian of our integrable system. We know that if we take $c = 0$, this system is of the form (4.8), so its Hamiltonian

$$\begin{cases} \frac{df}{d\xi} = p & = -\frac{\partial H}{\partial p} \\ \frac{dp}{d\xi} = f(f + as_0 - \alpha) & = \frac{\partial H}{\partial f}. \end{cases} \quad (4.9)$$

We can determine $H(f, p)$ itself by integrating over both equations in (4.9). We start by integrating over the first equation

$$H(f, p) = \int -p \, dp = -\frac{1}{2}p^2 + \varphi(f),$$

where φ is a real valued function that depends on f . We repeat this for the second equation

$$H(f, p) = \int f^2 + f(as_0 - \alpha) \, df = \frac{1}{3}f^3 + \frac{1}{2}f^2(as_0 - \alpha) + \psi(p),$$

where ψ is a real valued function that depends on p . If we combine these two expressions by taking $\varphi(f) = \frac{1}{3}f^3 + \frac{1}{2}f^2(as_0 - \alpha)$ and $\psi(p) = -\frac{1}{2}p^2$, we find the Hamiltonian $H(f, p)$ of system (4.9)

$$H(f, p) = \frac{1}{3}f^3 + \frac{1}{2}f^2(as_0 - \alpha) - \frac{1}{2}p^2. \quad (4.10)$$

We want to find the homoclinic orbits for this system. In the case $s_0 > \frac{\alpha}{a}$ we have that $(0, 0)$ is a saddle and that $(\alpha - as_0, 0)$ is a center point. So in that case we have a homoclinic orbit from $(0, 0)$ to $(0, 0)$ that goes around $(\alpha - as_0, 0)$. We want to find the equation of this orbit by using the Hamiltonian. The orbit goes through $(0, 0)$, so we want to determine the value of $H(0, 0)$. Easily we see that $H(0, 0) = 0$ holds. Thus the following equation must hold for the homoclinic orbit $\gamma(x) = (\hat{f}(x), \hat{p}(x))$:

$$\frac{1}{3}\hat{f}^3 + \frac{1}{2}\hat{f}^2(as_0 - \alpha) - \frac{1}{2}\hat{p}^2 = 0$$

We know that $\hat{p} = \dot{\hat{f}}$ holds, substituting this gives us:

$$\frac{1}{3}\hat{f}^3 + \frac{1}{2}\hat{f}^2(as_0 - \alpha) - \frac{1}{2}\dot{\hat{f}}^2 = 0$$

We remark that this is a first order ordinary differential equation, if we solve it we get the solution

$$\hat{f}(x) = -\frac{3}{2}(as_0 - \alpha)\operatorname{sech}^2\left(\frac{1}{2}\sqrt{as_0 - \alpha}x - \frac{\sqrt{3}}{2}\sqrt{as_0 - \alpha}k\right),$$

with $k \in \mathbb{R}$ a constant that we can determine. Because the orbit \hat{f} goes to zero for infinity and minus infinity, $\lim_{x \rightarrow \pm\infty} \hat{f}(x) = 0$, we can conclude that $k = 0$ must hold. Hence we find the following expression for the homoclinic orbit

$$\begin{aligned} \hat{f}(x) &= -\frac{3}{2}(as_0 - \alpha)\operatorname{sech}^2\left(\frac{1}{2}\sqrt{as_0 - \alpha}x\right), \\ \hat{p}(x) &= \dot{\hat{f}}(x) \\ &= \frac{3}{2}(as_0 - \alpha)\frac{3}{2}\tanh\left(\frac{1}{2}\sqrt{as_0 - \alpha}x\right)\operatorname{sech}^2\left(\frac{1}{2}\sqrt{as_0 - \alpha}x\right). \end{aligned}$$

We want to do the same for the case $s_0 > \frac{\alpha}{a}$. Then we have that $(\alpha - as_0, 0)$ is a saddle and that $(0, 0)$ is a center point. So in that case we have a homoclinic orbit from $(\alpha - as_0, 0)$ to $(\alpha - as_0, 0)$ that goes around $(0, 0)$. In order to find this orbit, we again use the Hamiltonian. We want to find the level set of $H(f, p)$ that goes through $(\alpha - as_0, 0)$, so we want to determine the value of $H(\alpha - as_0, 0)$.

$$\begin{aligned} H(\alpha - as_0, 0) &= \frac{1}{3}(\alpha - as_0)^3 + \frac{1}{2}(\alpha - as_0)^2(as_0 - \alpha) - \frac{1}{2}(0)^2 \\ &= \frac{1}{3}(\alpha - as_0)^3 - \frac{1}{2}(\alpha - as_0)^3 \\ &= -\frac{1}{6}(\alpha - as_0)^3 \\ &= \frac{1}{6}(as_0 - \alpha)^3 \end{aligned} \quad (4.11)$$

Setting $H(f, p)$ equal to the constant (4.11) that we found gives us the equation for the homoclinic orbit $\gamma^*(x) = (\bar{f}(x), \bar{p}(x))$

$$\frac{1}{3}\bar{f}^3 + \frac{1}{2}\bar{f}^2(as_0 - \alpha) - \frac{1}{2}\bar{p}^2 = \frac{1}{6}(as_0 - \alpha)^3.$$

We know that $\bar{p} = \dot{\bar{f}}$ holds because of system (4.5). We can find an implicit expression of this homoclinic orbit by substituting this.

$$\frac{1}{3}\bar{f}^3 + \frac{1}{2}\bar{f}^2(as_0 - \alpha) - \frac{1}{2}\dot{\bar{f}}^2 = \frac{1}{6}(as_0 - \alpha)^3.$$

4.2.3 Phase plane

We now know the characters of the critical points and we have determined the Hamiltonian. So we are able to plot the phase planes of the system (4.5) for different choices of our parameters. We first give another few definitions from the field of dynamical systems.

Definition 4.2.2. (Invariant set) A set Λ is invariant under a flow φ_t if $\varphi_t(\Lambda) = \Lambda$ for all t ; that is, for each $x \in \Lambda$, $\varphi_t(x) \in \Lambda$ for any t (Meiss, 2017).

Definition 4.2.3. (Heteroclinic orbit) An orbit Γ is a *heteroclinic orbit* from A to B if each $x \in \Gamma$ is backward asymptotic to an invariant set A and forward asymptotic to an invariant set B (Meiss, 2017).

Definition 4.2.4. (Homoclinic orbit) An orbit Γ is a *homoclinic orbit* to A if each $x \in \Gamma$ is both forward and backward asymptotic to the same invariant set A (Meiss, 2017).

If we take $c = 0$ and $s_0 < \frac{\alpha}{a}$, then we know that $(0, 0)$ is a center and $(\alpha - as_0, 0)$ is a saddle. In figure 4.1 we plot the phase plane to validate our analytical computations.

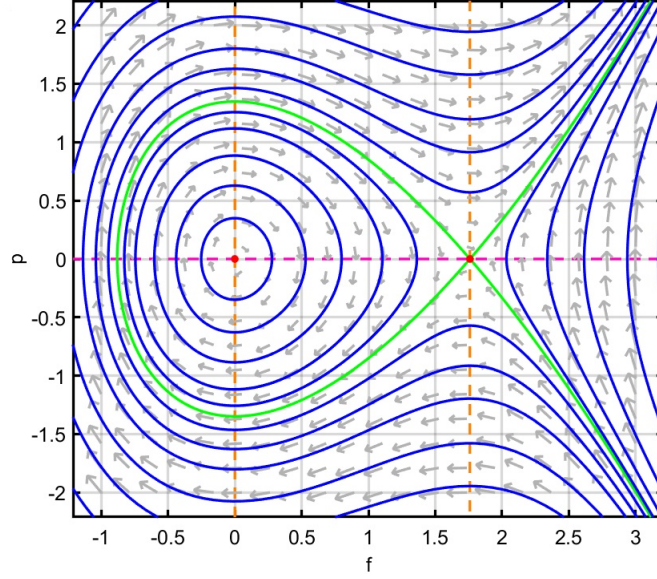


Figure 4.1: Phase planes for system (4.5).

The pink and the orange nullclines represents the values for which $\frac{df}{d\xi} = 0$ and $\frac{dp}{d\xi} = 0$ holds respectively.

We note that there is a homoclinic orbit from the saddle to itself. The homoclinic orbit goes around the other critical point, which is a center. Around the center point we see infinitely many periodic orbits. The green orbit describes the stable and unstable manifolds of the saddle. Which are defined below.

Definition 4.2.5. (Stable manifold) A *stable manifold* of an invariant set Λ as the set of points forward asymptotic to Λ (Meiss, 2017):

$$W^s(\Lambda) = \left\{ x \notin \Lambda : \lim_{t \rightarrow \infty} \rho(\varphi_t(x), \Lambda) = 0 \right\}.$$

Definition 4.2.6. (Unstable manifold) An *unstable manifold* of an invariant set Λ as the set of points backward asymptotic to Λ (Meiss, 2017):

$$W^u(\Lambda) = \left\{ x \notin \Lambda : \lim_{t \rightarrow -\infty} \rho(\varphi_t(x), \Lambda) = 0 \right\},$$

where $\rho(\varphi_t(x), \Lambda)$ is the distance between $\varphi_t(x)$ and Λ .

4.3 Slow system on \mathcal{M}_0^0

We have determined the manifolds \mathcal{M}_0^0 and \mathcal{M}_0^+ . Now we would like to determine the flow on both of these manifolds. We first look at \mathcal{M}_0^0 , on which we have $f = p = 0$. We substitute these

values of f and p into (4.4), which gives the following system

$$\begin{cases} \frac{ds}{d\chi} = q & =: E(s, q) \\ \frac{dq}{d\chi} = s(\mu s - \beta) & =: G(s, q). \end{cases} \quad (4.12)$$

4.3.1 Critical points and their character

Just like for the fast system we want to determine the critical points and their character of system (4.12). We first determine the nullclines. Setting the first equation of (4.12) equal to zero gives $q = 0$ and setting the second equation equal to zero gives $s = 0$ or $s = \frac{\beta}{\mu}$. Hence we know the critical points are equal to $(0, 0)$ and $\left(\frac{\beta}{\mu}, 0\right)$. In order to determine the character of the critical points we linearise the system. We first determine the Jacobian $J(s, q)$

$$J(s, q) = \begin{pmatrix} \frac{\partial E}{\partial s} & \frac{\partial E}{\partial q} \\ \frac{\partial G}{\partial s} & \frac{\partial G}{\partial q} \end{pmatrix} = \begin{pmatrix} 0 & 1 \\ 2\mu s - \beta & 0 \end{pmatrix}.$$

We evaluate this matrix in $(0, 0)$

$$J(0, 0) = \begin{pmatrix} 0 & 1 \\ -\beta & 0 \end{pmatrix}.$$

The characteristic polynomial is equal to $\lambda^2 + \beta$. We can determine the eigenvalues of the evaluated Jacobian by setting this expression to zero. Then we get $\lambda_{\pm} = \pm\sqrt{-\beta}$. We know that $\beta > 0$ holds, so we can conclude $\lambda_{\pm} \in i\mathbb{R}$. So for all possible parameter values we can conclude that $(0, 0)$ is a center.

We repeat this for $\left(\frac{\beta}{\mu}, 0\right)$, the Jacobian evaluated in this critical point is equal to

$$J\left(\frac{\beta}{\mu}, 0\right) = \begin{pmatrix} 0 & 1 \\ 2\beta - \beta & 0 \end{pmatrix} = \begin{pmatrix} 0 & 1 \\ \beta & 0 \end{pmatrix}.$$

The characteristic polynomial is equal to $\lambda^2 - \beta$, which gives the eigenvalues $\lambda_{\pm} = \pm\sqrt{\beta}$. Because β is positive we know that $\lambda_- < 0 < \lambda_+$ holds for the eigenvalues, again for all possible parameter values. So $\left(\frac{\beta}{\mu}, 0\right)$ is a saddle.

4.3.2 Phase plane

Now that we know the characters of the critical points, we plot the phase plane.

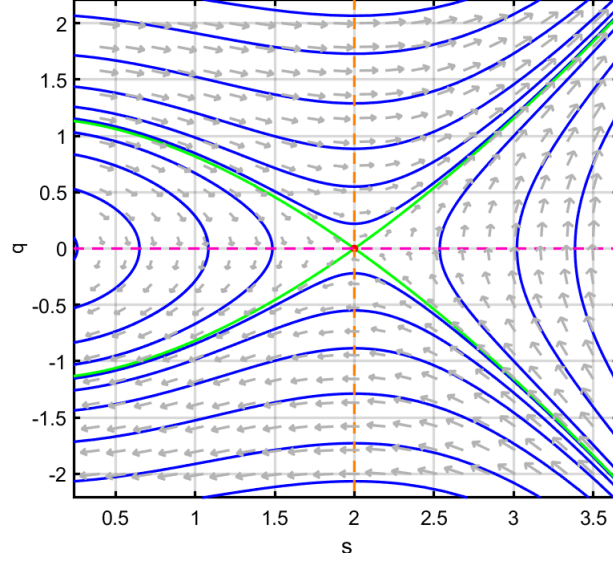


Figure 4.2: Phase planes for system (4.12).

The pink and the orange nullclines represents the values for which $\frac{ds}{d\chi} = 0$ and $\frac{dq}{d\chi} = 0$ holds respectively.

We know that $\left(\frac{\beta}{\mu}, 0\right)$ is a saddle, with stable and unstable manifolds. We plotted these as the green lines in figure 4.2. In this phase plane we took $s > \frac{\alpha}{a}$, because that is the only part of \mathcal{M}_0^0 that is normally hyperbolic. We also note that it is necessary that the condition $\frac{\alpha}{a} < \frac{\beta}{\mu}$ holds. Otherwise $\frac{\beta}{\mu}$ would not be normally hyperbolic and then we cannot find a front solution using Fenichel's theorems.

We can see that this phase plane contains a homoclinic orbit, this orbit goes from $\left(\frac{\beta}{\mu}, 0\right)$ to itself around the trivial critical point $(0, 0)$. This homoclinic orbit is a subset of the stable and unstable manifolds of $\left(\frac{\beta}{\mu}, 0\right)$. We determine an expression for this orbit implicitly in the next subsection using the Hamiltonian.

4.3.3 Hamiltonian

We remark that (4.12) is a Hamiltonian system, because it is of the form (4.2.1)

$$\begin{cases} \frac{ds}{d\chi} = q & = -\frac{\partial H}{\partial q} \\ \frac{dq}{d\chi} = s(\mu s - \beta) & = \frac{\partial H}{\partial s} \end{cases} \quad (4.13)$$

We first integrate the first equation over q , then we get the following expression for $H(s, q)$

$$H(s, q) = \int -q \, dq = -\frac{1}{2}q^2 + \varphi(s),$$

where φ is a real valued function that depends on s . Then we do the same for the second equation, but we integrate over the variable s

$$H(s, q) = \int s(-\beta + \mu s) \, ds = -\frac{1}{2}\beta s^2 + \frac{1}{3}\mu s^3 + \psi(q),$$

where ψ is a real valued function that depends on q . We can combine these two expressions for $H(s, q)$ by taking $\varphi(s) = -\frac{1}{2}\beta s^2 + \frac{1}{3}\mu s^3$ and $\psi(q) = -\frac{1}{2}q^2$. Substituting these functions gives us the Hamiltonian function

$$H(s, q) = -\frac{1}{2}\beta s^2 + \frac{1}{3}\mu s^3 - \frac{1}{2}q^2 \quad (4.14)$$

In this invariant plane we have two critical points $(0, 0)$, which is a center, and $\left(\frac{\beta}{\mu}, 0\right)$, which is a saddle. We want to find the homoclinic orbit that we saw in figure 4.2. In order to find an expression of this homoclinic orbit, we determine the Hamiltonian. Because the level sets of the Hamiltonian are the solutions to the system and the fact homoclinic orbit goes through $\left(\frac{\beta}{\mu}, 0\right)$, we evaluate the Hamiltonian in this point

$$\begin{aligned} H\left(\frac{\beta}{\mu}, 0\right) &= \frac{1}{2}\left(\frac{\beta}{\mu}\right)^2(-\beta) + \frac{1}{3}\mu\left(\frac{\beta}{\mu}\right)^3 \\ &= \frac{1}{3}\frac{\beta^3}{\mu^2} - \frac{1}{2}\frac{\beta^3}{\mu^2} \\ &= -\frac{1}{6}\frac{\beta^3}{\mu^2}. \end{aligned}$$

Setting the Hamiltonian equal to this value gives us the equation that describes the homoclinic orbit that we are looking for

$$\begin{aligned} -\frac{1}{2}\beta s^2 + \frac{1}{3}\mu s^3 - \frac{1}{2}q^2 &= -\frac{1}{6}\frac{\beta^3}{\mu^2} \\ \Rightarrow q^2 &= -\frac{2}{3}\mu\left(s - \frac{\beta}{\mu}\right)^2\left(s + \frac{\beta}{2\mu}\right) \end{aligned} \quad (4.15)$$

4.4 Slow system on M_0^+

Now we want to learn more about the flow on the other manifold. So we look at \mathcal{M}_0^+ , on which $f = \alpha - as$ holds. Substituting this value of f into the slow subsystem gives us the system

$$\begin{cases} \frac{ds}{d\chi} = q & =: I(s, q) \\ \frac{dq}{d\chi} = s(\mu s - \beta + b(\alpha - as)) & =: J(s, q). \end{cases} \quad (4.16)$$

4.4.1 Critical points and their character

For this system we also determine the critical points, in order to do that we determine the nullclines. $I(s, q) = 0$ gives $q = 0$ and setting $J(s, q)$ to zero together with $q = 0$ gives us $s = 0$ or $s = \frac{\beta - b\alpha}{\mu - ab}$. Hence we know the critical points are equal to $(0, 0)$ and $\left(\frac{\beta - b\alpha}{\mu - ab}, 0\right)$. The next step in order to determine the characters of these critical points is to linearise and determine the Jacobian.

$$J(s, q) = \begin{pmatrix} \frac{\partial I}{\partial s} & \frac{\partial I}{\partial q} \\ \frac{\partial J}{\partial s} & \frac{\partial J}{\partial q} \end{pmatrix} = \begin{pmatrix} 0 & 1 \\ 2\mu s - \beta + b(1 - 2as - m) & 0 \end{pmatrix}$$

Evaluating $(0, 0)$ into the Jacobian gives us

$$J(0, 0) = \begin{pmatrix} 0 & 1 \\ -\beta + b\alpha & 0 \end{pmatrix}$$

The characteristic polynomial is equal to $\lambda^2 + (\beta - b\alpha)$, setting it to zero gives us the eigenvalues $\lambda_{\pm} = \pm\sqrt{-\beta + b\alpha}$. We can conclude that $(0, 0)$ is a saddle because of the stability condition $\frac{\beta}{b} < \alpha$ we already found in section 3.

Not we evaluate the Jacobian into $\left(\frac{\beta - b\alpha}{\mu - ab}, 0\right)$, which gives

$$\begin{aligned} J\left(\frac{\beta - b\alpha}{\mu - ab}, 0\right) &= \begin{pmatrix} 0 & 1 \\ 2\mu\frac{\beta - b\alpha}{\mu - ab} - \beta + b\left(\alpha - 2a\frac{\beta - b\alpha}{\mu - ab}\right) & 0 \end{pmatrix} \\ &= \begin{pmatrix} 0 & 1 \\ (2(\mu - ab)\frac{\beta - b\alpha}{\mu - ab} - \beta + b\alpha) & 0 \end{pmatrix} \\ &= \begin{pmatrix} 0 & 1 \\ (2(\beta - b\alpha) - \beta + b\alpha) & 0 \end{pmatrix} \\ &= \begin{pmatrix} 0 & 1 \\ \beta + b\alpha & 0 \end{pmatrix} \end{aligned}$$

This matrix has characteristic polynomial $\lambda^2 - \beta - b\alpha$, which implies that the eigenvalues are equal to $\lambda_{\pm} = \pm\sqrt{\beta + b\alpha}$. Using the condition $\frac{\beta}{b} < \alpha$ again gives $\lambda_{\pm} \in \mathbb{R}$. This implies that $\left(\frac{\beta - b\alpha}{\mu - ab}, 0\right)$ is a center.

Because $\frac{\beta}{b} < \alpha$ holds, the numerator of $\frac{\beta - b\alpha}{\mu - ab}$ is negative. In subsection 3.1.1 we have shown that $\mu < ab$ holds, which implies that $\mu - ab$ is negative. So the s -component of the critical point $\left(\frac{\beta - b\alpha}{\mu - ab}, 0\right)$ is positive.

4.4.2 Phase planes

Now that we have determined the fixed points and their characters of system (4.16), we give the phase planes of the system for two different parameter choices.

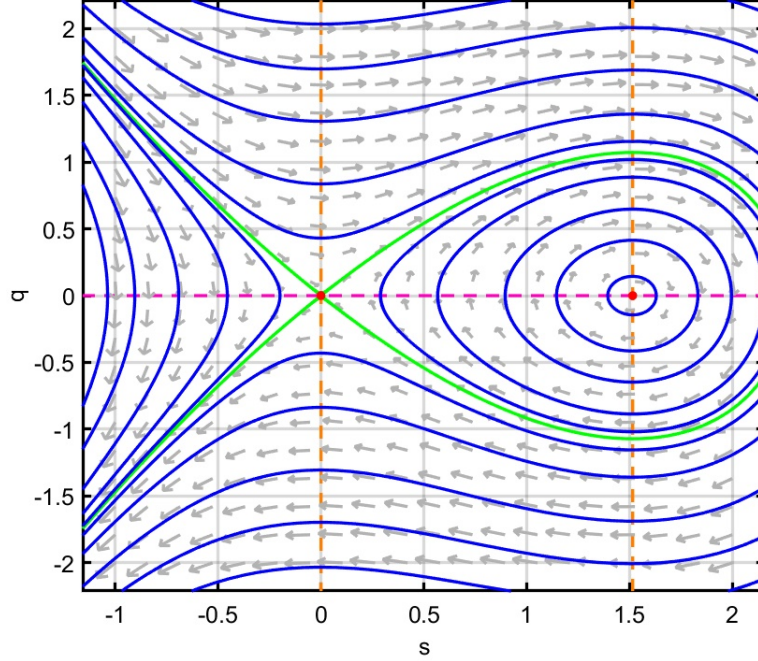


Figure 4.3: Phase planes for system (4.16).

The pink and the orange nullclines represents the values for which $\frac{ds}{d\chi} = 0$ and $\frac{dq}{d\chi} = 0$ holds respectively.

In this figure the plotted green lines are the stable and unstable manifolds of the saddle point $(0, 0)$. There exists a homoclinic orbit that goes from $(0, 0)$ to itself. In the next subsection we determine an implicit expression for the homoclinic orbit in figure 4.3. We are interested in the homoclinic orbit, because eventually we want to find a heteroclinic orbit from $(\alpha - as_0, 0)$ on M_ϵ^0 to $(0, 0)$ on M_ϵ^+ .

4.4.3 Hamiltonian

We remark that the system on the manifold M_0^+ (4.16) is Hamiltonian, because it is of the form (4.2.1)

$$\begin{cases} \frac{ds}{d\chi} = q & = -\frac{\partial H}{\partial q} \\ \frac{dq}{d\chi} = s(\mu s - \beta + b(\alpha - as)) & = \frac{\partial H}{\partial s}. \end{cases} \quad (4.17)$$

Integrating the first equation over q gives us the first expression for $H(s, q)$

$$H(s, q) = \int -q dq = -\frac{1}{2}q^2 + \varphi(s),$$

where $\varphi(s)$ is a real valued function dependent on s . Integrating the second equation over s gives the other expression that we need in order to determine $H(s, q)$.

$$\begin{aligned} H(s, q) &= \int s(-\beta + b(\alpha - as) + \mu s) ds \\ &= \int s(-\beta + b\alpha) + s^2(\mu - ab) ds \\ &= \frac{1}{2}s^2(-\beta + b\alpha) + \frac{1}{3}s^3(\mu - ab) + \psi(q) \end{aligned}$$

Combining these two expressions for $H(s, q)$ we get:

$$H(s, q) = \frac{1}{2}s^2(-\beta + b\alpha) + \frac{1}{3}s^3(\mu - ab) - \frac{1}{2}q^2 \quad (4.18)$$

We want to choose the parameter values in such a way that $\frac{\beta}{b} < \alpha$ holds. Because then both critical points lay in the half-plane $s \geq 0, q \in \mathbb{R}$ and then the homoclinic orbit also lies in this plane. Hence this choice is ecologically relevant. In this invariant plane we have two critical points $(0, 0)$, which is a saddle, and $\left(\frac{\beta - b\alpha}{\mu - ab}, 0\right)$, which is a center. We want to find an expression of the homoclinic orbit that goes from $(0, 0)$ around $\left(\frac{\beta - b\alpha}{\mu - ab}, 0\right)$ back to itself. We can determine this expression by using the Hamiltonian. Because the level sets of the Hamiltonian are the solutions to the system. The homoclinic orbit goes through $(0, 0)$, we evaluate the Hamiltonian in this saddle point

$$\begin{aligned} H(0, 0) &= \frac{1}{2}0^2(-\beta + b\alpha) + \frac{1}{3}0^3(\mu - ab) - \frac{1}{2}0^2 \\ &= 0 \end{aligned}$$

So the following equation describes the homoclinic orbit that we are looking for

$$\frac{1}{2}s^2(-\beta + b\alpha) + \frac{1}{3}s^3(\mu - ab) - \frac{1}{2}q^2 = 0. \quad (4.19)$$

Now we know a lot about system (2.5) for $\epsilon \rightarrow 0$, we can use this together with geometric singular perturbation theory to learn more about the dynamics of the system for $0 < \epsilon \ll 1$

4.5 Heteroclinic connection in the 4D space

4.5.1 Intersection of the manifolds

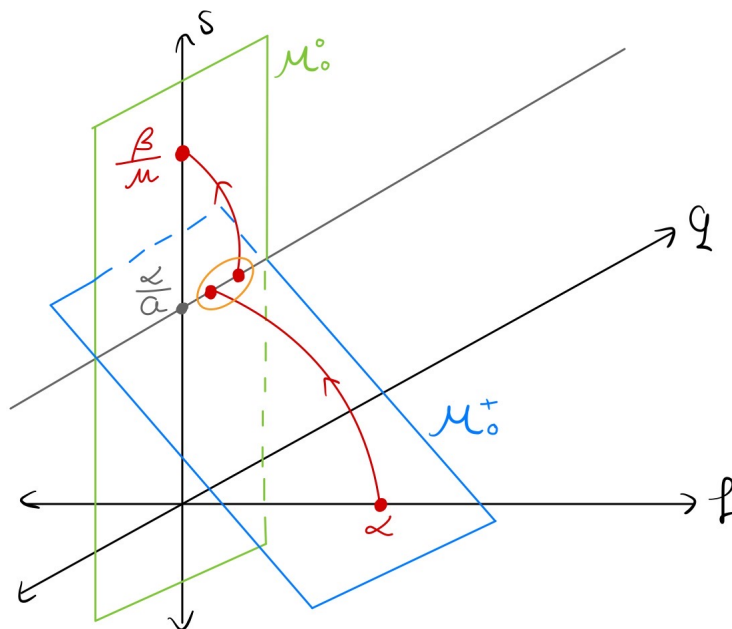


Figure 4.4: Intersection of the manifolds \mathcal{M}_ϵ^0 and \mathcal{M}_ϵ^+ , with the heteroclinic orbit we want to find.

We are looking for the heteroclinic orbit in figure 4.4, which consists parts of the homoclinic orbits on \mathcal{M}_ϵ^0 and \mathcal{M}_ϵ^+ . This heteroclinic orbit connects the critical point $(\alpha, 0, 0, 0)$, which is the pure trees state, to the critical point $(0, 0, \frac{\beta}{\mu}, 0)$. This last point is the pure grass state.

are the pure trees and pure grass state

This orbit represents the front in the savanna-forest transition zone. At this front the forest biomass starts at value α and then decreases to 0, and the front that represents the savanna biomass goes from 0 to $\frac{\beta}{\mu}$. We already determined that the two manifolds intersect in $f = 0, p = 0$ and $s = \frac{\alpha}{a}$. We want that the homoclinic orbits in both the manifolds intersect in this line.

4.5.2 Finding condition for heteroclinic connection using Hamiltonians

So we found two homoclinic orbits:

$$\begin{cases} \frac{1}{2}s^2(-\beta) + \frac{1}{3}\mu s^3 - \frac{1}{2}q^2 = -\frac{1}{6}\frac{\beta^3}{\mu^2} & \text{on } \mathcal{M}_\epsilon^0, \\ \frac{1}{2}s^2(-\beta + b\alpha) + \frac{1}{3}s^3(\mu - ab) - \frac{1}{2}q^2 = 0 & \text{on } \mathcal{M}_\epsilon^+ \end{cases} \quad (4.20)$$

We can rewrite these into:

$$\begin{cases} \frac{1}{2}q^2 = \frac{1}{2}s^2(-\beta) + \frac{1}{3}\mu s^3 + \frac{1}{6}\frac{\beta^3}{\mu^2} & \text{on } \mathcal{M}_\epsilon^0, \\ \frac{1}{2}q^2 = \frac{1}{2}s^2(-\beta + b\alpha) + \frac{1}{3}s^3(\mu - ab) & \text{on } \mathcal{M}_\epsilon^+ \end{cases} \quad (4.21)$$

We know that for in intersection of these manifolds $s = \frac{\alpha}{a}$ must hold. Substituting this gives:

$$\begin{cases} \frac{1}{2}q^2 = \frac{1}{2}\left(\frac{\alpha}{a}\right)^2(-\beta) + \frac{1}{3}\mu\left(\frac{\alpha}{a}\right)^3 + \frac{1}{6}\frac{\beta^3}{\mu^2} & \text{on } \mathcal{M}_\epsilon^0, \\ \frac{1}{2}q^2 = \frac{1}{2}\left(\frac{\alpha}{a}\right)^2(-\beta + b\alpha) + \frac{1}{3}\left(\frac{\alpha}{a}\right)^3(\mu - ab) & \text{on } \mathcal{M}_\epsilon^+ \end{cases} \quad (4.22)$$

Now we can combine these equations:

$$\begin{aligned} & \frac{1}{2}\left(\frac{\alpha}{a}\right)^2(-\beta) + \frac{1}{3}\mu\left(\frac{\alpha}{a}\right)^3 + \frac{1}{6}\frac{\beta^3}{\mu^2} = \frac{1}{2}\left(\frac{\alpha}{a}\right)^2(-\beta + b\alpha) + \frac{1}{3}\left(\frac{\alpha}{a}\right)^3(\mu - ab) \\ \Rightarrow & 3\left(\frac{\alpha}{a}\right)^2(-\beta) + 2\mu\left(\frac{\alpha}{a}\right)^3 + \frac{\beta^3}{\mu^2} = 3\left(\frac{\alpha}{a}\right)^2(-\beta + b\alpha) + 2\left(\frac{\alpha}{a}\right)^3(\mu - ab) \\ \Rightarrow & \frac{\beta^3}{\mu^2} = 3\left(\frac{\alpha}{a}\right)^2 b\alpha - 2ab\left(\frac{\alpha}{a}\right)^3 \\ \Rightarrow & \frac{\beta^3}{\mu^2} = 3b\frac{\alpha^3}{a^2} - 2b\frac{\alpha^3}{a^2} \\ \Rightarrow & \frac{\beta^3}{\mu^2} = b\frac{\alpha^3}{a^2} \\ \Rightarrow & a^2\beta^3 = b\mu^2\alpha^3 \end{aligned} \quad (4.23)$$

When parameters are chosen in such a way that this condition holds, there exists a heteroclinic orbit from $(\alpha, 0, 0, 0)$ to $\left(0, 0, \frac{\beta}{\mu}, 0\right)$ with $c = 0$. So we can conclude that this condition gives a standing front. We will confirm this numerically in section 4.6. For finding this heteroclinic orbit that we took $\epsilon = 0$. Because this orbit lies on the normally hyperbolic parts \mathcal{M}_0^0 and \mathcal{M}_0^+ we can use Fenichel's first and second theorem. Hence we know that this singular orbit persists for $\epsilon \neq 0$.

4.5.3 Heteroclinic connection for $c \neq 0$

We would also like to see if we can find such a connection for $c \neq 0$. Because there is no c in the slow limit, we look at the slow system without taking $\epsilon \rightarrow 0$.

$$\begin{cases} \frac{ds}{d\chi} = q \\ \frac{dq}{d\chi} = -\epsilon cq + s(\mu s - \beta + bf). \end{cases} \quad (4.24)$$

We want to find a heteroclinic connection from $(\alpha, 0, 0, 0)$, that lies on \mathcal{M}_ϵ^+ , to $\left(0, 0, \frac{\beta}{\mu}, 0\right)$ on \mathcal{M}_ϵ^0 . This orbit goes leaves from \mathcal{M}_ϵ^+ to \mathcal{M}_ϵ^0 at $s = \frac{\alpha}{a}$. On \mathcal{M}_ϵ^0 we know that $f = 0$ holds. We have already determined the Hamiltonian (4.14) for this system. We implement this in the Matlab code A.4.1. We want to plot this phase plane together with the orbit on \mathcal{M}_ϵ^+ from $(0, 0)$,

which is the critical value $(\alpha, 0, 0, 0)$ in the 4D space. On \mathcal{M}_ϵ^+ we have $f = \alpha - as$. For this system we use the Matlab function `ode45` (MATLAB, 2010). This function integrates a system of differential equations of the form $\frac{df}{dt} = f(t, y)$ from t_0 to t_f with initial condition y_0 . We implemented the equations of (4.24) together with $f = \alpha - as$ in the Matlab code in A.4.1.1. To use `ode45` we first define the parameters and we chose $\epsilon = 0.01$. Then we define the start the begin- and end time by `tspan=[0 5]`. Lastly we define the initial condition `y0=[0 0.001]`. So we took $y_0 = (s_0, q_0) = (0, 0.001)$, this initial condition lies really close to $(0, 0)$. We chose this initial condition because then we can see how the system behaves around $(0, 0)$. Then we use the line `[t,y] = ode45(@[t,y] eqns2(y,P), tspan, y0)` to find the solution. We also plot the value $s = \frac{\alpha}{a}$. Then we vary the value of c until the orbit from $(0, 0)$ on \mathcal{M}_ϵ^+ intersects with $\left(\frac{\beta}{\mu}, 0\right)$ on \mathcal{M}_0^0 in $s = \frac{\alpha}{a}$. We have found this connection in figure 4.5 for the value $c = -18$.

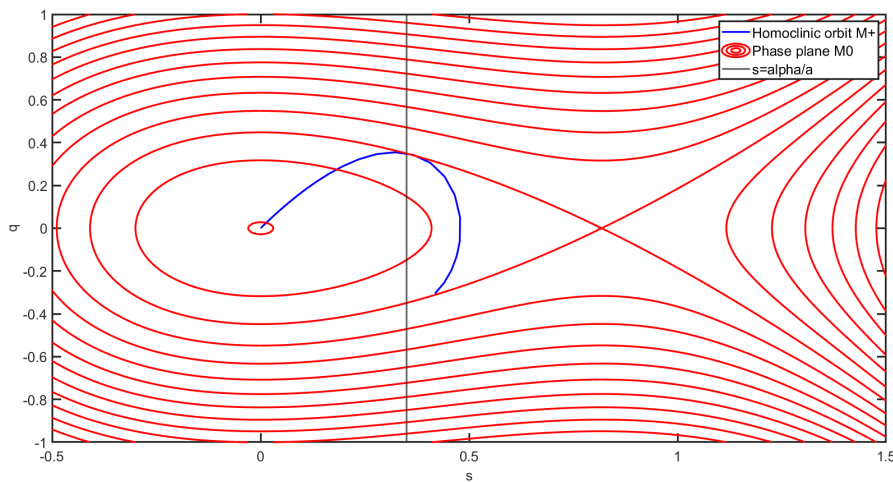


Figure 4.5: Intersection of the manifolds \mathcal{M}_ϵ^0 and \mathcal{M}_ϵ^+ at $s = \frac{\alpha}{a}$ for parameter values $\alpha = 0.7$, $a = 2$, $\beta = 0.9$, $\mu = 1.1$, $b = 6$, $\epsilon = 0.01$, $c = -18$.

So also for $c \neq 0$ we have found a heteroclinic connection that represents a bi-stable front solution.

4.6 Numerical simulations

4.6.1 Travelling front

We want to reproduce our analytical findings. We have introduced a traveling wave solution to system (2.3). Then we took $\epsilon = 0$ and provided a leading order analysis, which resulted in finding a condition for a heteroclinic connection from $(\alpha, 0)$ to $\left(0, \frac{\beta}{\mu}\right)$. Now we would like to take $c \neq 0$ again and construct the travelling wave solution numerically. If we look at the forest biomass f this heteroclinic connection goes from α to zero, so this gives a traveling front. The heteroclinic connection goes from zero to $\frac{\beta}{\mu}$ for the savanna biomass s , which gives a second

traveling front. We used the MATLAB function `pdepe` explained in section 2.4 to construct these fronts numerically.

We determine the solution for 500 time steps, but we don't have to plot them all to see what the solution looks like. We plot the solution at time $t = 10$ and then add 100 each time we make plot, we do this until $t = T$ is reached. In these numerical simulations we chose $\epsilon^2 = 0.005$. In figure 4.6 our traveling front solution is plotted.

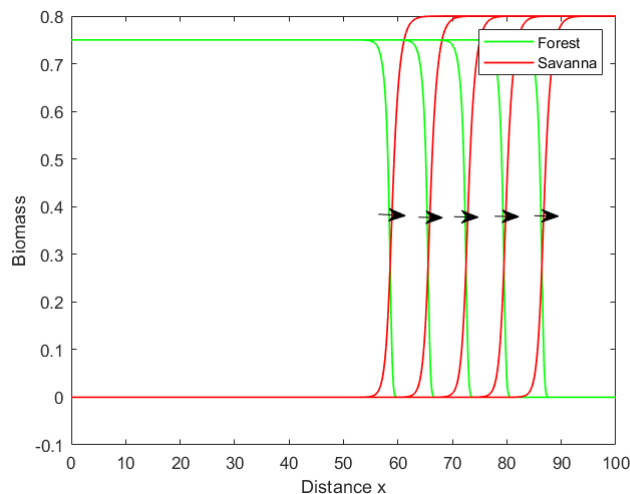


Figure 4.6: The green and the red plots represent the solutions of (2.8) for parameter values $\alpha = 0.75$, $a = 1.12$, $\beta = 1$, $b = 4.5$, $\mu = 1.25$, $\epsilon = 0.005$.

The front that describes the forest biomass decreases from $\alpha = 0.75$ to α and the front that describes the savanna biomass increases from 0 to $\beta/\mu = 0.8$. We see that the forest is invading the savanna for these parameter values. We can alter these values, then we see that the savanna invades the forest in figure (4.7).

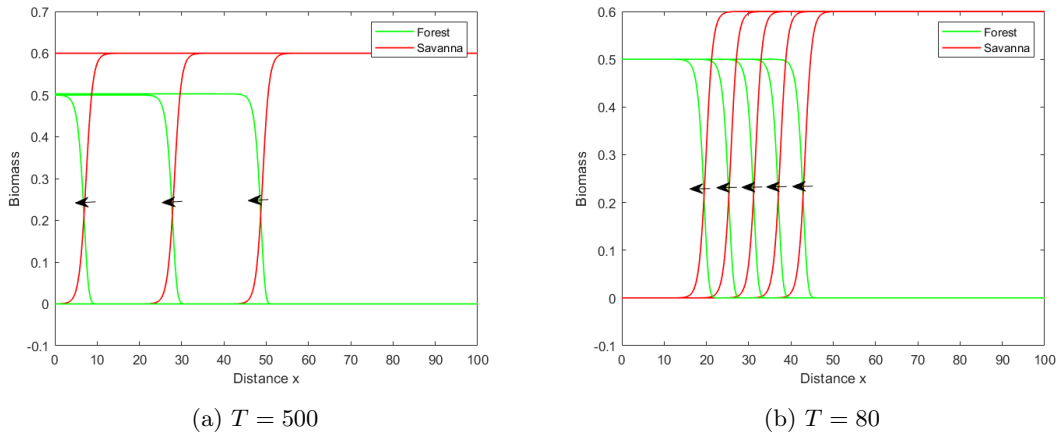


Figure 4.7: The green and the red plots represent the solutions of (2.8) for parameter values $\alpha = 0.5$, $a = 2.24$, $\beta = 2$, $b = 5.25$, $\mu = 2.5$, $\epsilon = 0.005$.

What we notice in this plot is that the wavespeed c for these parameter values is way bigger than for those in figure 4.6. So these fronts move faster. If we keep end time $T = 500$, the fronts leave our domain after a certain value of t . We plotted the solutions for $T = 500$ in figure 4.7a. If we want for the fronts to stay in our domain, we have to lower T . In figure 4.7b we plotted the solutions for $T = 150$.

It is also interesting to zoom in. In figure 4.8 we have only plotted one solution at $t = 10$, zoomed in from $x = 30$ to $x = 70$.

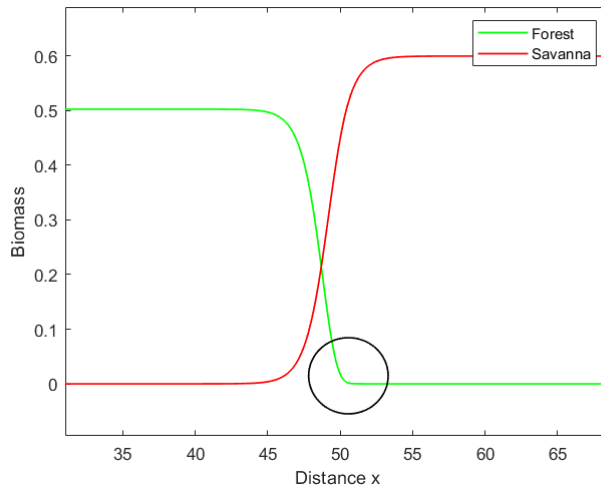


Figure 4.8: The green and the red plots represent the solutions of (2.8) at $t = 10$. for parameter values $\alpha = 0.75$, $a = 1.12$, $\beta = 1$, $b = 4.5$, $\mu = 1.25$, $\epsilon = 0.005$.

We can see that the forest front is sharper than the savanna front. So the savanna thins out more

slowly than the forest in the savanna-forest transition zone.

4.6.2 Standing front

Now we want to use result (4.23) in our simulations. This is a condition for a heteroclinic condition from $(\alpha, 0)$ to $(0, \frac{\beta}{\mu})$ when $c = 0$ holds. So if we use this condition in our simulations, we must get a standing front, because the wavespeed c is equal to zero. We implemented this condition by rewriting the equation to

$$b = \frac{a^2 \beta^3}{\mu^2 \alpha^3}.$$

Hence we change b in the parameter vector P in the Matlab code A.1.1. We keep the other parameter values the same as in figure 4.6.

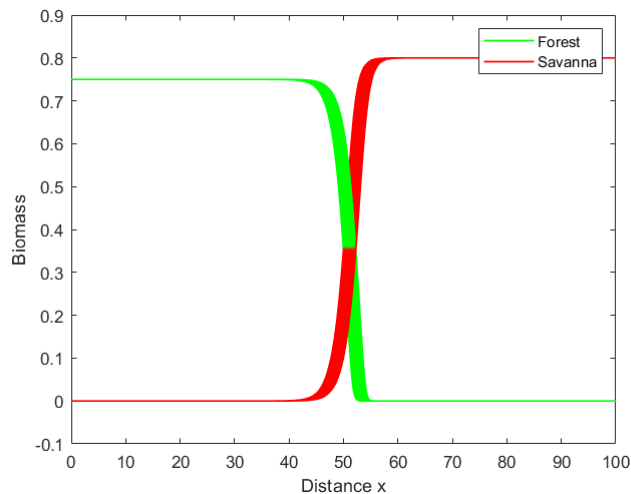


Figure 4.9: The green and the red plots represent the solutions of (2.8) for parameter values $\alpha = 0.5$, $a = 2.24$, $\beta = 2$, $\mu = 2.5$, $b = \frac{a^2 \beta^3}{\mu^2 \alpha^3} \approx 1.903$, $\epsilon = 0.005$.

In figure 4.9 we see that the fronts move way slower than in 4.6, where we did not use this condition. But we see that the front does not completely stand still and hence wavespeed c is not equal to zero. This is because we made an order ϵ error determining condition (4.23). We want to change parameter value b a bit in order for c to be zero. First we just try to add a small term to b and we see that this increases our wavespeed, which is the opposite of what we want. So we want to decrease b a little. In Matlab code A.1.5 we write a for-loop that goes from $i = -0.1$ to $i = 0$ with step size 0.01. Then we add this number i to b and plot the solution for $t = T = 500$ in figure 4.10.

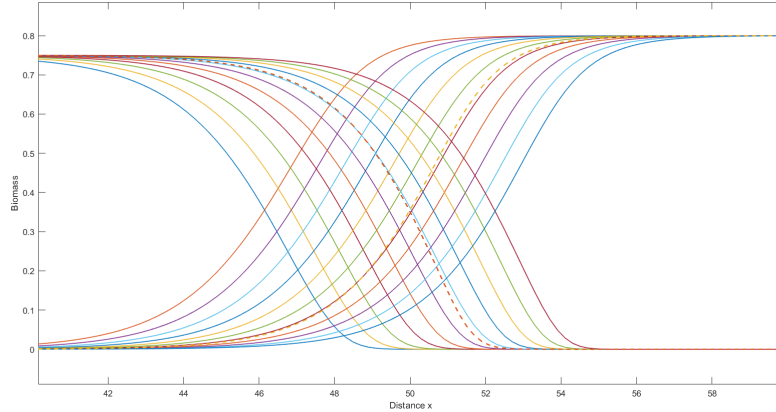


Figure 4.10: Solutions of (2.8) at $T = 500$ for different values of b on the interval $[40, 60]$. The dotted line is the solution for $t = 20$, we can use this to compare the other solutions with.

In this figure we also plotted the solution for $t = 20$ this is the dotted line. We choose the value $b + i$ for which the solution is closest to the solution at $t = 20$. Because for this value of b the front does barely shift after many timesteps. We can see that for the seventh iteration $i = -0.04 = \mathcal{O}(\epsilon)$, so we get $b = \frac{a^2 \beta^3}{\mu^2 \alpha^3} - 0.04$. If we plot the solutions from $t = 1$ until $t = T$ again for this new b we get the following figure 4.11.

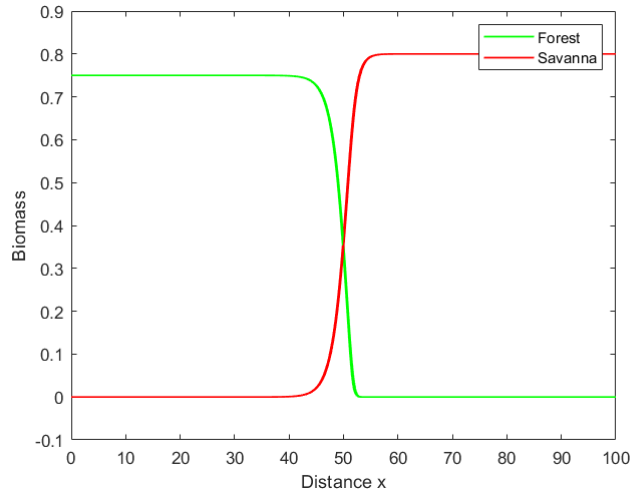


Figure 4.11: The green and the red plots represent the solutions of (2.8) for parameter values $\alpha = 0.5$, $a = 2.24$, $\beta = 2$, $\mu = 2.5$, $b = \frac{a^2 \beta^3}{\mu^2 \alpha^3} - 0.04 \approx 1.863$, $\epsilon = 0.005$.

We remark that this front does almost stand still, but still we see that the front moves a little. We

can repeat this procedure again to choose b more precisely. We know that b must be approximately $b = \frac{a^2\beta^3}{\mu^2\alpha^3} - 0.04$. Creating another for-loop that goes from $i = -0.045$ to $i = -0.035$ with step size 0.001 will show us how we could choose b even more precisely. The solutions of system (2.8) at time $t = T$ for $b = \frac{a^2\beta^3}{\mu^2\alpha^3} + i$ are shown in figure 4.12.

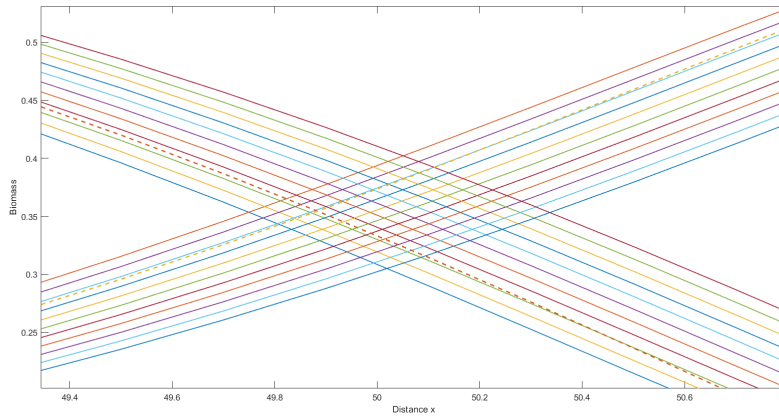


Figure 4.12: Solutions of (2.8) at $T = 500$ for different values of b on the interval $[49, 50]$ for parameter values $\alpha = 0.5$, $a = 2.24$, $\beta = 2$, $\mu = 2.5$, $b = \frac{a^2\beta^3}{\mu^2\alpha^3} - 0.043 \approx 1.860$, $\epsilon = 0.005$.

All of these solutions get really close to a standing front, so it is hard to see which one gets the closest to this front. That is why we zoomed in for this plot. Now we can see that the solution for the third iteration $i = -0.043$ is the one with the lowest wavespeed. So we choose $b = \frac{a^2\beta^3}{\mu^2\alpha^3} - 0.043$. If we plot the solutions again from $t = 1$ to $t = T$ we get the following plot.

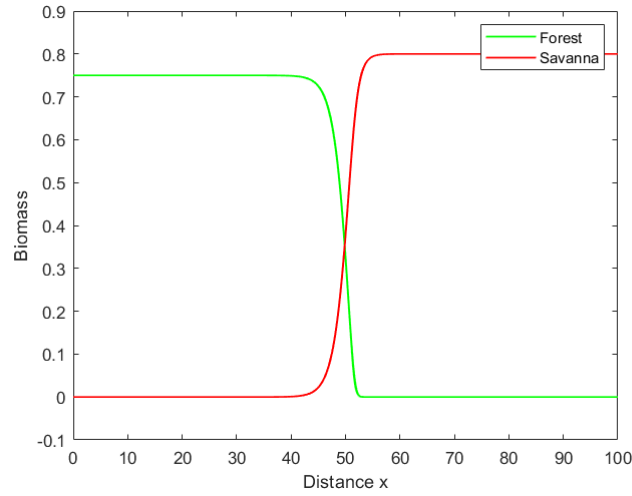


Figure 4.13: The green and the red plots represent the solutions of (2.8) for parameter values $\alpha = 0.5$, $a = 2.24$, $\beta = 2$, $\mu = 2.5$, $b = \frac{a^2\beta^3}{\mu^2\alpha^3} - 0.043 \approx 1.861.94$, $\epsilon = 0.005$.

The solutions in figure 4.13 seem to stand still. If we zoom in we see that the fronts move a little, but we can conclude that if $b \approx \frac{a^2\beta^3}{\mu^2\alpha^3} - 0.043$ holds the wavespeed c is equal to zero.

Chapter 5

A more realistic model: saturation with respect to forest trees

In this section we add a saturation term to the first equation of the system

$$\begin{cases} \frac{\partial F}{\partial t} = F \left(\alpha - F - \frac{aS}{1 + \sigma F} \right) + \Delta F \\ \frac{\partial S}{\partial t} = S(\beta - bF - \mu S) + \frac{1}{\epsilon^2} \Delta S, \end{cases} \quad (5.1)$$

where $\sigma > 0$ holds. This makes sure that the term $\frac{aS}{1 + \sigma F}$ cannot keep growing. This term can only get as big as its saturation value $\frac{aS}{\sigma}$. Adding this term makes this system more ecologically realistic than system (2.1). First we look at the non-spatial model, hence we take $\Delta F = \Delta S = 0$

$$\begin{cases} \frac{df}{dt} = f \left(\alpha - f - \frac{as}{1 + \sigma f} \right) & =: K(f, s) \\ \frac{ds}{dt} = s(\beta - bf - \mu s) & =: L(f, s). \end{cases} \quad (5.2)$$

We remark that if we take σ equal to zero, we get system (2.1). We start the analysis of this model by determining the nullclines. In order to determine these we set both equations to zero. The first one gives $f = 0$ or $s = \frac{1}{a}(\alpha - f)(1 + \sigma f)$ and the second one gives $s = 0$ or $s = \frac{1}{\mu}(\beta - bf)$. We want to plot the nullclines. First we would like to know more about the nullcline $s = \frac{1}{a}(\alpha - f)(1 + \sigma f)$ where $K(f, s) = 0$ holds. This nullcline intersects the s -axis in $s = \frac{\alpha}{a}$. This function is a concave parabola, because the conditions $\sigma, a > 0$ makes sure that $-\frac{\sigma}{a}$ is always negative. The value of f where this parabola reaches its maximum value can be determined by computing the derivative and setting it to zero. First we define the function

$$s(f) = \frac{1}{a}(-\sigma f^2 + f(\alpha\sigma - 1) + \alpha),$$

then we differentiate and set to zero

$$\begin{aligned} s'(f_{\max}) = 0 &\Rightarrow \frac{1}{a}(-2\sigma f_{\max} + \alpha\sigma - 1) = 0 \\ &\Rightarrow -2\sigma f_{\max} + \alpha\sigma - 1 = 0 \\ &\Rightarrow f_{\max} = \frac{1}{2\sigma}(\alpha\sigma - 1). \end{aligned}$$

We look into two cases, we see that f_{\max} is positive whenever $\alpha\sigma > 1$ holds and it's negative when $\alpha\sigma < 1$. Plotting these nullclines for these cases gives the following plots.

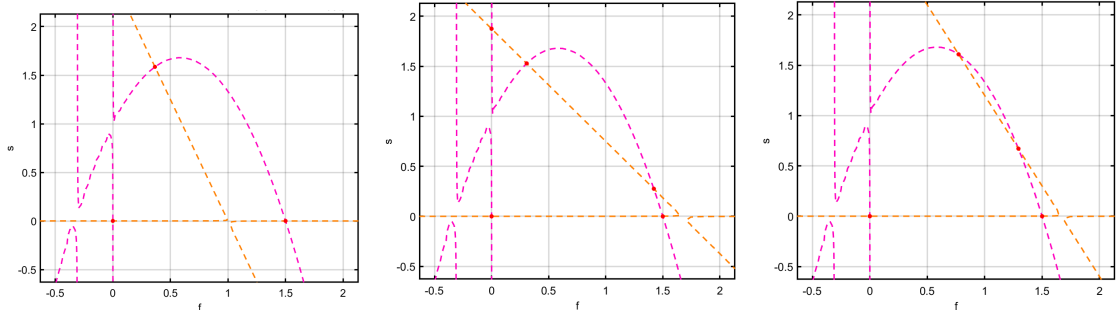


Figure 5.1: Nullclines for system (2.1) when $\alpha\sigma > 1$ holds.

The pink and the orange nullclines represents the values for which $\frac{df}{dt} = 0$ and $\frac{ds}{dt} = 0$ holds respectively

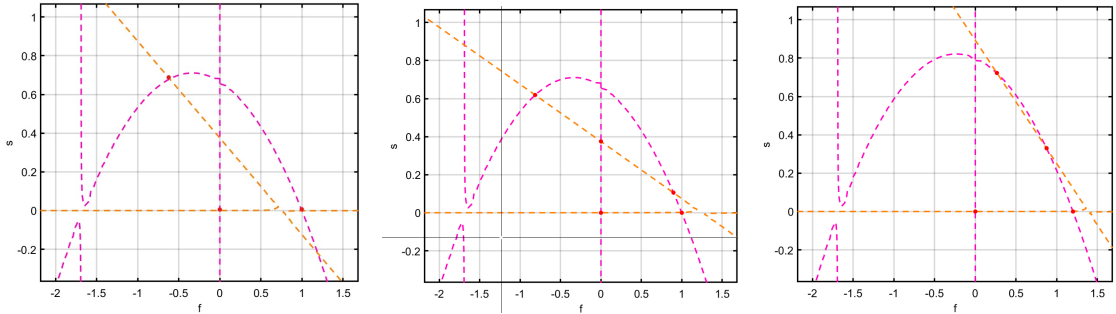


Figure 5.2: Nullclines for system (2.1) when $\alpha\sigma < 1$ holds.

The pink and the orange nullclines represents the values for which $\frac{df}{dt} = 0$ and $\frac{ds}{dt} = 0$ holds respectively

Now we that know for which f value the function $s(f)$ reaches its maximum, therefore substituting

this value of f into $s(f)$ to determines its maximum value

$$\begin{aligned}
s_{\max} &= s \left(\frac{1}{2\sigma}(\alpha\sigma - 1) \right) \\
&= \frac{1}{a} \left(\alpha - \frac{1}{2\sigma}(\alpha\sigma - 1) \right) \left(1 + \sigma \frac{1}{2\sigma}(\alpha\sigma - 1) \right) \\
&= \frac{1}{a} \left(\frac{2\alpha\sigma - \alpha\sigma + 1}{2\sigma} \right) \left(\frac{2 + \alpha\sigma - 1}{2} \right) \\
&= \frac{(\alpha\sigma + 1)^2}{4a\sigma}.
\end{aligned}$$

So we cannot study this system for values of s larger than this maximum value. Hence we will only look at $s \geq s_{\max}$ in our analysis. We would like to determine the critical values of system (5.2). The trivial point $(0, 0)$ is a critical value. If we combine $s = 0$ with $s = \frac{1}{a}(\alpha - f)(1 + \sigma f)$ we get $f = \alpha$ or $f = -\frac{1}{\sigma}$. This gives us critical values $(\alpha, 0)$ and $(-\frac{1}{\sigma}, 0)$. Now we want to combine $f = 0$ together with $s = \frac{1}{\mu}(\beta - bf)$, which gives $(0, \frac{\beta}{\mu})$. The last two critical points can be found by combining $s = \frac{1}{a}(\alpha - f)(1 + \sigma f)$ together with $s = \frac{1}{\mu}(\beta - bf)$. Just like for the system in section 4 we would like to determine the characters of these critical values. In order to do this we compute the Jacobian of system (5.2).

$$J(f, s) = \begin{pmatrix} \frac{\partial K}{\partial f} & \frac{\partial K}{\partial s} \\ \frac{\partial L}{\partial f} & \frac{\partial L}{\partial s} \end{pmatrix} = \begin{pmatrix} \alpha - 2f - \frac{as}{(1 + \sigma f)^2} & -\frac{af}{1 + \sigma f} \\ -bs & \beta - 2\mu s - bf \end{pmatrix}.$$

For this bi-stable front to exist we require that both of these critical values are stable nodes. First we determine the eigenvalues of the Jacobian evaluated in $(\alpha, 0)$.

$$J(\alpha, 0) = \begin{pmatrix} -\alpha & -\frac{a\alpha}{1 + \sigma\alpha} \\ 0 & \beta - b\alpha \end{pmatrix}.$$

Because this is a upper triangular matrix we can directly conclude that the eigenvalues are equal to $\lambda_1 = -\alpha < 0$ and $\lambda_2 = \beta - b\alpha$. We require that $\lambda_2 < 0$ holds. Hence we get the stability condition $\frac{\beta}{b} < \alpha$, which is the same condition as the one we found in section 3.

We repeat this for the critical value $(0, \frac{\beta}{\mu})$.

$$J\left(0, \frac{\beta}{\mu}\right) = \begin{pmatrix} \alpha - \frac{a\beta}{\mu} & 0 \\ -\frac{b\beta}{\mu} & -\beta \end{pmatrix}.$$

This gives eigenvalues $\lambda_1 = -\beta < 0$ and $\lambda_2 = \alpha - \frac{a\beta}{\mu}$. For the second eigenvalue to be negative, we need $\alpha\mu < a\beta$ to hold. So we have found these two conditions that are necessary for the bi-stable front to exist.

$$\frac{\beta}{b} < \alpha, \quad \alpha\mu < a\beta \tag{5.3}$$

5.1 Four dimensional system

Just like for the other system, we add diffusion terms to both equations.

$$\begin{cases} \frac{\partial F}{\partial t} = F(\alpha - F) - a \frac{SF}{1 + \sigma F} + \Delta F \\ \frac{\partial S}{\partial t} = S(\beta - \mu S) - bFS + \frac{1}{\epsilon^2} \Delta S. \end{cases} \quad (5.4)$$

To apply the geometric singular perturbation theory we want to rewrite this system again to system of four equations in the form (2.9). We are also looking for a wave solution, hence we take $F = F(x, t) = f(\xi)$ and $S = S(x, t) = s(\xi)$, with $\xi = x - ct$. Then we get a two dimensional system of second order ordinary differential equations

$$\begin{cases} \frac{d^2 f}{d\xi^2} = -c \frac{df}{d\xi} + f \left(f - \alpha + \frac{as}{1 + \sigma f} \right) \\ \frac{d^2 s}{d\xi^2} = \epsilon^2 \left[-c \frac{ds}{d\xi} + s(\mu s - \beta + bf) \right]. \end{cases} \quad (5.5)$$

Which can be rewritten into this four dimensional system by taking $p := \frac{df}{d\xi}$ and $q := \frac{1}{\epsilon} \frac{ds}{d\xi}$

$$\begin{cases} \frac{df}{d\xi} = p \\ \frac{dp}{d\xi} = -cp + f \left(f - \alpha + \frac{as}{1 + \sigma f} \right) \\ \frac{ds}{d\xi} = \epsilon q \\ \frac{dq}{d\xi} = \epsilon (-\epsilon c q + s(\mu s - \beta + bf)). \end{cases} \quad (5.6)$$

The values $(\alpha, 0, 0, 0)$ and $(0, 0, \frac{\beta}{\mu}, 0)$ are critical values for system (6.2). It can be shown that both of these critical values are saddles using the same analysis as before together with the bistability conditions (5.3).

5.2 Fast and slow sub-system

Again we want to apply geometric singular perturbation theory. We can use this theory because system (6.2) is of the form (2.10). We call this system the fast system. If we take the limit $\epsilon \rightarrow 0$ we get the system

$$\begin{cases} \frac{df}{d\xi} = p \\ \frac{dp}{d\xi} = -cp + f \left(f - \alpha + \frac{as}{1 + \sigma f} \right) \\ \frac{ds}{d\xi} = 0 \\ \frac{dq}{d\xi} = 0. \end{cases} \quad (5.7)$$

To get the slow system (2.12), we use a different scale, namely $\chi = \epsilon\xi$. We call this scale the slow scale. Then we get the following slow system

$$\begin{cases} \epsilon \frac{df}{d\chi} = p \\ \epsilon \frac{dp}{d\chi} = -cp + f \left(f - \alpha + \frac{as}{1 + \sigma f} \right) \\ \frac{ds}{d\chi} = q \\ \frac{dq}{d\chi} = -\epsilon cq + s(\mu s - \beta + bf). \end{cases} \quad (5.8)$$

We look at the $\epsilon \rightarrow 0$ limit, then we get the following system:

$$\begin{cases} 0 = p \\ 0 = -cp + f \left(f - \alpha + \frac{as}{1 + \sigma f} \right) \\ \frac{ds}{d\chi} = q \\ \frac{dq}{d\chi} = s(\mu s - \beta + bf) \end{cases} \quad (5.9)$$

The first equation gives $p = 0$, and the second one $f = 0$ or $f - \alpha + \frac{as}{1 + \sigma f} = 0$. This last equation can be rewritten into $s = \frac{1}{a}(\alpha - f)(1 + \sigma f)$. We can express this expression in terms of f by doing the following analysis.

$$\begin{aligned} s = \frac{1}{a}(\alpha - f)(1 + \sigma f) &\Rightarrow as = -\sigma f^2 - (1 - \alpha\sigma)f + \alpha \\ &\Rightarrow \sigma f^2 + (1 - \alpha\sigma)f - \alpha + as = 0 \\ &\Rightarrow f_{\pm} = \frac{\alpha\sigma - 1 \pm \sqrt{(\alpha\sigma - 1)^2 + 4\sigma(\alpha - as)}}{2\sigma} \end{aligned} \quad (5.10)$$

This implies that there are three critical points in the fast system, namely $(0, 0)$, $(f_+, 0)$ and $(f_-, 0)$. Now we want to define the critical manifolds. Because s describes the savanna biomass density, this variable must be positive.

$$\begin{aligned} \mathcal{M}_0^0 &= \{f = 0, p = 0, s, q \geq 0\}, \\ \mathcal{M}_0^+ &= \left\{ f = \frac{1}{2\sigma} \left(\alpha\sigma - 1 + \sqrt{(\alpha\sigma - 1)^2 + 4\sigma(\alpha - as)} \right), p = 0, s \geq 0, q \right\} \\ \mathcal{M}_0^- &= \left\{ f = \frac{1}{2\sigma} \left(\alpha\sigma - 1 - \sqrt{(\alpha\sigma - 1)^2 + 4\sigma(\alpha - as)} \right), p = 0, s \geq 0, q \right\} \end{aligned}$$

We would like to determine whether these critical manifolds are normally hyperbolic, so that we can use Fenichel's theorems. We first state the fast subsystem. Because $\frac{ds}{d\xi} = \frac{dq}{d\xi} = 0$ holds, we know that the value of s is constant for this system. Hence we take $s \equiv s_0$.

$$\begin{cases} \frac{df}{d\xi} = p \\ \frac{dp}{d\xi} = -cp + f \left(f - \alpha + \frac{as_0}{1 + \sigma f} \right) \end{cases} \quad (5.11)$$

The Jacobian of this system is equal to

$$J(f, p) = \begin{pmatrix} 0 & 1 \\ 2f - \alpha + \frac{as}{(1 + \sigma f)^2} & -c \end{pmatrix} \quad (5.12)$$

We would like to determine the characters of the critical points $(0, 0)$, $(f_-(s_0), 0)$ and $(f_+(s_0), 0)$. We remark that if we evaluate the Jacobian in $(0, 0)$, we get the same matrix as in (4.7). Hence we can conclude that the character of $(0, 0)$ is the same as the character of $(0, 0)$ for the fast subsystem in section 4. So for this system we also know that \mathcal{M}_0^0 is only normally hyperbolic whenever $s_0 > \frac{\alpha}{a}$ holds.

Now we evaluate the Jacobian in the critical values $(f_{\pm}(s_0), 0)$. We know that $s_0 = \frac{1}{a}(\alpha - f_{\pm})(1 + \sigma f_{\pm})$ holds for these values. So the evaluated Jacobian becomes

$$\begin{aligned} J(f_{\pm}(s_0), 0) &= \begin{pmatrix} 0 & 1 \\ 2f_{\pm}(s_0) - \alpha + \frac{(\alpha - f_{\pm}(s_0))(1 + \sigma f_{\pm}(s_0))}{(1 + \sigma f_{\pm}(s_0))^2} & -c \end{pmatrix} \\ &= \begin{pmatrix} 0 & 1 \\ 2f_{\pm}(s_0) - \alpha + \frac{\alpha - f_{\pm}(s_0)}{1 + \sigma f_{\pm}(s_0)} & -c \end{pmatrix}. \end{aligned}$$

The eigenvalues of this matrix are equal to $\lambda_{\pm} = \frac{1}{2} \left(-c \pm \sqrt{c^2 + 4 \left(2f_{\pm}(s_0) - \alpha + \frac{\alpha - f_{\pm}(s_0)}{1 + \sigma f_{\pm}(s_0)} \right)} \right)$.

These eigenvalues are only bounded away from the imaginary axis whenever the expression $2f_{\pm}(s_0) - \alpha + \frac{\alpha - f_{\pm}(s_0)}{1 + \sigma f_{\pm}(s_0)}$ is positive. This function is equal to zero on $f_{\pm}(s_0) = \frac{\alpha\sigma - 1}{2\sigma}$, this is exactly the value where s_0 reaches its maximum value. When $f_{\pm}(s_0)$ is smaller than $\frac{\alpha\sigma - 1}{2\sigma}$, then the expression is negative. Otherwise it is positive. So this expression is only positive on \mathcal{M}_0^+ , thus this critical manifold is normally hyperbolic. The manifold \mathcal{M}_0^- is not normally hyperbolic.

5.3 Heteroclinic orbit

We want to construct a front solution for this system as well. So we are again looking for a heteroclinic orbit from $(\alpha, 0, 0, 0)$ to $\left(0, 0, \frac{\beta}{\mu}, 0\right)$. We already found this heteroclinic orbit for $\sigma = 0$ in section (4), this orbit is depicted in figure 5.3. We naturally expect that this persists for $0 < \sigma \ll 1$. For the other two cases we are looking for a heteroclinic orbit as in figure 5.4.

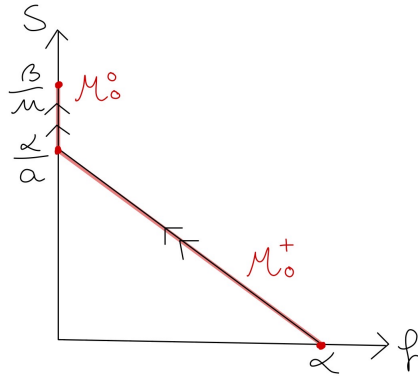


Figure 5.3: Heteroclinic orbit of system (6.2) for $0 < \sigma \ll 1$

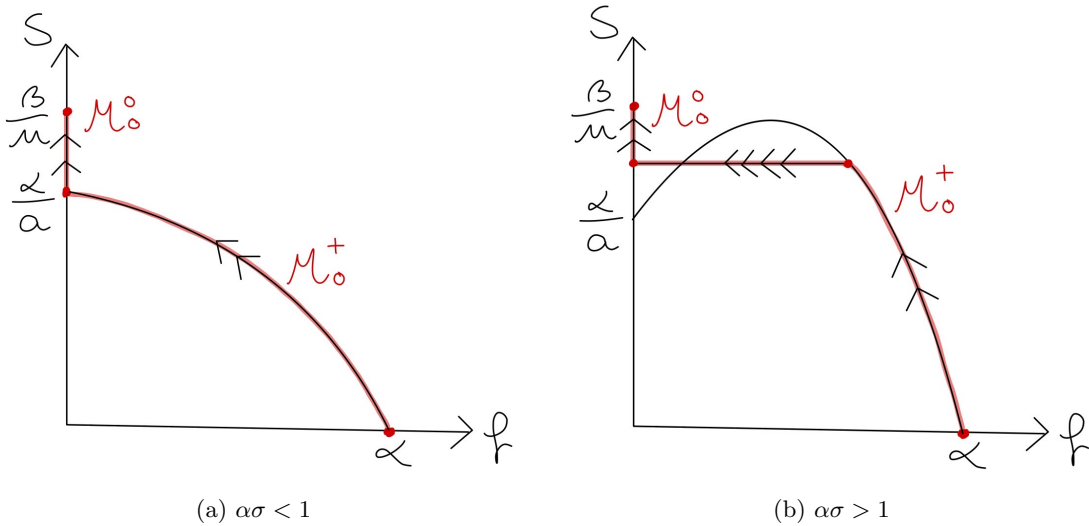


Figure 5.4: Heteroclinic orbit of system (6.2) for two different cases.

In figure 5.4a the heteroclinic connection is a fully slow orbit as the one in section (4). In this case there is no sharp transition in $f(\xi)$. This means that the forest thins out slowly towards the savanna. The heteroclinic connection figure 5.4b contains a jump from \mathcal{M}_0^+ to \mathcal{M}_0^0 in the $f - p$ space, this is called the fast jump. So this connection consists of a slow part, a fast jump and another slow part. The fast jump occurs at $s = s^*$ from $f = f^+(0)$ to $f = 0$. Because of the fast jump there is a sharp interface between a relatively dense forest and the savanna.

In this section we will focus on finding a heteroclinic connection as depicted in figure 5.4b that contains a fast jump, hence we take $\alpha\sigma > 1$. First we study the flow on the slow manifolds. Then we can see where this fast jump occurs. In other words, we would like to find out what the value of this s^* is.

On \mathcal{M}_0^0 we have $f = 0$, so on this invariant plane we have the following system

$$\begin{cases} \frac{ds}{dx} = q & = -\frac{\partial H}{\partial q} \\ \frac{dq}{dx} = s(\mu s - \beta) & = \frac{\partial H}{\partial s}, \end{cases} \quad (5.13)$$

which is the same as system (4.13). We have already concluded that this is a Hamiltonian system. Its Hamiltonian is equal to (4.14). We have also shown that the homoclinic orbit in figure 4.2 that goes from $\left(\frac{\beta}{\mu}, 0\right)$ to itself is equal to (4.15). We already determined the equation for the homoclinic orbit in (4.15).

On \mathcal{M}_0^+ we have $f = f_+ = \frac{1}{2\sigma} \left(\alpha\sigma - 1 + \sqrt{(\alpha\sigma - 1)^2 + 4\sigma(\alpha - as)} \right)$. If we substitute this f into system (5.9), we get (5.14).

$$\begin{cases} \frac{ds}{d\chi} = q \\ \frac{dq}{d\chi} = s(\mu s - \beta + bf_+) \end{cases} \quad (5.14)$$

We remark that it is really complicated to determine the Hamiltonian of this system. So we will not use the Hamiltonian to find out what the slow flow looks like on \mathcal{M}_0^+ , but we use MATLAB to analyse this numerically.

5.3.1 Orbit from $(0, 0)$ on \mathcal{M}_0^+

Eventually we want to find a heteroclinic connection from $(\alpha, 0, 0, 0)$ to $(0, 0, \frac{\beta}{\mu}, 0)$. This first critical value lies on \mathcal{M}_0^+ . We use numerical simulations to analyse the flow on this manifold. Because this system is not Hamiltonian we cannot use the Hamiltonian to plot the phase plane. We want to use the Matlab function `ode45` (MATLAB, 2010). This function integrates a system of differential equations of the form $\frac{df}{dt} = f(t, y)$ from t_0 to t_f with initial condition y_0 . We remark that our slow limit (5.14) on \mathcal{M}_0^+ is of this form. We implemented the equations of (5.14) in the Matlab code in A.4.2.2. Because we substituted f_+ into these equations we implemented this expression (5.10) into the Matlab `ode` A.4.2.3. In (A.4.2.1) we start by defining all of our parameters. Then we define the start- and end time by `tspan=[0 20]`. Lastly we define the initial condition `y0=[0 0.01]`. So we took $y_0 = (s_0, q_0) = (0, 0.01)$, this initial condition lies really close to $(\alpha, 0, 0, 0)$. We chose this initial condition because then we can see how the system behaves around $(0, 0)$. Then we use the line `[t,y] = ode45(@(t,y) eqns(y,P), tspan, y0)` to find the solution.

5.3.2 Combine dynamics of fast and slow system

We already know what the phase plane (4.2) looks like on \mathcal{M}_0^0 . We know that there is a homoclinic orbit from $\left(\frac{\beta}{\mu}, 0\right)$ back to itself. We check if we can find certain parameter values such that the homoclinic orbits on \mathcal{M}_0^0 and \mathcal{M}_0^+ intersect if we project them on the same plane. If we can find this intersection we call it (s^*, q^*) . Because if this is the case, there exists an orbit from $(\alpha, 0, 0, 0)$

to $(f_+(s^*), 0, s^*, q^*)$. Then we can look for the fast jump that goes from $(f_+(s^*), 0, s^*, q^*)$ to $(0, 0, s^*, q^*)$ in the $f - p$ space. Now the orbit is on the critical manifold \mathcal{M}_0^0 and then it follows the homoclinic orbit to $(0, 0, \frac{\beta}{\mu}, 0)$. We depicted what this heteroclinic orbit looks like in figure 5.5.

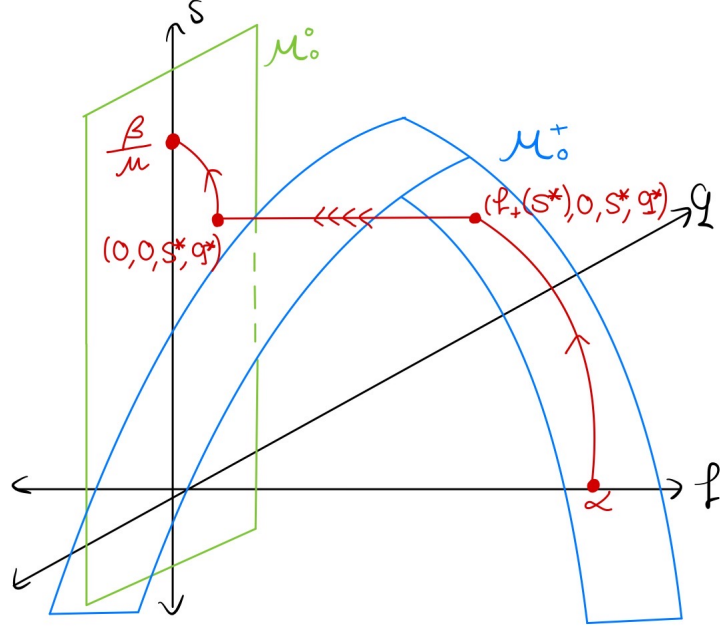


Figure 5.5: Heteroclinic connection from $(\alpha, 0, 0, 0)$ to $(0, 0, \frac{\beta}{\mu}, 0)$ for $\alpha\sigma > 1$.

5.3.3 Heteroclinic orbit in fast system

We want to find the fast jump that we saw in figure (5.5). So we take $s = s^*$ in the fast system. We already determined the critical points $(0, 0)$, $(f_-^*, 0)$, $(f_+^*, 0)$ of the fast system (5.15), with

$$f_{\pm}^* = f_{\pm}(s^*) = \frac{\alpha\sigma - 1 \pm \sqrt{(\alpha\sigma - 1)^2 + 4\sigma(\alpha - as^*)}}{2\sigma}.$$

In the $f - p$ space this heteroclinic connection goes from $(f_+^*, 0)$ to $(0, 0)$. We have determined the following fast system, by taking ϵ to zero.

$$\begin{cases} \frac{df}{d\xi} = p \\ \frac{dp}{d\xi} = -cp + f \left(f - \alpha + \frac{as}{1 + \sigma f} \right) \end{cases} \quad (5.15)$$

For this case we need $(0, 0)$ and $(f_+^*, 0)$ to be saddles and $(f_-^*, 0)$ to be a center, together with the condition $0 < f_-^* < f_+^*$. We also need f_-^* and f_+^* to be real values. Hence we know that the

following conditions must hold for the parameter values.

$$\begin{cases} \alpha\sigma > 1 \\ \alpha < as \\ (\alpha\sigma - 1)^2 > 4\sigma(as^* - \alpha) \end{cases} \quad (5.16)$$

We want to choose these parameters in such a way that this heteroclinic orbit from $(f_+^*, 0)$ to $(0, 0)$ exists.

5.3.4 Intersection of the orbits on \mathcal{M}_0^0 and \mathcal{M}_0^+

Now we would like to plot both homoclinic orbits on \mathcal{M}_0^0 and \mathcal{M}_0^+ in one plane. We already computed the equation of the homoclinic orbit (4.15) on \mathcal{M}_0^0 . We implemented this equation in A.4.2.1 as well. If we run the code we see that the orbit that goes from $(0, 0)$ on \mathcal{M}_0^+ shoots to infinity. That is why we shorten our running time to `tspan=[0 3]`. Then we get the following plot.

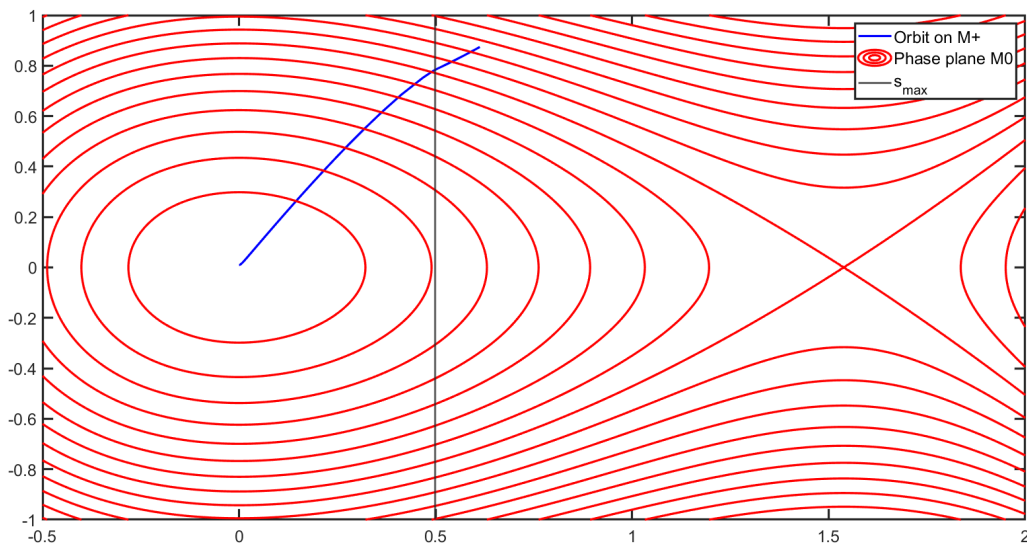


Figure 5.6: Intersection of orbit from $(0, 0)$ on \mathcal{M}_0^+ and the homoclinic orbit on \mathcal{M}_0^0 for parameter values $\alpha = 0.75$, $a = 2.8$, $\beta = 1$, $\mu = 0.65$, $b = 6$, $\sigma = 7$.

We can see that the orbits from $(0, 0)$ on \mathcal{M}_0^+ and from $\left(\frac{\beta}{\mu}, 0\right)$ on \mathcal{M}_0^0 intersect. The value of the intersection $(s^*, q^*) = (0.49, 0.77)$ is where the fast jump occurs. We know that the value of s cannot get bigger than $s_{\max} = \frac{(\alpha\sigma + 1)^2}{4a\sigma}$, which is approximately equal to 0.498. We remark that the value of s^* is smaller than this maximum value for s . Now we can substitute this value into the fast plane.

5.4 Fast jump

The fast system then becomes equal to

$$\begin{cases} \frac{df}{d\xi} = p \\ \frac{dp}{d\xi} = -cp + f \left(f - \alpha + \frac{0.49a}{1 + \sigma f} \right). \end{cases} \quad (5.17)$$

We would like to find a heteroclinic orbit from $(f_+^*, 0)$ to $(0, 0)$. Because our goal is to find a heteroclinic orbit as in figure 5.5. We found the value of s^* for certain parameter values, hence we need to choose the parameter values in the same way in the fast system. In order to find this orbit we use the Matlab function `ode45` again. We have implemented this function in the Matlab code A.4.3.1. We have found out that it is easier to find a heteroclinic orbit from $(0, 0)$ to $(f_+^*, 0)$. Hence we try to find this orbit and then take $\xi \rightarrow -\xi$. First we implement the equations in A.4.4. Then we can run our code. Just like for determining the homoclinic orbits on the slow manifolds we set the initial condition close to zero, so we set `y0 = [0.0001 0]`. Furthermore we choose our running time equal to 500, we implement this like `tspan = [0 500]`. We start by choosing $c = 0$, then we see in figure 5.7a that the solution shoots to infinity. If we choose this value a little bigger, $c = 0.5$, then we get the orbit in figure 5.7b. We see that this solution does not reach $(f_+^*, 0)$ and that it spirals to $(f_-^*, 0)$. Thus we know that there must exist a variable c in the interval $(0, 0.5)$ such that there exists a heteroclinic orbit. We call this value c^* .

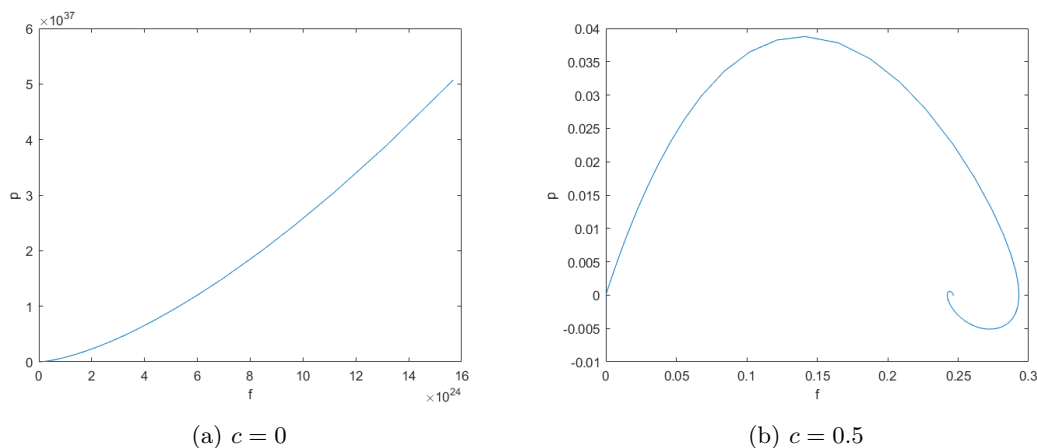


Figure 5.7: Orbit of (6.3) with initial condition close to $(0, 0)$ for different values of c .

Now we would like to vary c to see if we can find a heteroclinic solution. We use a for loop to do this, starting by the for loop `for i=0:0.01:0.5`. Then we can see what the solution looks like for $0, 0.01, 0.02, \dots, 0.5$. If we keep reducing the size of this interval and picking a smaller step-size, we get closer to the value of c^* . Repeating this procedure we find that c^* must lie in the interval $(0.20676, 0.20677)$. In the figures below we plotted the solutions for these values of c .

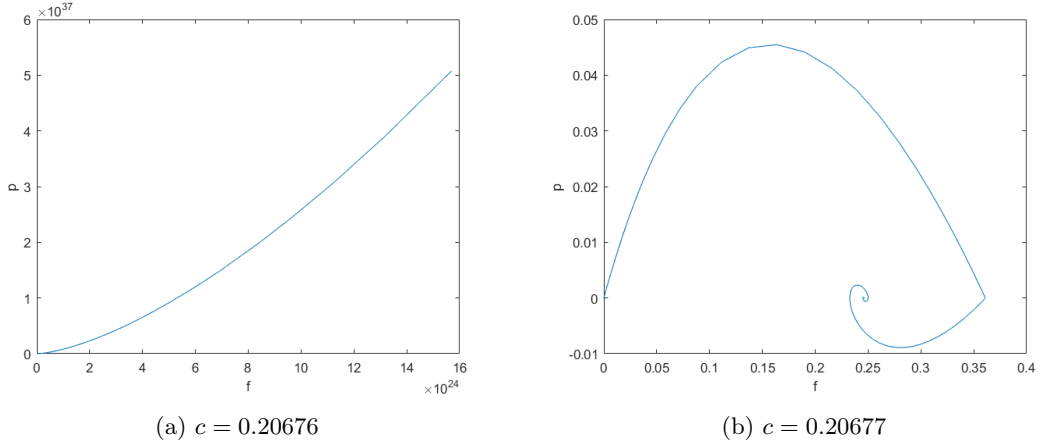


Figure 5.8: Orbit of (6.3) with initial condition close to $(0, 0)$ for different values of c .

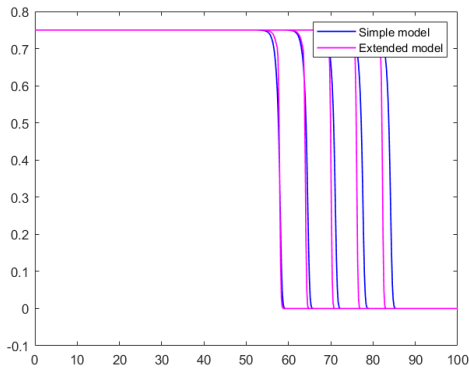
We see that the solution again shoots to infinity for $c = 0.20676$, if we add 0.00001 the solution spirals to $(f_+^*, 0)$. Hence we can conclude that for $c = c^* = 0.20676 + \mathcal{O}(10^{-6})$ there exists a heteroclinic orbit from $(f_+^*, 0)$ to $(0, 0)$. Therefore the heteroclinic orbit in figure 5.5 exists.

5.5 Finding the fast jump numerically

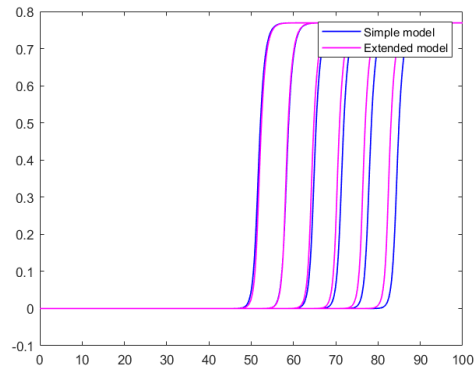
In this section we saw that the heteroclinic orbit for system (5.4) makes a fast jump. We are interested in finding out if that also happens numerically. Again we are looking for fronts, so it is sufficient to only look into one dimension. Hence system (5.4) becomes

$$\begin{cases} \frac{\partial f}{\partial t} = f \left(\alpha - f - \frac{as}{1 + \sigma f} \right) + \frac{\partial^2 f}{\partial x^2} \\ \frac{\partial s}{\partial t} = s(\beta - \mu s - bf) + \frac{1}{\epsilon^2} \frac{\partial^2 s}{\partial x^2}. \end{cases} \quad (5.18)$$

We can use the code that we used to solve (2.8), we only have to change the equations in `eqn.m` in A.1.2 and took $\epsilon^2 = 0.0005$. We plotted the solutions of this system at times $t = 10, 110, \dots, 510$. We also plotted the solutions of (2.8) in the same plot, so that we can compare the fronts.



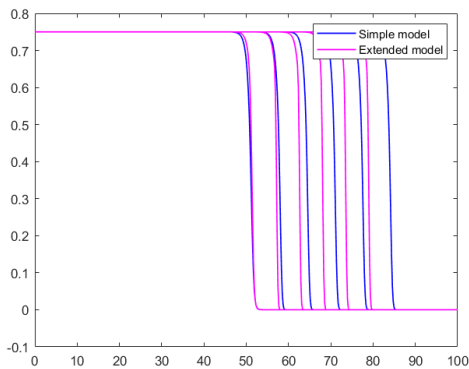
(a) Forest biomass solution.



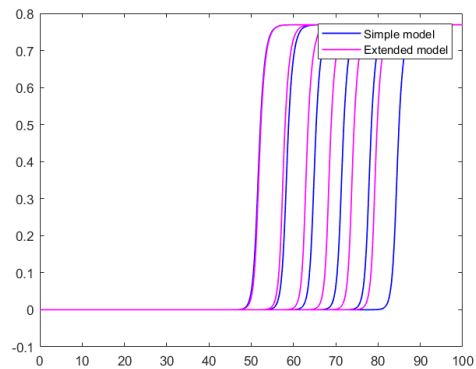
(b) Savanna biomass solution.

Figure 5.9: The blue and magenta plots represent the solutions of (2.8) and (5.18) respectively for parameter values $\alpha = 0.75$, $a = 1.12$, $\beta = 1$, $b = 4.5$, $\mu = 1.25$, $\sigma = 2.5$.

In figure 5.9a and 5.9b we plotted the solution of the forest- and the savanna biomass respectively. The solutions of (2.8) differ from the ones of (5.18). In this case we have $\alpha\sigma > 1$, in this case the critical manifolds of this system are shown in figure 5.4b. This is where the fast jump occurs. In the other case $\alpha\sigma < 1$ the critical manifolds are shown in 5.4a where the fast jump does not occur. So just like in figure 5.10 we plot the numerical solutions of (5.18), but now for $\sigma = 1.2$.



(a) Forest biomass solution.



(b) Savanna biomass solution.

Figure 5.10: The blue and magenta plots represent the solutions of (2.8) and (5.18) respectively for parameter values $\alpha = 0.75$, $a = 1.12$, $\beta = 1$, $b = 4.5$, $\mu = 1.25$, $\sigma = 1.2$.

In these plots it is hard to see if the fronts of the extended model (5.18) have a fast jump. In figure 5.11 we plotted the solution at $T = 500$ in the $f - s$ space. So we can compare them with the heteroclinic orbits in figures 5.3, 5.4a and 5.4b.

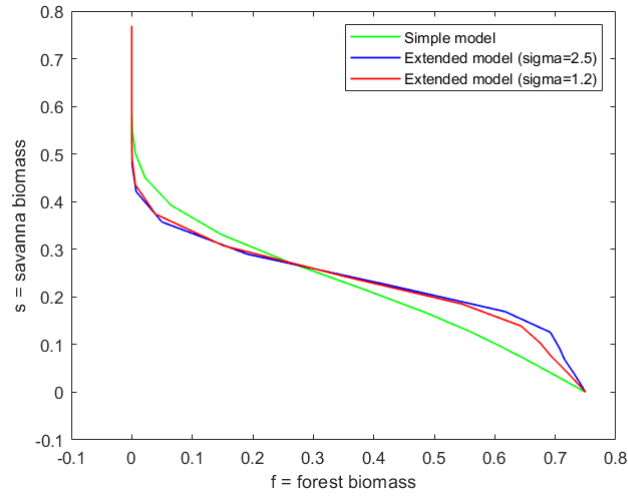


Figure 5.11: Solutions of (2.8) and (5.18) at $T = 500$ in the $f - s$ space. The green line is the solution of (2.8), the blue and red lines are the solutions of (5.18) for $\sigma = 2.5$ and $\sigma = 1.2$ respectively.

We remark that the solution of (2.8) looks like the heteroclinic orbit in figure 5.3. The solution of (5.18) for $\sigma = 1.2$ also looks like the heteroclinic orbit in 5.4a, this solution is more curved than the solution of (2.8). The blue line in figure 5.11 that represents the solution of (5.18) for $\sigma = 2.5$ should have a fast jump in 5.4b. We see that this solution reaches the s -axis faster than the other two solutions. But we don't see the sharp fast jump. This is because in 5.4b we took $\epsilon = 0$, now we took $\epsilon = \sqrt{0.0005}$. Hence we make an order ϵ error in these plots.

Chapter 6

Front (in-)stability

We alter the system a little. We change the term in front of the FS term in the S -equation. We are curious to see whether we can find the heteroclinic connection for this system. Furthermore, other dryland vegetation models that have been studied have generated vegetation patterns named fingering fronts. Front instability results in these vegetation fingers that grow into bare soil (Fernandez-Oto et al., 2019). So we would like to investigate whether this system gives a fingering front for a suitable parameter combination. The extended model becomes the following

$$\begin{cases} \frac{\partial F}{\partial t} = F(\alpha - F) - a \frac{SF}{1 + \sigma F} + \Delta F \\ \frac{\partial S}{\partial t} = S(\beta - \mu S) - \frac{bF - d}{F + 1} FS + \frac{1}{\epsilon^2} \Delta S. \end{cases} \quad (6.1)$$

Again we want to rewrite this system into a four dimensional system. We also take only one spatial variable and introduce a wave solution again. Analogue to the earlier models we get the following system

$$\begin{cases} \frac{df}{d\xi} = p \\ \frac{dp}{d\xi} = -cp + f \left(f - \alpha + \frac{as}{1 + \sigma f} \right) \\ \frac{ds}{d\xi} = \epsilon q \\ \frac{dq}{d\xi} = \epsilon \left(-\epsilon c q + s \left(\mu s - \beta + \frac{bf - d}{f + 1} f s \right) \right). \end{cases} \quad (6.2)$$

We also want to find a heteroclinic orbit for this system. To do this we look at the fast and the slow system again. The fast- and slow limits become

$$\begin{cases} \frac{df}{d\xi} = p \\ \frac{dp}{d\xi} = -cp + f \left(f - \alpha + \frac{as}{1 + \sigma f} \right), \end{cases} \quad (6.3)$$

$$\begin{cases} \frac{ds}{d\chi} = q \\ \frac{dq}{d\chi} = s \left(\mu s - \beta + \frac{bf-d}{f+1} fs \right). \end{cases} \quad (6.4)$$

The fast system is exactly the same as the fast system of the extended model in section 5. This also implies that we have the same critical manifolds \mathcal{M}_0^0 and \mathcal{M}_0^+ as in section 5.2. So we have the same conditions on the parameters for the heteroclinic orbit in the fast plane to exist. So our parameters have to meet the conditions (5.16). Because these systems are equal, we have the same condition for normal hyperbolicity as in section 5.

6.1 Intersection homoclinic orbits

Now we would like to determine the value of s^* for this model. So we try to determine the homoclinic orbits on both the manifolds \mathcal{M}_0^0 and \mathcal{M}_0^+ and find the intersection. We use the same Matlab codes to plot both homoclinic orbits. We have found the intersection in figure 6.1.

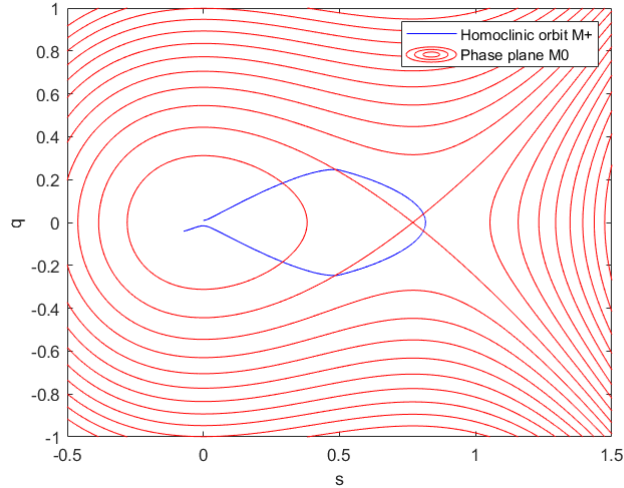


Figure 6.1: The phase plane on \mathcal{M}_0^0 together with homoclinic orbit on \mathcal{M}_0^+ of system (6.4). For parameter values $\alpha = 0.75$, $a = 2.8$, $\beta = 1$, $\mu = 1.3$, $b = 6$, $d = 1$, $\sigma = 7$.

The value of the intersection $(s^*, q^*) = (0.49, 0.25)$ is where the fast jump occurs. Now we can substitute this value into the fast plane.

6.2 Fast jump

We remark that the fast system is equal to the one in (6.3). We also see that the parameter values that we took for finding the intersection in figure 6.1 are equal to the ones that we took for the intersection in figure (5.6). Hence we know that we have the same fast jump as in section (5.4) and we know that for $c^* = c = 0.20676 + \mathcal{O}(10^{-6})$ there exists a heteroclinic orbit from $(f_+^*, 0)$ to $(0, 0)$. Therefore the heteroclinic orbit in figure 5.5 also exists for this system.

6.3 Condition for fingering fronts

In Carter, Doelman, Lilly, Overmayer, and Rao (2022) this general system of 2-component singularly perturbed reaction-diffusion equation is stated

$$\begin{cases} \tau \frac{\partial F}{\partial t} = \Delta F + M(F, S; \vec{P}) \\ \frac{\partial S}{\partial t} = \frac{1}{\epsilon^2} \Delta S + N(F, S; \vec{P}), \end{cases} \quad (6.5)$$

where $(x, y) \in \mathbb{R}^2$, $F(x, y, t), S(x, y, t) : \mathbb{R}^2 \times \mathbb{R}^+ \rightarrow \mathbb{R}$, $M(F, S; \vec{P})$ and $N(F, S; \vec{P})$ sufficiently smooth, $0 < \epsilon \ll 1$, and $\tau > 0$, $\vec{P} \in \mathbb{R}^m$, parameters (Carter et al., 2022). This paper assumes that system (6.5) has at least two stable homogeneous background states $(F(x, y, t), V(x, y, t)) \equiv (\bar{F}^\pm, \bar{S}^\pm)$. Then the travelling wave coordinate $\xi = x - ct$ is introduced, together with $f(\xi) = F(x, y, t)$ and $s(\xi) = S(x, y, t)$. This gives the following system of ordinary differential equations.

$$\begin{cases} \frac{\partial^2 f}{\partial \xi^2} = -c \frac{\partial f}{\partial \xi} - M(f, s, \vec{P}) \\ \frac{\partial^2 s}{\partial \xi^2} = -\epsilon^2 \left(c \frac{\partial s}{\partial \xi} + N(f, s, \vec{P}) \right) \end{cases} \quad (6.6)$$

Equation (6.5) is equal to the systems that we have analysed for these choices of τ, \vec{P}, M and N

$$\begin{aligned} \tau &= 1, \quad \vec{P} = (\alpha, a, \beta, \mu, b, d, \sigma, \sigma_S)^\top \\ M(f, s; \vec{P}) &= f(\alpha - f) - \frac{asf}{1 + \sigma f} \\ N(f, s; \vec{P}) &= s(\beta - \mu s) - sf \frac{bf - d}{f + 1}. \end{aligned}$$

For system (2.3) we have $\sigma = 0$ and $b = -d > 0$, for (5.4) $\sigma > 0$ and $b = -d > 0$ and for (6.1) $\sigma > 0$ and $d > 0$. Then the paper defines the following values

$$M_*(\vec{P}) = \int_{\mathbb{R}} M_s(f_*(\xi), s^*) f_{*,\xi}(\xi) e^{c_* \tau \xi} d\xi \quad (6.7)$$

$$N_*(\vec{P}) = N(f_*^+, s^*) - N(f_*^-, s^*) \quad (6.8)$$

where s^* is the value where the fast jump occurs. In our case the fast jump $f_*(\xi)$ goes from $f_*^+ = 0$ to $f_*^- = f_+(s^*) = f_*$, like in figure 5.4b. Then the following condition must hold for front instability (Carter et al., 2022)

$$-\text{sign}(M_*(\vec{P})) \times \text{sign}(N_*(\vec{P})) > 0 \quad (6.9)$$

Only in the case of front instability it is possible for the fronts to finger (Carter et al., 2022). The front solutions we found before are stable. Only when they are unstable, fingering could occur. We would like to determine such a condition for system (6.1). We start by determining the value of $M_*(\vec{P})$

$$\begin{aligned} M_*(\vec{P}) &= \int_{\mathbb{R}} \frac{\partial}{\partial s} \left(f_*(\alpha - f_*) - \frac{asf_*}{1 + \sigma f_*} \right) f_{*,\xi}(\xi) e^{c_* \tau \xi} d\xi \\ &= - \int_{\mathbb{R}} \frac{af_*}{1 + \sigma f_*} f_{*,\xi}(\xi) e^{c_* \tau \xi} d\xi \end{aligned}$$

We know that $f_* \leq 0$ holds, which implies that the term $\frac{af_*}{1 + \sigma f_*}$ is positive. $f_{*,\xi}(\xi)u$ is negative, because $f_*(\xi)$ is a decreasing function. We also know that $e^{c_*\xi}$ is positive. Hence we can conclude that $M_*(\vec{P}) > 0$ holds. Now we want to determine $N_*(\vec{P})$.

$$\begin{aligned} N_*(\vec{P}) &= N(0, s^*) - N(f_*^-, s^*) \\ &= s^*(\beta - \mu s^*) - \left(s^*(\beta - \mu s^*) - s^* f_+^* \frac{bf_+^* - d}{f_+^* + 1} \right) \\ &= s^* f_+(s^*) \frac{bf_+^* - d}{f_+^* + 1} \end{aligned}$$

We remark that the term $\frac{s^* f_+^*}{f_+^* + 1}$ is positive. We have also shown that $M_*(\vec{P})$ is positive. So the condition for instability (6.9) only holds whenever $bf_+^* - d < 0$ holds. Hence we can conclude that for fingering fronts to exist, we need $bf_+^* - d$ to be negative. We also remark that the term $\frac{bf-d}{f+1}$ is crucial for fingering fronts. Therefore we know that the fronts (2.3) and (5.4) will not finger.

We have found a heteroclinic connection in this chapter for certain parameter values and a certain value $c = c^*$. We are curious to see if the instability condition holds for these parameter values.

$$\begin{aligned} bf_+^* - d &= bf_+(s^*) - d \\ &= \frac{b}{2\sigma} \left(\alpha\sigma - 1 + \sqrt{(\alpha\sigma - 1)^2 + 4\sigma(\alpha - as^*)} \right) - d \\ &\approx 1.4616 > 0 \end{aligned}$$

Hence we know that the system will not give fingering fronts for these parameter values.

6.4 Numerical simulations in 2D (Still have to do these simulations for the second extended model)

In this section we want to do numerical simulations in two dimensions. We want to see if we get similar results as in the one dimensional case. Equation (6.1) is implemented in the Matlab code A.3. We define the solutions of (6.1) as matlab variables popS and popF. These are 100×100 matrices. In this code we have a two dimensional domain, we use spatial variables x and y . The domain we use is $(x, y) \in [0, 100] \times [0, 100]$, with $m = 100$ grid points for each variable. The running time is EndTime = 1000 with time step $dT = 1$. For the initial condition we use a two-dimensional front, which is defined in the following way:

$$\text{popF}_{ij} = \begin{cases} \alpha & , \text{ if } j < \frac{m}{2} \\ 0 & , \text{ if } j \geq \frac{m}{2}, \end{cases}$$

$$\text{popS}_{ij} = \begin{cases} 0 & , \text{ if } j < \frac{m}{2} \\ \frac{\beta}{\mu} & , \text{ if } j \geq \frac{m}{2}, \end{cases}$$

for every $i \in \{1, \dots, 100\}$. For the boundary conditions we use zero flux Neumann boundary conditions. So there is no flow in or out of the boundary in the x and in the y direction. Running

the Matlab code gives the following plots for the forest biomass in the $x - y$ plane, for different values of t .

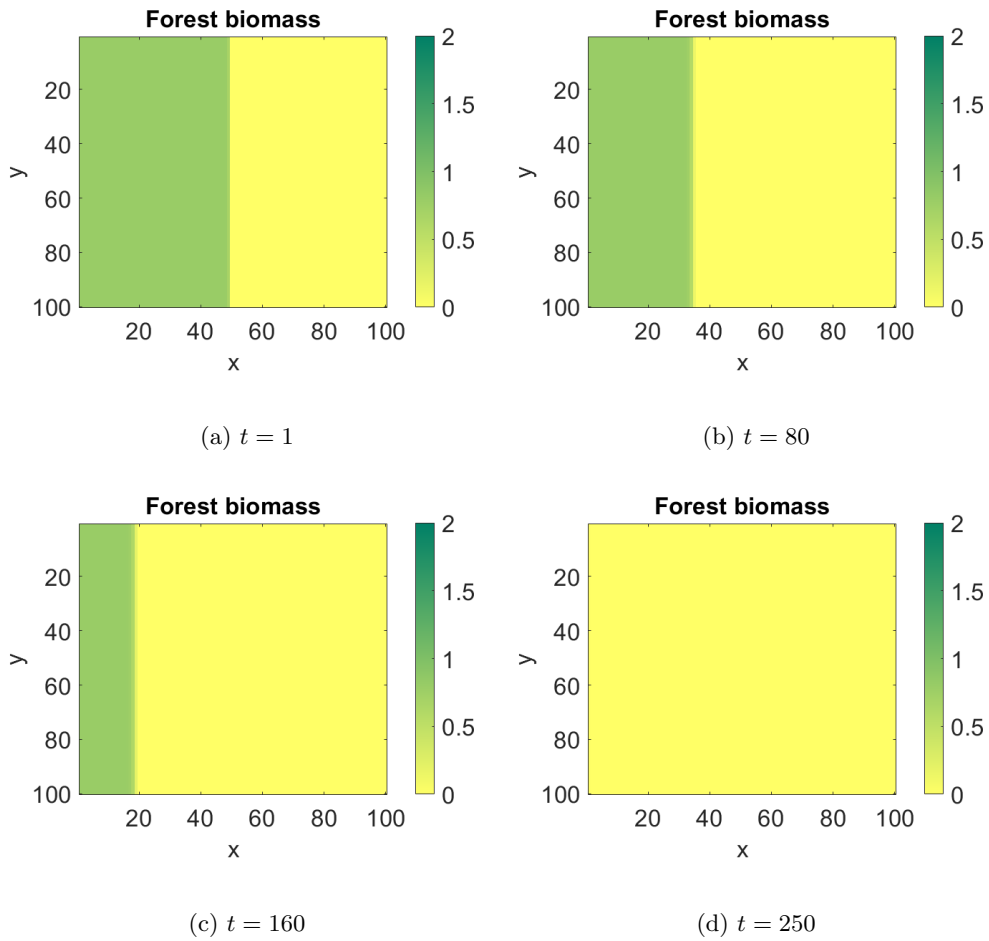


Figure 6.2: Forest biomass solution for different time values of (6.1), with parameter values: $\alpha = 0.8$, $a = 2.5$, $\beta = 1.5$, $\mu = 2.5$, $b = 5.25$, $d = 1$, $\sigma = 1$

If we plot the savanna biomass, we get the same figures. Except that the colors are interchanged. Which makes sense because for this front the savanna biomass decreases from a positive value to zero.

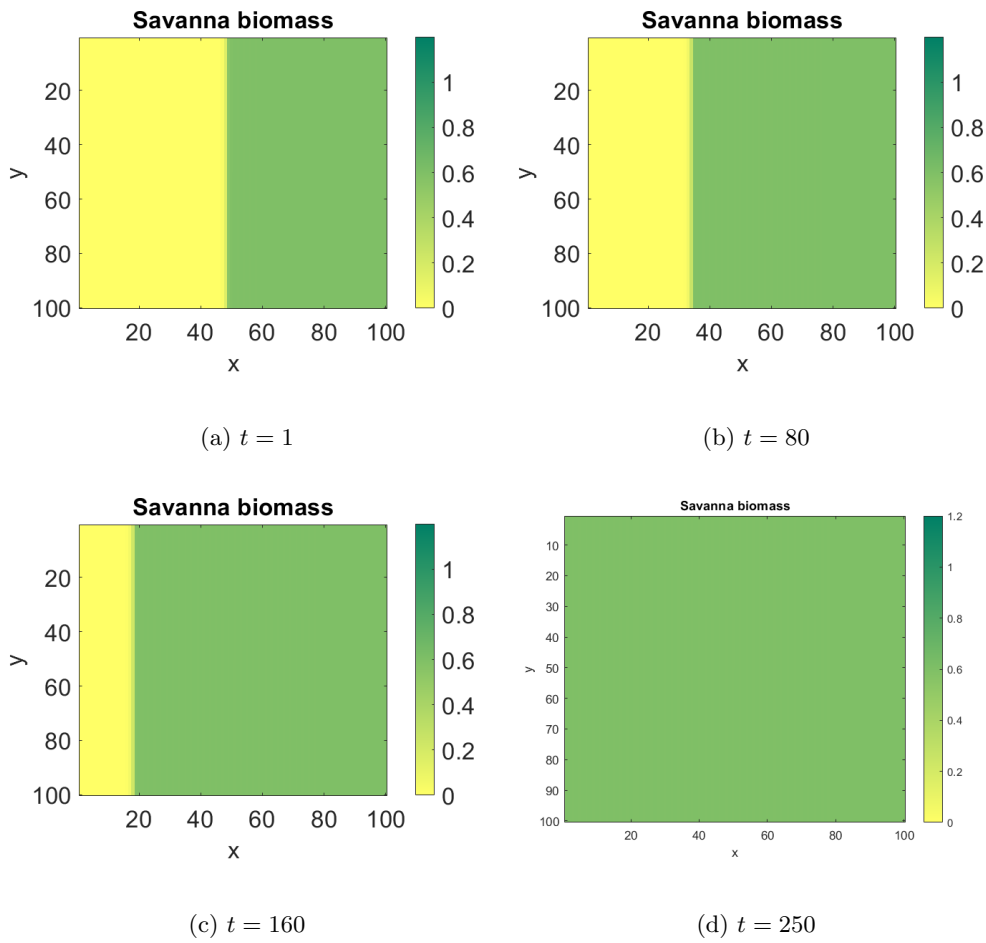


Figure 6.3: Savanna biomass solution for different time values of (6.1), with parameter values: $\alpha = 0.8$, $a = 2.5$, $\beta = 1.5$, $\mu = 2.5$, $b = 5.25$, $d = 1$, $\sigma = 1$

We see that the solution is a two-dimensional invasion front. For these parameter values the front moves to the right, which implies that the savanna biomass is invading the forest biomass for these parameter values.

We remark that these fronts are bi-stable, so these fronts do not finger. Varying the parameter values for system (6.1) did not result in these vegetation patterns. There may exist a parameter combination such that these patterns do exist, but we are not sure.

Chapter 7

Discussion

In this thesis, we have analysed system (1.1) that describes the savanna-forest transition zone. Because this model is a singularly perturbed system of differential equations with a clear separation in spatial scales, we were able to use geometric singular perturbation theory (Hek, 2009). We start by reducing the number of parameters by non-dimensionalising our system. Followed by the analysis of the two dimensional system of ordinary differential equation. We determined its critical points and plotted its phase plane. The critical points $(\alpha, 0)$ and $(0, \frac{\beta}{\mu})$ are stable. We are interested in finding a heteroclinic orbit that connects these points. This orbit represents the bi-stable front that has been observed in the tropics (Ametsitsi, 2021).

In section 2.3 we have introduced geometric singular perturbation theory. First we gave a basic set-up and defined the slow and fast limit systems. Afterwards we stated Fenichel's first and second theorem that uses the knowledge of the limit systems to understand the full system (Fenichel, 1979). We applied this theory to our system in section 4. In this section we added a diffusion term, introduced the wave solution and rewrote the system into a four dimensional system of first order ordinary differential equations. Because of the clear separation in spatial scales we were able to split this system into two systems, the fast and the slow system. These systems are both two dimensional. By analysing these systems and combining their dynamics using geometric singular perturbation theory we found the heteroclinic orbit that we were looking for. We found a condition for which this orbit exist, with wave-speed zero. So we found a standing front analytically. Furthermore, we also found a travelling front numerically.

We continued with extending the model. In the extended model we added a saturation term. For large values of F this term saturates. This is a reflection of the limited savanna- and forest capability, when one of these biomes are abundant (Murray, 2002). Again we use geometric singular perturbation theory on these equations to find a heteroclinic orbit that represents the bi-stable front. We were able to find a heteroclinic connection that represents the bi-stable fronts. This orbit consists of a slow part on the two slow manifolds that are connected with a fast jump on the fast plane. We found this connection for a certain wavespeed c^* . We also performed numerical simulations for this system using Matlab.

Lastly we made a second extension on the model, because we wanted to see if we could find fingering fronts for this model. These patterns have been observed in other models. We used a different term instead of the saturation term in the S -equation. This also resulted in finding the

heteroclinic orbit that we were looking for. Then we used Atassi (n.d.) to derive a condition for when fingering fronts exist for this model. Unfortunately the parameter choices that we made for finding the heteroclinic connection does not meet this condition. So we know that this will not result in fingering fronts. It is hard to find parameter values such that the heteroclinic orbit exists, especially when you have to take the stability condition into account. This is because this condition depends on f_+^* , which you can find after you have already found the heteroclinic connection. We have also done some two-dimensional simulations in this section, unfortunately we have not found fingering fronts.

Because we have found a bi-stable front solution for the unextended and two extended models, we can conclude that these models describe the savanna-forest boundary properly.

These results are promising, it gives insight in the ecology, but a lot has to be considered. Because the models, especially the extended model, are complicated it is hard to find a solution. Hence it is difficult to predict how this savanna-forest will evolve over time. A logical research suggestion would be to analyse the system analytically in two dimensions. We also assumed that our domain Ω is one dimensional, because we can already get a lot of information of the systems for this assumption. But actually this area is two dimensional. Hence it would be interesting to find out what solutions for these systems will look like in this case even if it makes the problem more complicated.

We have found bi-stable fronts for these models and we have derived a condition that may result in fingering fronts. Further research could result in finding a front solution that will give fingering fronts. A way to do this may be to follow the procedure as in section 6 and choose the parameters in such a way that the instability condition holds.

Another research suggestion could be to change the model (6.1) such that the instability condition can still hold. We chose equation (6.1) for mathematical reasons. But changing the model such that it makes more sense ecologically, would give better insight in the savanna-forest transition zone.

Further studies could result in finding a more precise solution for this system, so we might get a better insight in how the savanna-forest boundary will evolve over time. This could lead to finding precautionary measures that will slow down the desertification process.

References

- Ametsitsi, G. (2021). *A study of drivers and dynamics of forest-savanna boundaries in west africa* (Doctoral dissertation, Wageningen University). (WU thesis 7764 Includes bibliographical references. - With summaries in English and Dutch) doi: 10.18174/539002
- Atassi, H. M. (n.d.). *Class notes on quasilinear partial differential equations*. University of Notre Dame.
- Bel, G., Hagberg, A., & Meron, E. (2012, 11). Gradual regime shifts in spatially extended ecosystems. *Theoretical Ecology*, 5. doi: 10.1007/s12080-011-0149-6
- Berry, R. S., & Kulmatiski, A. (2017, 04). A savanna response to precipitation intensity. *PLOS ONE*, 12(4), 1-18. Retrieved from <https://doi.org/10.1371/journal.pone.0175402> doi: 10.1371/journal.pone.0175402
- Bonan, G. B. (2008). Forests and climate change: Forcings, feedbacks, and the climate benefits of forests. *Science*, 320, 1444-1449. doi: 10.1126/science.1155121
- Braun, M. (1983). *Differential equations and their applications*. New York: Springer.
- Carter, P., Doelman, A., Lilly, K., Overmayer, E., & Rao, S. (2022). Criteria for the (in)stability of planar interfaces in singularly perturbed 2-component reaction-diffusion equations.
- Cuni-Sanchez, A., White, L. J. T., Calders, K., Jeffery, K. J., Abernethy, K., Burt, A., ... Lewis, S. L. (2016). African savanna-forest boundary dynamics: A 20-year study. *PLOS ONE*, 11, 1-23. Retrieved from <https://doi.org/10.1371/journal.pone.0156934> doi: 10.1371/journal.pone.0156934
- Doelman, A. (n.d.). Pattern formation in reaction-diffusion systems — an explicit approach. In *Complexity science* (p. 129-182). Retrieved from https://www.worldscientific.com/doi/abs/10.1142/9789813239609_004 doi: 10.1142/9789813239609_004
- D. Schwartz, A. M. J. B. e. a., H. De Foresta. (2013). Present dynamics of the savanna-forest boundary in the congolese mayombe: a pedological, botanical and isotopic (¹³C and ¹⁴C) study. , 106, 516-524.
- Fenichel, N. (1979). Geometric singular perturbation theory for ordinary differential equations. *Journal of Differential Equations*, 31(1), 53-98. Retrieved from <https://www.sciencedirect.com/science/article/pii/0022039679901529> doi: [https://doi.org/10.1016/0022-0396\(79\)90152-9](https://doi.org/10.1016/0022-0396(79)90152-9)
- Fernandez-Oto, C., Tzuk, O., & Meron, E. (2019). Front instabilities can reverse desertification. *Phys. Rev. Lett.*, 122, 048101. Retrieved from <https://link.aps.org/doi/10.1103/PhysRevLett.122.048101> doi: 10.1103/PhysRevLett.122.048101
- Gillison, A. (1983, 01). Gillison. a.n. (1983). tropical savannas of australia and the south-west pacific. in: F. bourlière (ed.) 'tropical savannas', in: D.w. goodall (ed.-in-chief) 'ecosystems of the world' 13, 183-243. (elsevier, amsterdam). In (p. 183-243).

- Goel, N. (2020). *High elevation savanna-forest mosaics, commonly referred to as shola grasslands, in human-dominated regions of western ghats, karnataka, india*. Retrieved from <https://www.annat.org/an/newpapers/May-Goel.html>
- Goel, N., Guttal, V., Levin, S., & Staver, C. (2018, 11). Dispersal increases the resilience of tropical savanna and forest distributions:. doi: 10.1101/476184
- Grace, J., José, J. S., Meir, P., Miranda, H. S., & Montes, R. A. (2006). Productivity and carbon fluxes of tropical savannas. *Journal of Biogeography*, 33(3), 387-400. Retrieved from <https://onlinelibrary.wiley.com/doi/abs/10.1111/j.1365-2699.2005.01448.x> doi: <https://doi.org/10.1111/j.1365-2699.2005.01448.x>
- Hek, G. (2009). Geometric singular perturbation theory in biological practice. *Journal of mathematical biology*, 60, 347-86. doi: 10.1007/s00285-009-0266-7
- Janssen, T., Ametsitsi, G., Collins, M., Adu-Bredu, S., Oliveras, I., Mitchard, E., & Veenendaal, E. (2018). Extending the baseline of tropical dry forest loss in ghana (1984–2015) reveals drivers of major deforestation inside a protected area.
- Kershaw, A. (1992). The development of rainforest-savanna boundaries in tropical australia. , 255-271. <https://eurekamag.com/research/033/754/033754704.php>.
- MATLAB. (2010). *version r2022a*. Natick, Massachusetts: The MathWorks Inc.
- Meiss, J. (2017). *Differential dynamical systems, revised edition*. Society for Industrial and Applied Mathematics. Retrieved from <https://books.google.nl/books?id=TqEJDgAAQBAJ>
- Mitchard, E. T. A., & Flintrop, C. M. (2013). Woody encroachment and forest degradation in sub-saharan africa's woodlands and savannas 1982–2006. *Philosophical Transactions of the Royal Society B: Biological Sciences*, 368(1625), 20120406. Retrieved from <https://royalsocietypublishing.org/doi/abs/10.1098/rstb.2012.0406> doi: 10.1098/rstb.2012.0406
- Murray, J. D. (2002). *Mathematical biology i. an introduction* (3rd ed., Vol. 17). New York: Springer. doi: 10.1007/b98868
- Oliveras, I., & Malhi, Y. (2016). Many shades of green: the dynamic tropical forest-savannah transition zones. *Philosophical Transactions of the Royal Society B: Biological Sciences*, 371(1703), 20150308. Retrieved from <https://royalsocietypublishing.org/doi/abs/10.1098/rstb.2015.0308> doi: 10.1098/rstb.2015.0308
- Solbrig, O. T. (1996). The diversity of the savanna ecosystem. In O. T. Solbrig, E. Medina, & J. F. Silva (Eds.), *Biodiversity and savanna ecosystem processes: A global perspective* (pp. 1–27). Berlin, Heidelberg: Springer Berlin Heidelberg. Retrieved from https://doi.org/10.1007/978-3-642-78969-4_1 doi: 10.1007/978-3-642-78969-4_1
- Staver, C. (2011).
- Wiggins, S. (1990). *Introduction to applied nonlinear dynamical systems and chaos*. New York: Springer.
- Zelnik, Y. R., & Meron, E. (2018). Regime shifts by front dynamics. *Ecological Indicators*, 94, 544-552. Retrieved from <https://www.sciencedirect.com/science/article/pii/S1470160X17307057> doi: <https://doi.org/10.1016/j.ecolind.2017.10.068>

Appendix A

Matlab codes

A.1 Unextended model

A.1.1 Main code for using pdepe

This Matlab code uses pdepe to determine the solution of (2.8).

```
1 %PDE: MATLAB script M-file that solves the PDE
2 % u=(u1,u2)=(s,f)
3 m = 0;
4
5 %% Parameters for forest invading the savanna
6 % P(1) = 0.75;           %alpha
7 % P(2) = 1.12;         %a
8 % P(3) = 1;            %beta
9 % P(4) = 4.5;          %b
10 % P(5) = 1.25;         %mu
11
12
13 %% Parameters for savanna invading the forest
14 P(1) = 0.5;           %alpha
15 P(2) = 2.26;         %a
16 P(3) = 1.5;          %beta
17 P(4) = 5.25;         %b
18 P(5) = 2.5;          %mu
19
20 %% Here we define the other variables
21 T = 510;              %End time
22 L = 100;              %Domain [0,L]
23 P(6) = L;             %We want to use L in initial.m
24
25 t=linspace(0,T,510); %tspan
26 x=linspace(0,L,510); %xmesh
27
28 %% Using pdepe to solve the system
29 sol = pdepe(m,@eqn,@initial,@bc,x,t,[],P); %Determine solution
30 u1 = sol(:, :, 1);   %Solution forest biomass
```

```

31 u2 = sol(:, :, 2); %Solution savanna biomass
32
33 %% Plotting solutions
34 for i=10:100:510
35 figure(1)
36 plot(x,u1(i,:), 'green', 'LineWidth', 1) %Plot solution forest biomass
37 hold on
38 plot(x,u2(i,:), 'red', 'LineWidth', 1) %Plot solution savanna biomass
39 drawnow
40 end
41 xlabel('Distance x')
42 ylabel('Biomass')
43 legend('Forest', 'Savanna')
44
45 %% Plotting initial conditions
46 figure(2)
47 plot(x,u1(1,:), 'green') %Plot initial condition forest biomass
48 hold on
49 plot(x,u2(1,:), 'red') %Plot initial condition savanna biomass
50 drawnow
51 xlabel('Distance x')
52 ylabel('Biomass')
53 legend('Forest', 'Savanna')
54
55 figure(5)
56 plot(u1(i,:), u2(i,:), 'green', 'LineWidth', 1) %Plot solution forest biomass

```

A.1.2 Defining equations for pdepe

The equations of (2.8) are implemented in this code.

```

1 function [c, b, s] = eqn(x, t, u, DuDx, P)
2 %EQN2: MATLAB M-file that contains the coefficients for
3 %a system of two PDE in time and one space dimension.
4
5 fo = u(1); %forest variable
6 sa = u(2); %savanna variable
7
8 c = [1; 1]; %function omega
9 b = [0.005; 1] .* DuDx; %function varphi
10 s = [fo*(P(1)-fo-P(2)*sa);
11      sa*(P(3)-P(4)*fo-P(5)*sa)]; %function psi

```

A.1.3 Defining initial condition for pdepe

```

1 function value = initial(x, P);
2 %INITIAL2: MATLAB function M-file that defines initial conditions
3 %for a system of two PDE in time and one space variable.
4
5 f=1/2*(1+tanh(-x+1/2*P(6))); %Initial condition (front) forest biomass
6 s=1/2*(1+tanh(x-1/2*P(6))); %Initial condition (front) savanna biomass
7
8 value=[f; s]; %Return initial condition

```


A.1.4 Defining boundary conditions for pdepe

```

1 function value = initial(x,P);
2 %INITIAL2: MATLAB function M-file that defines initial conditions
3 %for a system of two PDE in time and one space variable.
4
5 f=1/2*(1+tanh(-x+1/2*P(6))); %Initial condition (front) forest biomass
6 s=1/2*(1+tanh(x-1/2*P(6))); %Initial condition (front) savanna biomass
7
8 value=[f;s]; %Return initial condition

```

A.1.5 Finding still front

```

1 %PDE: MATLAB script M-file that solves the PDE
2 % u=(u1,u2)=(s,f)
3 m = 0;
4
5 %Parameters
6 %% Forest invading the savanna
7 P(1) = 0.75; %alpha
8 P(2) = 1.12; %a
9 P(3) = 1; %beta
10 P(5) = 1.25; %amu
11
12 %% Here we define the other variables
13 T = 500; %End time
14 L = 100; %Domain [0,L]
15 P(6) = L; %We want to use L in initial.m
16
17 t=linspace(0,T,500); %tspan
18 x=linspace(0,L,500); %xmesh
19
20 %% Determine solution
21 C = {'k','b','r','g','y',[.5 .6 .7],[.8 .2 .6]} %Define different colors
22
23 for i=-0.1:0.01:0 %For loop with time step 0.01
24 %for i=-0.045:0.001:-0.035 %For loop with time step 0.001
25 P(4)= (P(2)^2*P(3)^3)/(P(5)^2*P(1)^3)+i; %Add i to b
26 sol = pdepe(m,@eqn,@initial,@bc,x,t,[],P); %Determine solution
27 %for b=b+1
28 u1 = sol(:,:,1); %Solution forest biomass
29 u2 = sol(:,:,2); %Solution savanna biomass
30 figure(3)
31 plot(x,u1(i,:), 'green', 'LineWidth', 1) %Plot solution forest biomass
32 hold on
33 plot(x,u2(i,:), 'red', 'LineWidth', 1) %Plot solution savanna biomass
34 drawnow
35 end
36 plot(x,u1(20,:), '—', 'LineWidth', 1.5) %Plot solution for t=20
37 hold on
38 plot(x,u2(20,:), '—', 'LineWidth', 1.5) %Plot solution for t=20
39 xlabel('Distance x')
40 ylabel('Biomass')
41 drawnow

```

A.2 Extended model: saturation term in F- and S-equation

```

1  %PDE: MATLAB script M-file that solves the PDE
2  % u=(u1,u2)=(s,f)
3  m = 0;
4
5  %% Parameters for forest invading the savanna
6  P(1) = 0.75;           %alpha
7  P(2) = 1.12;          %a
8  P(3) = 1;             %beta
9  P(4) = 4.5;           %b
10 P(5) = 1.25;          %amu
11 P(7) = 2.5;           %sigma
12
13 %% Here we define the other variables
14 T = 500;               %End time
15 L = 100;               %Domain [0,L]
16 P(6) = L;              %We want to use L in initial.m
17
18 t=linspace(0,T,500);   %tspan
19 x=linspace(0,L,500);   %xmesh
20
21 %% Using pdepe to solve the system
22 %This gives the solution of the unextended model
23 sol = pdepe(m,@eqnold,@initial,@bc,x,t,[],P); %Determine solution
24 u1 = sol(:,:,1);       %Solution forest biomass
25 u2 = sol(:,:,2);       %Solution savanna biomass
26
27 %This gives the solution of the extended model for sigma=2.5
28 sol2 = pdepe(m,@eqn,@initial,@bc,x,t,[],P); %Determine solution
29 w1 = sol2(:,:,1);      %Solution forest biomass
30 w2 = sol2(:,:,2);      %Solution savanna biomass
31
32 %This gives the solution of the extended model for sigma=1.2
33 P(7) = 1.2;             %sigma
34 sol3 = pdepe(m,@eqn,@initial,@bc,x,t,[],P); %Determine solution
35 v1 = sol3(:,:,1);      %Solution forest biomass
36 v2 = sol3(:,:,2);      %Solution savanna biomass
37
38 %% Plotting solutions
39 %Plot forest biomass solution (sigma=2.5)
40 for i=1:100:500
41 figure(1)
42 plot(x,u1(i,:), 'blue', 'linewidth',1) %Plot solution forest biomass
43 hold on
44 plot(x,w1(i,:), 'magenta', 'linewidth',1) %Plot solution forest biomass
45 drawnow
46 end
47 xlabel('Distance x')
48 ylabel('Biomass')
49 legend('Simple model', 'Extended model')
50
51 %Plot savanna biomass solution (sigma=2.5)
52 for i=1:100:500

```

```

53 figure(2)
54 plot(x,u2(i,:), 'blue', 'linewidth',1)           %Plot solution savanna biomass
55 hold on
56 plot(x,w2(i,:), 'magenta', 'linewidth',1)       %Plot solution savanna biomass
57 drawnow
58 end
59 xlabel('Distance x')
60 ylabel('Biomass')
61 legend('Simple model', 'Extended model')
62
63 %Plot forest biomass solution (sigma=1.2)
64 for i=1:100:500
65 figure(3)
66 plot(x,u1(i,:), 'blue', 'linewidth',1)           %Plot solution forest biomass
67 hold on
68 plot(x,v1(i,:), 'magenta', 'linewidth',1)       %Plot solution forest biomass
69 drawnow
70 end
71 xlabel('Distance x')
72 ylabel('Biomass')
73 legend('Simple model', 'Extended model')
74
75 %Plot savanna biomass solution (sigma=1.2)
76 for i=1:100:500
77 figure(4)
78 plot(x,u2(i,:), 'blue', 'linewidth',1)           %Plot solution savanna biomass
79 hold on
80 plot(x,v2(i,:), 'magenta', 'linewidth',1)       %Plot solution savanna biomass
81 drawnow
82 end
83 xlabel('Distance x')
84 ylabel('Biomass')
85 legend('Simple model', 'Extended model')
86
87 figure(5)
88 plot(u1(i,:), u2(i,:), 'green', 'LineWidth', 1) %f-s plot simple model
89 hold on
90 plot(w1(i,:), w2(i,:), 'blue', 'LineWidth', 1) %f-s plot extended model
91 hold on
92 plot(v1(i,:), v2(i,:), 'red', 'LineWidth', 1) %f-s plot extended model
93 drawnow
94 xlabel('f = forest biomass')
95 ylabel('s = savanna biomass')
96 legend('Simple model', 'Extended model', 'Extended model')

```

A.3 Unextended model 2D

```

1 % Rietkerk 2002 AmNat
2 clear all
3
4 %% System discretisation
5 DeltaX=101;           % (m)
6 DeltaY=101;           % (m)

```

```

7
8 DifS=1000; % (m2 d-1)
9 DifF=1; % (m2 d-1)
10
11 %% Parameter values
12 P(1) = 0.8; %alpha
13 P(2) = 2.5; %a
14 P(3) = 1.5; %beta
15 P(4) = 5.25; %b
16 P(5) = 2.5; %mu
17 P(6) = 1; %sigma
18 P(7) = 1; %d
19
20 %% Number of grid cells
21 m=100;
22 NX=m;
23 NY=m;
24
25 %% Timesteps
26 dT=1; %timestep
27 Time=1; % begin time
28 EndTime=1000; % end time
29 PlotStep=1; % (d)
30 PlotTime=PlotStep; % (d)
31 count=1;
32
33 % Initialisation
34 popS = zeros(m,m);
35 popF = zeros(m,m);
36
37 dS=zeros(m,m);
38 dF=zeros(m,m);
39
40 NetS=zeros(m,m);
41 NetF=zeros(m,m);
42
43 %% Boundary conditions
44 FYS = zeros(NY+1,NX); % bound.con. no flow in/out to Y-direction
45 FXS = zeros(NY,NX+1); % bound.con. no flow in/out to X-direction
46 FYF = zeros(NY+1,NX); % bound.con. no flow in/out to Y-direction
47 FXF = zeros(NY,NX+1); % bound.con. no flow in/out to X-direction
48
49 %% Initial state
50 for i=1:m
51     for j=1:m
52         if(j<m/2)
53             popS(i,j)=0; % Homogeneous equilibrium surface water in
                    absence of plants
54             popF(i,j)=P(1); % Homogeneous equilibrium soil water
                    in absence of plants
55         else
56             popS(i,j)=P(3)/P(5); % Homogeneous equilibrium surface water
                    in absence of pla

```

```

57         popF(i,j)=0;           % Homogeneous equilibrium soil water in
                                absence of plants
58     end
59 end
60 end
61
62 %% Timesteps
63 while Time<=EndTime
64
65     dF=popF.*(P(1)-popF-P(2).*popS./(1+P(6).*popF));
66     dS=popS.*(P(3)-P(5).*popS-popF.*(P(4).*popF-P(7))./(popF+1));
67
68     %% Diffusion: calculate Flow in x direction: Flow= -D*dpopF/dx
69     FXS(1:NY,2:NX)= -DifS.*(popS(1:NY,2:NX)-popS(1:NY,1:NX-1))./DeltaX;
70     FXF(1:NY,2:NX)= -DifF.*(popF(1:NY,2:NX)-popF(1:NY,1:NX-1))./DeltaX;
71
72     %% Calculate the flow in y direction: Flow= -D*dpopF/dy
73     FYS(2:NY,1:NX)= -DifS.*(popS(2:NY,1:NX)-popS(1:NY-1,1:NX))./DeltaY;
74     FYF(2:NY,1:NX)= -DifF.*(popF(2:NY,1:NX)-popF(1:NY-1,1:NX))./DeltaY;
75
76     %% Calculate net flow
77     NetS(1:NY,1:NX)=(FXS(1:NY,1:NX)-FXS(1:NY,2:NX+1))./DeltaX+(FYS(1:NY,1:
78         NX)-FYS(2:NY+1,1:NX))./DeltaY;
79     NetF(1:NY,1:NX)=(FXF(1:NY,1:NX)-FXF(1:NY,2:NX+1))./DeltaX+(FYF(1:NY,1:
80         NX)-FYF(2:NY+1,1:NX))./DeltaY;
81
82     %% Update
83     popS = popS +NetS*dT+dS*dT;
84     popF = popF +NetF*dT+dF*dT;
85
86     Time=Time+dT
87
88     %% Plotting
89     PlotTime=PlotTime-dT;
90     if PlotTime<=0
91         %         imagesc (popS); title 'Savanna biomass'
92         %         caxis([0 1.2]);
93         imagesc (popF); title 'Forest biomass'
94         caxis([0 2]);
95         colorbar
96         colormap (flipud (summer))
97         xlabel ('x')
98         ylabel ('y')
99         drawnow;
100        PlotTime=PlotStep;
101        count=count+1;
102    end
103 end

```

A.4 Heteroclinic orbit

A.4.1 Heteroclinic orbit for (2.7)

```
1 % other parameter values in vector P (forest invading savanna)
2 P(1)=1.1;           %mu
3 P(2)=0.9;           %beta=mu-n
4 P(3)=6;             %b
5 P(4)=0.7;           %alpha=1-m
6 P(5)=2;             %a
7 P(6)=-18;           %c
8 P(7)=0.01;          %epsilon
9
10 tspan = [0 5]; %Time span
11 y0 = [0 0.001]; %Initial condition
12 [t,y] = ode45(@(t,y) eqns2(y,P), tspan, y0);
13 plot(y(:,1),y(:,2), 'blue') %Plot solution M+ in phase plane near (0,0)
14 hold on
15
16 [s, q] = meshgrid(-0.5:0.01:1.5, -1:0.01:1); %Define s-q grid
17 g=@(s,q) 1/3*P(1)*s.^3-1/2*P(2)*s.^2-1/2*q.^2+1/6*P(2)^3/(P(1)^2);
18                                     %Levelcurve Hamiltonian through (0,0) in M0
19 w=g(s,q);
20 contour(s,q,w,[-0.5:0.05:1], 'red') %plotting M0 phaseplane
21 legend('Homoclinic orbit M+', 'Phase plane M0')
22
23 xline(P(4)/P(5))
24
25 xlabel('s')
26 ylabel('q')
```

A.4.1.1 Defining equations for ode45

```
1 function dydt = eqns(y,P)
2 s=y(1);
3 q=y(2);
4 dydt = [q; -P(6)*P(7)*q+s*(P(1)*s-P(2)+P(3).*(P(4)-P(5).*s)]];
5 return
```

A.4.2 Heteroclinic orbit for (5.4)

A.4.2.1 Find intersection homoclinic orbits

```
1 % other parameter values in vector P (forest invading savanna)
2 P(1)=1.3;           %mu
3 P(2)=1;             %beta=mu-n
4 P(3)=6;             %b
5 P(4)=1;             %d
6 P(5)=0.75;          %alpha=1-m
7 P(6)=7;             %sigma
8 P(7)=2.8;           %a
9 Sstar = 0.49;       %s*
10
11 tspan = [0 20]; %Time span
12 y0 = [0 0.01]; %Initial condition
```

```

13 [t,y] = ode45(@(t,y) eqns(y,P), tspan, y0);
14 plot(y(:,1),y(:,2), 'blue') %Plot solution M+ in phase plane near (0,0)
15 hold on
16
17 [s, q] = meshgrid(-0.5:0.01:1.5, -1:0.01:1); %Define s-q grid
18 g=@(s,q) 1/3*P(1)*s.^3-1/2*P(2)*s.^2-1/2*q.^2+1/6*P(2)^3/(P(1)^2);
19 %Levelcurve Hamiltonian through (0,0) in M0
20 w=g(s,q);
21 contour(s,q,w,[-0.5:0.05:1], 'red') %plotting M0 phaseplane
22 legend('Homoclinic orbit M+', 'Phase plane M0')
23 xlabel('s')
24 ylabel('q')

```

A.4.2.2 Defining equations for ode45

```

1 function dydt = eqns(y,P)
2 s=y(1);
3 q=y(2);
4 dydt = [q; s*(P(1)*s-P(2)+(P(3)*fplus(s,P))/(1+P(6)*fplus(s,P)))]];
5 %dydt = [q; s*(P(1)*s-P(2)+fplus(s,P)*(P(3)*fplus(s,P)-P(4))/(fplus(s,P)+1)
6 return

```

A.4.2.3 Defining f_+

```

1 function y = fplus(s,P)
2 y = (P(5)*P(6)-1+sqrt((P(5)*P(6)-1)^2+4*P(6)*(P(5)-P(7)*s)))/(2*P(6));
3 return

```

A.4.3 Heteroclinic orbit for (6.2)

A.4.3.1 Find heteroclinic connection $f^*(\xi)$

```

1 %other parameter values in vector P (forest invading savanna)
2
3 P(1)=1.3; %mu
4 P(2)=1; %beta=mu-n
5 P(3)=6; %b
6 P(4)=1; %c
7 P(5)=0.75; %alpha=1-m
8 P(6)=7; %sigma
9 P(7)=2.8; %a
10 P(8)=0.49; %s*
11
12 plus = fplus(P(8),P)
13
14 tspan = [0 500]; %Time span
15 y0 = [0.0001 0]; %Initial condition
16
17 figure(1) %c=0
18 P(9)=0; %c
19 [t,y] = ode45(@(t,y) eqnsfp(y,P), tspan, y0); %Find solution
20 plot(y(:,1),y(:,2)) %Plot solution
21 xlabel('f')
22 ylabel('p')

```

```

23
24 figure(2)           %c=0
25 P(9)=0.3;           %c
26 [t,y] = ode45(@(t,y) eqnsfp(y,P), tspan, y0); %Find solution
27 plot(y(:,1),y(:,2)) %Plot solution
28 xlabel('f')
29 ylabel('p')
30
31 for i=0:0.01:0.5
32 figure(3)           %c=0
33 P(9)=i;             %c
34 [t,y] = ode45(@(t,y) eqnsfp(y,P), tspan, y0); %Find solution
35 plot(y(:,1),y(:,2)) %Plot solution
36 end
37 xlabel('f')
38 ylabel('p')
39
40 figure(4)           %c=0
41 P(9)=0.20676;       %c
42 [t,y] = ode45(@(t,y) eqnsfp(y,P), tspan, y0); %Find solution
43 plot(y(:,1),y(:,2)) %Plot solution
44 xlabel('f')
45 ylabel('p')
46
47 figure(5)           %c=0
48 P(9)=0.20677;       %c
49 [t,y] = ode45(@(t,y) eqnsfp(y,P), tspan, y0); %Find solution
50 plot(y(:,1),y(:,2)) %Plot solution
51 xlabel('f')
52 ylabel('p')

```

A.4.4 Defining equations for ode45

```

1 function dydt = eqnsfp(y,P)
2 f=y(1);
3 p=y(2);
4 dydt = [p; -P(9)*p+f*(f-P(5)+(P(7)*P(8))/(1+P(6)*f))];
5 return

```